# *Příloha 1*

**Iveta Vranová**, Michaela Moserová, Petr Hodek, René Kizek, Eva Frei, Marie Stiborová

**THE ANTICANCER DRUG ELLIPTICINE INDUCES CYTOCHROMES P450 1A1, 1A2 AND 3A, CYTOCHROME $B_5$ AND NADPH:CYTOCHROME P450 OXIDOREDUCTASE IN RAT LIVER, KIDNYE AND LUNG**

*Int. J. Electrochem. Sci. 8*, 1586-1597, 2013

$IF_{2013} = 1.956$

*Int. J. Electrochem. Sci.*, 8 **(2013)** 1586 - 1597

International Journal of
ELECTROCHEMICAL
SCIENCE
www.electrochemsci.org

# The Anticancer Drug Ellipticine Induces Cytochromes P450 1A1, 1A2 and 3A, Cytochrome $b_5$ and NADPH:Cytochrome P450 Oxidoreductase in Rat Liver, Kidney and Lung

*Iveta Vranová[1], Michaela Moserová[1], Petr Hodek[1], Rene Kizek[2,3], Eva Frei[4], Marie Stiborová[1*]*

[1] Department of Biochemistry, Faculty of Science, Charles University, Albertov 2030, CZ-128 40 Prague 2, Czech Republic
[2] Department of Chemistry and Biochemistry, Faculty of Agronomy, Mendel University in Brno, Zemedelska 1, CZ-613 00 Brno, Czech Republic
[3] Central European Institute of Technology, Brno University of Technology, Technicka 3058/10, CZ-616 00 Brno, Czech Republic
[4] Division of Preventive Oncology, National Center for Tumor Diseases, German Cancer Research Center (DKFZ), Im Neuenheimer Feld 280, 69 120 Heidelberg, Germany
[*]E-mail: stiborov@natur.cuni.cz

*Received:* 31 July 2012 / *Accepted:* 19 October 2012 / *Published:* 1 February 2013

The antineoplastic alkaloid ellipticine is a prodrug, the pharmacological efficiency of which is dependent on its cytochrome P450 (CYP)- and/or peroxidase-mediated activation in target tissues. Using the Western blotting, we found that this compound increases protein expression of cytochrome $b_5$, CYP1A1, 1A2, 3A and NADPH:CYP oxidoreductase (POR) in livers, lungs and kidneys of rats treated (i.p.) with ellipticine. The ellipticine-mediated induction of these enzymes resulted in an increase in their enzymatic activities and ellipticine oxidation to 7-hydroxy-, 9-hydroxy-, 12-hydroxy- and 13-hydroxyellipticine, the metabolites that are both detoxication products (7-hydroxy-, 9-hydroxyellipticine) and metabolites responsible for generation ellipticine-derived DNA adducts (12-hydroxy- and 13-hydroxyellipticine). The results demonstrate that by inducing CYP1A1/2, 3A, POR and cytochrome $b_5$, ellipticine increases its own metabolism in rats, thereby modulating its own pharmacological and/or genotoxic potential.

**Keywords:** Ellipticine; Cytochromes P450; Protein Expression; Western Blotting; Metabolism

## 1. INTRODUCTION

Ellipticine (5,11-dimethyl-6*H*-pyrido[4,3-*b*]carbazole, Fig. 1) and its derivatives are efficient anticancer compounds that function through multiple mechanisms participating in cell cycle arrest and

initiation of apoptosis (for a summary see [1-6]). Ellipticine was found (i) to arrest cell cycle progression due to modulation of levels of cyclinB1 and Cdc2, and phosphorylation of Cdc2 in human mammary adenocarcinoma MCF-7 cells, (ii) to initiate apoptosis due to formation of toxic free radicals, stimulation of the Fas/Fas ligand system and modulation of proteins of Bcl-2 family in several tumor cell lines, and (iii) to induce the mitochondria-dependent apoptotic processes (for a summary see [3,4]). The predominant mechanisms of ellipticine's biological effects were suggested to be (i) intercalation into DNA [5,6] and (ii) inhibition of topoisomerase II [3-6]. Further, we showed that this antitumor agent forms covalent DNA adducts after its enzymatic activation with cytochromes P450 (CYP) and peroxidases [1-4,7-11], suggesting an additional DNA-damaging effect of ellipticine.

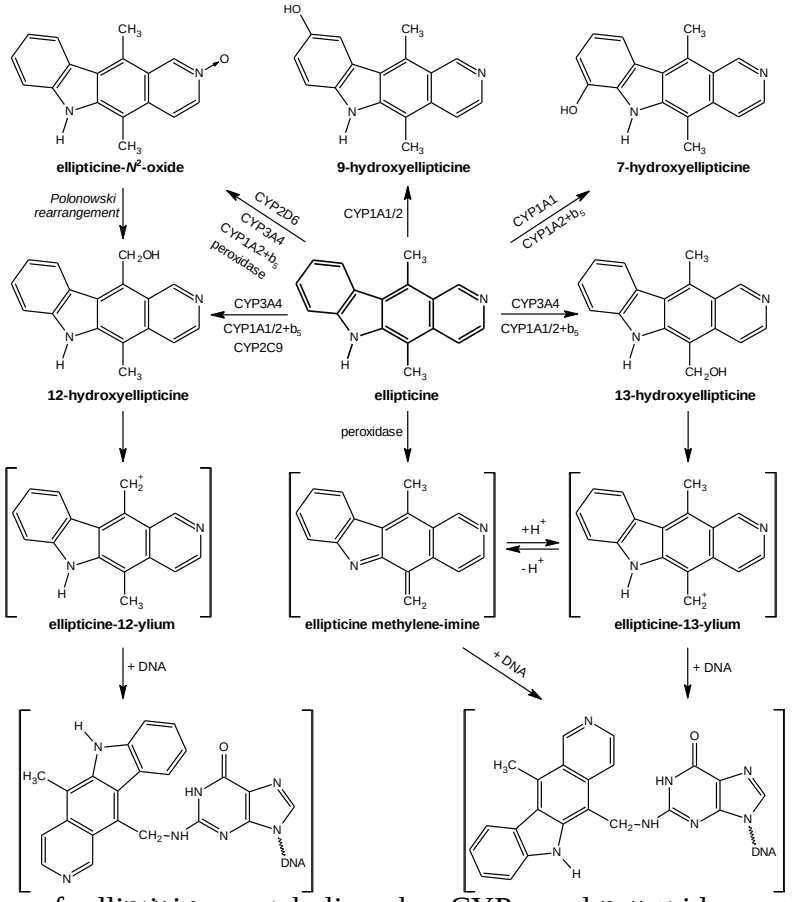


**Figure 1.** Scheme of ellipticine metabolism by CYPs and peroxidases showing the identified metabolites and those proposed to form DNA adducts. The compounds shown in brackets were not detected under the experimental conditions and/or not structurally characterized. The CYP enzymes predominantly oxidizing ellipticine shown in the figure were identified in our previous studies [7,10,11].

Of the CYP enzymes investigated, human CYP3A4 and rat CYP3A1 are the most active enzymes oxidizing ellipticine to 12-hydroxy- and 13-hydroxyellipticine, the reactive metabolites that dissociate to ellipticine-12-ylium and ellipticine-13-ylium which bind to DNA [3,7,8,10], while the CYP1A isoforms preferentially form the other ellipticine metabolites, 7-hydroxy- and 9-hydroxyellipticine, which are the detoxication products (Fig. 1). Recently we have found that

cytochrome $b_5$ alters the ratio of ellipticine metabolites formed by CYP1A1, 1A2 and 3A4. While the amounts of the detoxication metabolites (7-hydroxy- and 9-hydroxyellipticine) were either decreased or not changed with added cytochrome $b_5$, 12-hydroxy-, 13-hydroxyellipticine and ellipticine $N^2$-oxide increased considerably. The change in amounts of metabolites resulted in an increased formation of covalent ellipticine-DNA adducts, one of the DNA-damaging mechanisms of ellipticine antitumor action [10,11].

Because of the important role of cytochrome $b_5$ in CYP1A- and CYP3A-mediated ellipticine metabolism, expression levels of all these proteins are crucial for antitumor, cytostatic and/or genotoxic activities of this drug in individual tissues.

Recently we found that ellipticine as a ligand of aryl hydrocarbon receptor (AHR) [12] is a strong inducer of CYP1A1 and 1A2 in rat liver *in vivo* [13] and in several cancer cell lines *in vitro* [14,15]. In addition, levels of cytochrome $b_5$ are increased by ellipticine in liver of rats treated with this drug [11]. Moreover, ellipticine also induces expression of *CYP3A4* mRNA and CYP3A4 protein in several cancer cell lines [14,15]. However, in contrast to induction of CYP1A by ellipticine *in vivo* that has been partially studied previously [13], the effect of ellipticine on expression of CYP3A and cytochrome $b_5$ *in vivo* remains to be investigated.

Therefore, Western blotting analysis was used in this work to evaluate the effect of ellipticine on protein levels not only of CYP1A1/2, but also of CYP3A, POR and cytochrome $b_5$ proteins in rats *in vivo*.

## 2. EXPERIMENTAL PART

### *2.1 Animal experiments*

The study was conducted in accordance with the Regulations for the Care and Use of Laboratory Animals (311/1997, Ministry of Agriculture, Czech Republic), which is in compliance with the Declaration of Helsinki. Male Wistar rats (~100 g) were treated with a single dose of 4 or 40 mg/kg body weight (n=3) of ellipticine by intraperitoneal (i.p.) injection as described previously [13]. Ellipticine was dissolved in 1% acetic acid at a concentration of 6 mg/ml. Three control animals received an equal volume of solvent only. Rats were placed in cages in temperature and humidity controlled rooms. Standardized diet and water were provided *ad libitum*. The animals were killed 48 hours after treatment by cervical dislocation. Livers, lungs and kidneys were removed immediately and directly used for the isolation of microsomal fractions. Microsomes were isolated from the livers, kidneys and lungs of rats as described [1].

### *2.2 Electrochemical determination of CYP, POR and cytochrome $b_5$ protein levels in microsomes of rat liver, kidney and lung*

Immunoquantitation of rat liver, kidney and lung microsomal cytochrome $b_5$ , CYPs (CYP1A1, 1A2, and 3A) and POR was done by sodium dodecyl sulfate-polyacrylamide gel electrophoresis (SDS-

PAGE). Samples containing 30-75 μg microsomal proteins were subjected to electrophoresis on 10% polyacrylamide gels (for CYPs and POR) and 15% gels (for cytochrome $b_5$) polyacrylamide gels [11,16,17]. After migration, proteins were transferred onto a polyvinylidene fluoride (PVDF) membrane and incubated with 5% non-fat milk to block non-specific binding. The membranes were then exposed to specific rabbit polyclonal anti-cytochrome $b_5$ (1:750, AbCam, MA, USA), anti-CYP1A1 (1:1000, Millipore, MA, USA), anti-CYP3A4 (1:5000, AbD Serotec, Oxford, UK) and anti-POR (1:1000, Millipore, MA, USA) antibodies overnight at 4 $^{o}$C. The antigen-antibody complex was visualized with an alkaline phosphatase-conjugated goat anti-rabbit IgG antibody (1:1428, Sigma-Aldrich, USA) and 5-bromo-4-chloro-3-indolylphosphate/nitrobluetetrazolium as chromogenic substrate [16,17]. Antibody against glyceraldehyde phosphate dehydrogenase (GAPDH) (1:750, Millipore, MA, USA) was used as loading control.

### 2.3 *CYP1A, 3A and POR enzyme activity assays*

The rat liver, kidney and lung microsomal samples were characterized for CYP1A activity using 7-ethoxyresorufin *O*-deethylation (EROD) [18], for 6-β-hydroxylation of testosterone (a marker for CYP3A) [19] and for POR activity using reduction of cytochrome *c* [10,13].

### *2.4 CYP1A mRNA contents in rat liver, kidney and lung*

The mRNA contents of CYP1A in rat liver, kidney and lung were carried out as described previously [13].

### 2.5 *Determination of cytochrome $b_5$ content*

The concentration of cytochrome $b_5$ was determined spectrophotometrically (the absolute absorbance spectrum) using the molar extinction coefficient $\varepsilon_{413}$ = 117 $mM^{-1}.cm^{-1}$ [20,21], or from the difference spectrum of reduced minus oxidized form, using molar extinction coefficient $\varepsilon_{424\text{-}409}$ = 185 $mM^{-1}.cm^{-1}$, respectively [21].

### *2.6 Oxidation of ellipticine by rat hepatic, renal and pulmonary microsomes*

Incubation mixtures used to study ellipticine oxidation to its metabolites contained 50 mM potassium phosphate buffer (pH 7.4), 1 mM $NADP^{+}$, 10 mM D-glucose 6-phosphate, 1 U/ml D-glucose 6-phosphate dehydrogenase (NADPH-generation system), 0.2 mg protein of pooled hepatic, renal and pulmonary microsomal fraction from 3 male rats, either untreated or treated with 40 mg/kg body weight ellipticine and 10 μM ellipticine (dissolved in 5 μl methanol) in a final volume of 500 μl. The reaction was initiated by adding the substrate. In the control incubation, ellipticine was omitted from the incubation mixture. After incubation in open glass tubes (37 $^{o}$C, 20 min) the reaction was stopped by adding 100 μl of 2 M NaOH. The oxidation of ellipticine is linear up to 30 min of

incubation [7]. After incubation, 5 µl of 1 mM phenacetine in methanol was added as an internal standard and the ellipticine metabolites were extracted twice with ethyl acetate (2 x 1 ml). Analyzes of ellipticine metabolites were performed by HPLC as described [7,10,11]. Recoveries of ellipticine metabolites were around 95%.

## 3. RESULTS AND DISCUSSION

Using Western blot analysis with antibodies raised against CYP1A1, 3A4, POR and cytochrome $b_5$, the expression levels of these proteins were analyzed in livers, kidneys and lungs of rats exposed to ellipticine. Rats treated i.p. with 4 and 40 mg/kg body weight were used as a model. Microsomes isolated from livers, kidneys and lungs of untreated (control) and ellipticine-treated rats were used for the analyses.

### *3.1 CYP1A1, 1A2 and 3A protein levels and enzymatic activities in rat liver, kidney and lung*

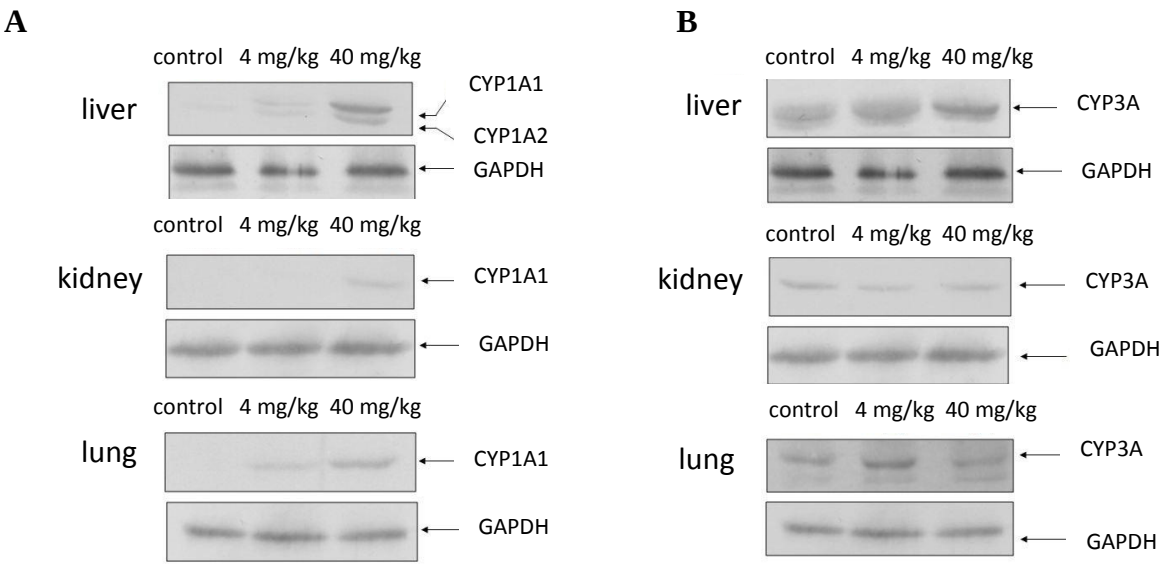


**Figure 2.** Immunoblots of microsomal CYP1A1, 1A2 (**A**) and 3A (**B**) from livers, lungs, and kidneys of untreated and ellipticine-treated (4 and 40 mg/kg) rats stained with antibody against rat CYP1A1 (**A**) and human CYP3A4 (**B**). Microsomes isolated from rat organs were subjected to SDS-polyacrylamide gel electrophoresis, and proteins were transferred to PVDF membranes and probed with antibodies. Glyceraldehyde phosphate dehydrogenase (GAPDH) was used as loading control.

As shown in Figure 2A, ellipticine is capable of inducing expression levels of CYP1A1 and 1A2 proteins in liver, kidney and lung of rats treated i.p. with this compound. The increase in CYP1A1 and 1A2 protein levels in rat organs is dose-dependent; the highest expression levels of these enzymes were found in the liver of rats treated with 40 mg/kg body weight of ellipticine (Fig. 2A). A dose-dependent increase in CYP1A1 and 1A2 protein levels due to ellipticine correlated with their

enzymatic activities (EROD for CYP1A1/2) in all organs studied (Fig. 3A). Moreover, as we found in our former work [13], this increase in CYP1A1 protein levels corresponded also to higher expression of *CYP1A1* mRNAs in liver, kidney and lung (see [13] and Table 1). mRNA levels of *CYP1A2* showed no significant difference between ellipticine treated and control rats in all three organs. Interestingly the highest *CYP1A2* mRNA levels were observed in lung and kidney, while protein expression determined by Western blot was only seen in livers of ellipticine treated rats.

**Table 1**. Expression of mRNA of CYP1A1 and 1A2

| | CYP1A1 | | CYP1A2 | |
|---|---|---|---|---|
| | $\Delta c_T$[a] | Fold Change | $\Delta c_T$ | Fold Change |
| control rats | | | | |
| liver | 6.37 ± 0.07 | | -3.9 ± 0.12 | |
| kidney | 4.45 ± 0.36 | | 14.07 ± 0.54 | |
| lung | 10.48 ± 0.16 | | 13.97 ± 1.06 | |
| ellipticine-treated rats | | | | |
| liver | 3.87 ± 1.73 | 5.66* | -4.04 ± 0.22 | 1.1 |
| kidney | 1.12 ± 0.13 | 10.08** | 13.8 ± 0.76 | 1.21 |
| lung | 5.89 ± 0.59 | 24.2** | 15.37 ± 0.03 | 0.38 |

[a]Results shown are mean ± standard deviation from data found for three male rats (control and treated with 40 mg/kg body weight) and are taken from our previous work [13].
Significantly different from controls: $^{*}p<0.05$; $^{**}p<0.001$ (Student's t-test).

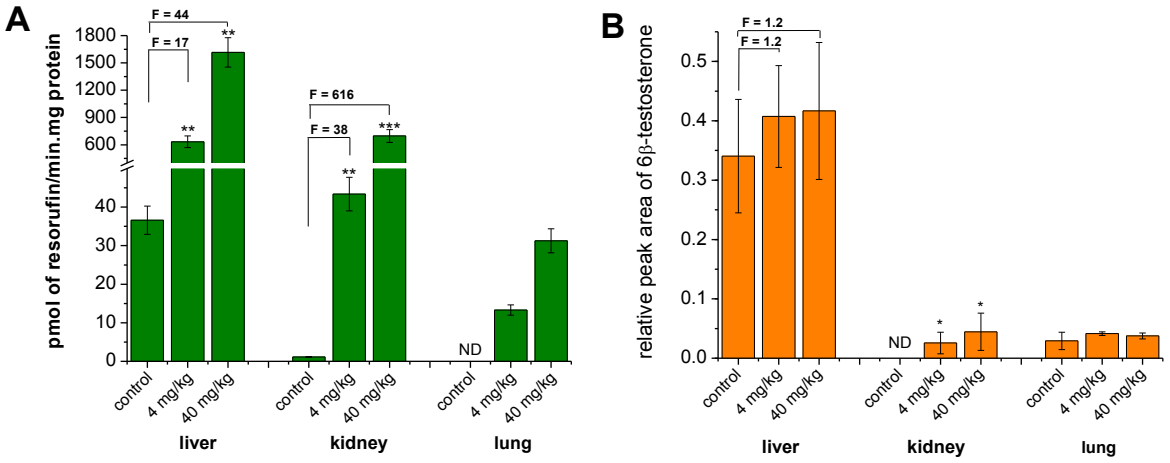


**Figure 3.** CYP1A enzymatic activity measured by 7-ethoxyresorufin *O*-deethylation (EROD) (**A**) and CYP3A enzymatic activity measured by testosterone 6-β-hydroxylation (**B**) in microsomes of control and ellipticine-treated rats (ND – not detected). F, fold of increase in CYP1A and 3A enzymatic activities in rats treated with ellipticine compared with those of control (uninduced) rats. Values significantly different from control: **p*<0.05, ***p*<0.01, ****p*<0.001 (Student's t-test).

Besides CYP1A1 and 1A2, expression levels of CY3A protein were also increased in livers of rats treated with ellipticine (Fig. 2B). In contrast, lower CYP3A protein levels were found in kidney of rats treated with both doses of ellipticine and in lung of rats exposed to the higher dose of ellipticine (40 mg/kg). Dose-dependent increases in marker activity of the CYP3A enzymes, testosterone 6-β-hydroxylation, were produced in all studied organs of rats treated with ellipticine (Fig. 3B). Nevertheless, an increase in this enzymatic activity in liver and lung was not statistically significant.

### *3.2 Cytochrome $b_5$ protein levels and its specific content in rat liver, kidney and lung*

Similarly to CYP1A and 3A enzymes, expression of additional protein of the mixed-function oxidase system located in the membrane of endoplasmic reticulum, cytochrome $b_5$, was increased in liver and kidney of rats treated with ellipticine (Fig. 4). Using only 30 μg microsomal proteins were sufficient to detect expression of this protein in rat livers by Western blotting (Fig. 4A), but higher levels of microsomal proteins (75 μg) were utilized to detect expression of this protein in rat kidney (Fig. 4B). An increase in expression levels of cytochrome $b_5$ by treating rats with ellipticine was dose-dependent. No cytochrome $b_5$ expression was detectable in lung microsomes.

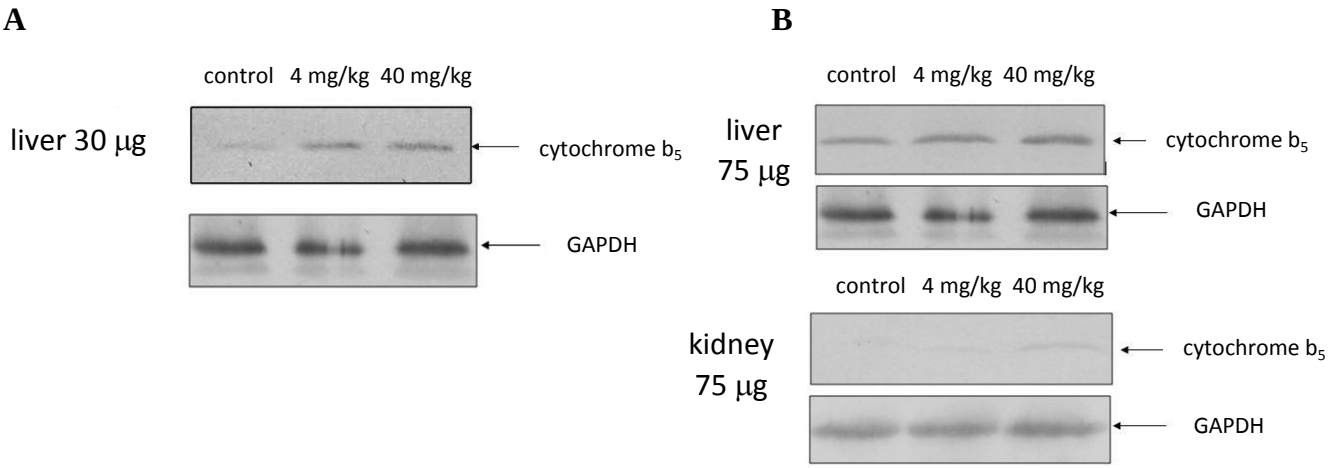


**Figure 4.** Immunoblots of microsomal cytochrome $b_5$ from livers (30 μg microsomal proteins) (A), and livers and kidneys (75 μg microsomal proteins) (B) of untreated and ellipticine-treated (4 and 40 mg/kg) rats stained with antibody against rat cytochrome $b_5$. Microsomes isolated from rat organs were subjected to SDS-polyacrylamide gel electrophoresis, and proteins were transferred to PVDF membranes and probed with antibody. Glyceraldehyde phosphate dehydrogenase (GAPDH) was used as loading control.

An increase in expression of liver and kidney cytochrome $b_5$ in rats after treatment with ellipticine was paralleled by the specific content of this protein determined spectrophotometrically (Fig. 5).

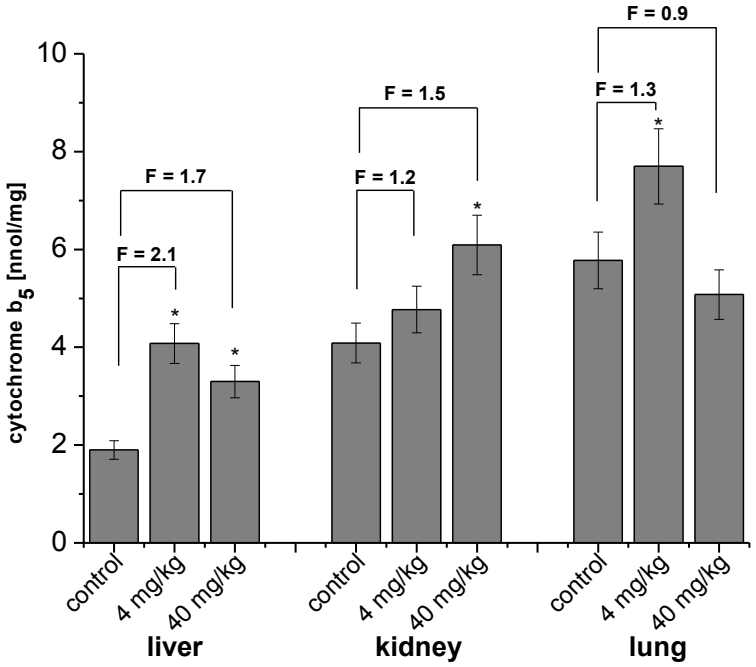


**Figure 5.** Specific contents of cytochrome $b_5$ in microsomes of control and ellipticine-treated rats. F, fold of increase in cytochrome $b_5$ in rats treated with ellipticine compared with those of control (uninduced) rats. Values significantly different from control: *$p$<0.05 (Student's t-test).

In contrast to the cytochrome $b_5$ protein detected by Western blot, spectrophotometric analyses revealed higher cytochrome $b_5$ contents in lung (approximately three fold over liver) than liver or kidney (Fig. 5). Low interaction of antibody with cytochrome $b_5$ caused by worse availabilities of epitopes of this protein in lung microsomes or the presence of certain inhibitor(s) in these microsomes that decrease interaction of the protein with its antibody might the reasons of this observation. Nevertheless, these suggestions remain to be investigated.

*3.3 POR protein levels and enzymatic activity in rat liver, kidney and lung*

Another enzyme that is a component of the mixed-function oxidase system, POR, was also detected by Western blotting in the liver, kidney and lung microsomes of rats treated with ellipticine (Fig. 6), whereas almost no expression of this enzyme was detected in kidney of untreated (control) rats. An increase in levels of rat liver POR protein by ellipticine was paralleled by an increase in its enzymatic activity measured as reduction of cytochrome *c* (Fig. 7).

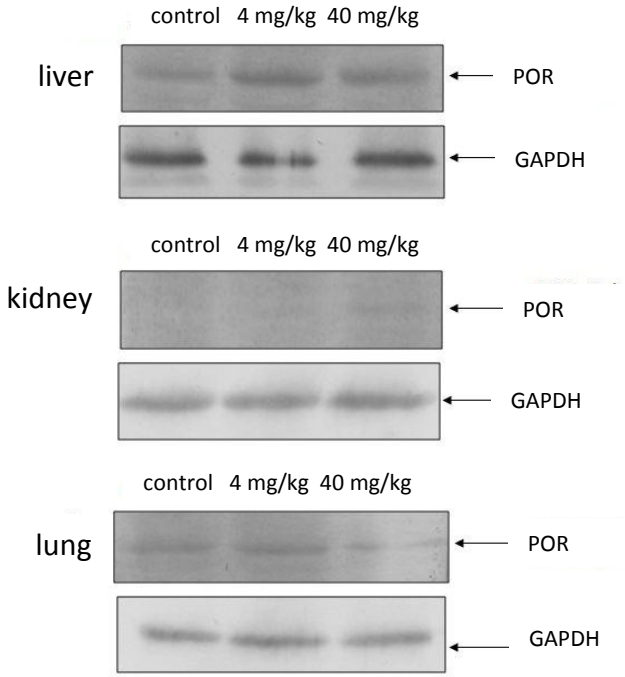


**Figure 6.** Immunoblots of microsomal POR from livers, kidneys and lungs of untreated and ellipticine-treated (4 and 40 mg/kg) rats stained with antibody against rat POR. Microsomes isolated from rat organs were subjected to SDS-polyacrylamide gel electrophoresis, and proteins were transferred to a PVDF membrane and probed with antibody. Glyceraldehyde phosphate dehydrogenase (GAPDH) was used as loading control.

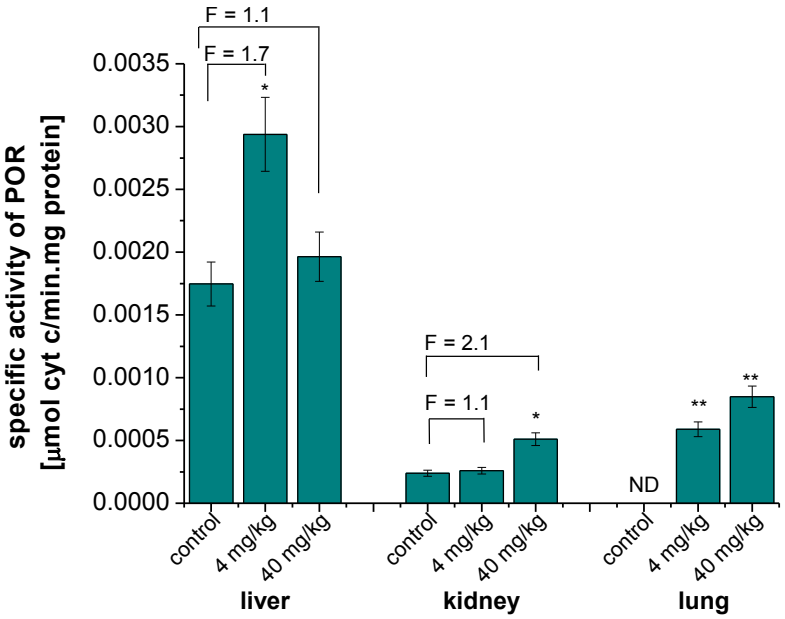


**Figure 7.** POR enzymatic activity in microsomes of control and ellipticine-treated rats (ND – not detected). F, fold of increase in POR enzymatic activities in rats treated with ellipticine compared with those of control (uninduced) rats. Values significantly different from control: *$p$<0.05, **$p$<0.01, ***$p$<0.001 (Student's t-test).

The mechanisms responsible for induction of CYP1A have already been investigated [12,22,,23]. CYP1A1 and 1A2 induction might be a consequence of the binding of ellipticine to AHR [12]. Binding of ellipticine allows cytosolic AHR to translocate into the nucleus and to dimerize with AHR nuclear translocator (ARNT). The AHR-ARNT complex functions as a transcriptional activator by binding to the aryl hydrocarbon responsive element in the regulatory domains of *CYP1A1* and *CYP1A2* genes [12], thus stimulating their transcription as we previously found in livers [13] and in kidneys and lungs in the present study. Another mechanism of CYP1A1 induction might result from inhibitory potential of ellipticine to this enzyme [22]. As shown previously [23], a decrease in levels of CYP1A1 enzymatic activity by ellipticine results in an increase in constitutive activation of AHR-ARNT transcriptional complexes. Moreover, low levels of ellipticine antagonize AHR activation by inducing ligands such as 2,3,7,8-tetrachlorodibenzo-*p*-dioxin or certain azo dyes.

Effects of ellipticine upon CYP3A, POR and cytochrome $b_5$ protein expression and enzymatic activities were much lower than upon CYP1A. For these proteins the induction mechanisms are not yet entirely elucidated and await further investigation. Because the pregnane X receptor (PXR) and the constitutive active receptor (CAR) are known to coordinate multifaceted responses to inducers of CYPs of a 3A subfamily and POR [24, 25], we plan to investigate whether ellipticine or its metabolites function as ligands of either of these receptors, thereby inducing expression of these enzymes.

### *3.3 Ellipticine as an inducer of cytochrome $b_5$, CYP1A and 3A increases efficiencies of rat hepatic, pulmonary and renal microsomes to oxidize ellipticine to its hydroxylated metabolites*

Ellipticine is oxidized by hepatic, pulmonary and renal microsomes to four metabolites, 7-hydroxy-, 9-hydroxy-, 12-hydroxy and 13-hydroxyellipticine (Fig. 8). Ellipticine $N^2$-oxide (Fig. 1) was also produced, but this metabolite was not quantitated in this study because of its spontaneous rearrangement to 12-hydroxyellipticine [7,8].

Treatment of rats with 40 mg/kg of ellipticine resulted in changes of patterns of metabolites formed by microsomes isolated from all three organs of these rats. In all organs 9-hydroxyellipticine was formed at significantly higher amounts by "ellipticine microsomes" than by those of control rats, while 7-hydroxyellipticine formation was induced in kidney and liver only. The influence of ellipticine exposure on the levels of these two metabolites was expected, because they are predominantly formed by CYP1A1/2 [7,11] and CYP1A1 was induced in all three organs. An up to 2-fold increase in formation of 13-hydroxy- and 12-hydroxyellipticine, the metabolites generating DNA adducts 1 and 2 (see Fig. 1), was induced in hepatic microsomes (Fig. 8A). This phenomenon is caused not only by a strong induction of CYP1A1/2, but also by induction of CYP3A (Fig. 2B) and cytochrome $b_5$ (Fig. 4) in livers of rats treated with ellipticine. Ellipticine treatment causing induction of cytochrome $b_5$ seems to play a crucial role for these metabolic changes. Cytochrome $b_5$ influences the enzymatic activity of CYP1A1/2 [11] and CYP3A [10], mediating the increased formation of 12-hydroxy- and 13-hydroxyellipticine *in vitro*. Hence, higher levels of cytochrome $b_5$ protein in liver (Fig. 4) results in the elevated formation of 12-hydroxy- and 13-hydroxyellipticine in rat liver microsomes shown in this study (Fig. 8A). In order to prove that elevated formation of these ellipticine metabolites leads to

higher levels of ellipticine-derived DNA adducts will be analyzed in our laboratory in future. The $^{32}$P-postlabeling assay [1-3,4-11] or electrochemical techniques [26,27] will be used for such a study. In contrast to liver microsomes, no increase in formation of 12-hydroxy- and 13-hydroxyellipticine was found during oxidation of ellipticine catalyzed by lung and kidney nicrosomes of rats treated with ellipticine (Fig. 8B,C). Only an increase in oxidation of ellipticine to 7-hydroxyellipticine and/or 9-hydroxyellipticine was found in lung and kidney microsomes. These results are consequences of both the effective ellipticine-mediated induction of CYP1A1 in these organs and a lower induction effect of ellipticine on expression levels of CYP3A and cytochrome $b_5$ in these tissues (compare Figs. 2 and 4).

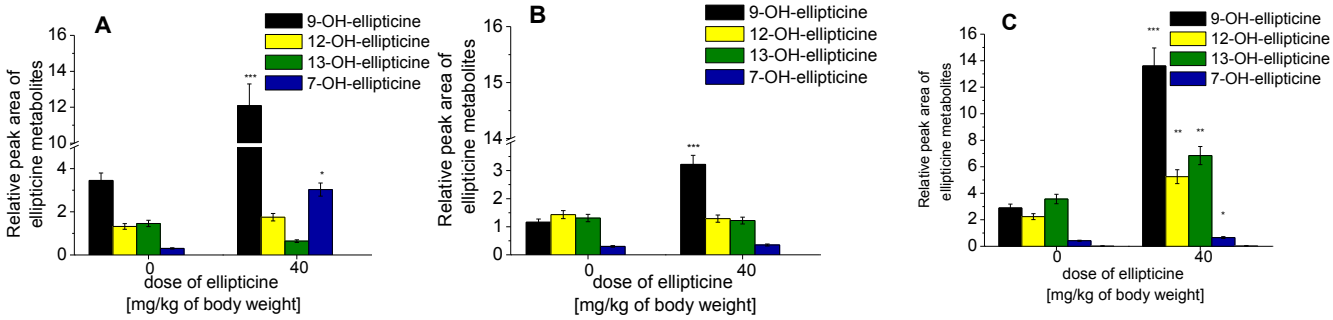


**Figure 8.** Ellipticine metabolism in rat liver (A), lung (B) and kidney microsomes (C) of control animals and those treated with 40 mg/kg ellipticine. Microsomes containing 0.2 mg microsomal protein, and 10 μM ellipticine were used in all experiments. Levels of ellipticine metabolites are averages ± standard deviations of triplicate incubations. Values significantly different from control: *$p$<0.05, **$p$<0.01, ***$p$<0.001 (Student's t-test).

## 4. CONCLUSIONS

Utilizing the Western blotting, protein levels of CYP1A, 3A, POR and cytochrome $b_5$ were found to be increased by treating rats with ellipticine. The most prominent change observed was the induction of CYP1A expression in all organs analyzed, namely liver, kidney and lung. This induction of expression resulted in an increase in CYP1A, 3A and POR marker activities as well as in an enhanced oxidation of ellipticine itself. By inducing these proteins, ellipticine modulates its own metabolism in rats, thereby dictating its own pharmacological and/or genotoxic potential. Therefore, further studies that would shad more light on the mechanism(s) of this induction are needed to be carried out. Studies investigating whether ellipticine or its metabolites activates receptors such as AHR, CAR and PXR which consequently leads to induction of CYP1A, 3A, and POR expression is planned to be performed in our laboratory in future.

ACKNOWLEDGEMENTS
Financial support from GACR (grant P301/10/0356) and Charles University in Prague (UNCE 204025/2012) is highly acknowledged.

**References**


1. M. Stiborova, C.A. Bieler, M. Wiessler and E. Frei, *Biochem. Pharmacol.*, 62 (2001) 1675.
2. M. Stiborova, M. Rupertova, H. H. Schmeiser and E. Frei, *Biomed. Pap. Med. Fac. Univ. Palacky Olomouc Czech Repub.*, 150 (2006) 13.
3. M. Stiborova, M. Rupertova and E. Frei, *Biochim. Biophys. Acta*, 1814 (2011) 175.
4. R. Kizek, V. Adam, J. Hrabeta, T. Eckschlager, S. Smutny, J. V. Burda, E. Frei and M. Stiborova, *Pharmacol. Ther.*, 133 (2012) 26.
5. C. Auclair, *Arch. Biochem. Biophys.*, 259 (1987) 1.
6. N. C. Garbett and D. E. Graves, *Curr. Med. Chem. Anti-Cancer Agents*, 4 (2004) 149.
7. M. Stiborova, J. Sejbal, L. Borek-Dohalska, D. Aimova, J. Poljakova, K. Forsterova, M. Rupertova, J. Wiesner, J. Hudecek, M. Wiessler and E. Frei, *Cancer Res.*, 64 (2004) 8374.
8. M. Stiborova, J. Poljakova, H. Ryslava, M. Dracinsky, T. Eckschlager and E. Frei, *Int. J. Cancer*, 120 (2007) 243.
9. M. Stiborova, M. Rupertova, D. Aimova, H. Ryslava and E. Frei, *Toxicology*, 236 (2007) 50.
10. M. Stiborova, R. Indra, M. Moserova, V. Cerna, M. Rupertova, V. Martinek, T. Eckschlager, R. Kizek and E. Frei, *Chem. Res. Toxicol.*, 25 (2012) 1075.
11. V. Kotrbova, B. Mrazova, M. Moserova, V. Martinek, P. Hodek, J. Hudecek, E. Frei and M. Stiborova, *Biochem. Pharmacol.*, 82 (2011) 669.
12. Gasiewicz T.A., Kende R.S., Rucci G., B. Whitney and J. J. Willey, *Biochem. Pharmacol*., 52 (1996) 787.
13. D. Aimova, L. Svobodova, V. Kotrbova, B. Mrazova, P. Hodek, J. Hudecek, R. Vaclavikova, E. Frei and M. Stiborova, *Drug Metab. Dispos.* 35 (2007) 1926.
14. E. Martinkova, M. Dontenwill, E. Frei and M. Stiborova, *Neuro Endocrinol. Lett.*, 30, Suppl. 1 (2009) 60.
15. J. Poljakova, J. Hrebackova, M. Dvorakova, M. Moserova, T. Eckschlager, J. Hrabeta, M. Göttlicherova, B. Kopejtkova, E. Frei, R. Kizek and M. Stiborova, *Neuro Endocrinol. Lett.*, 32, Suppl. 1 (2011) 101.
16. M. Stiborova, V. Martinek, H. Rydlova, P. Hodek and E. Frei, *Cancer Res.*, 62 (2002) 5678.
17. M. Stiborova, V. Martinek, H. Rydlova, T. Koblas and P. Hodek, *Cancer Lett*. 220 (2005) 145.
18. F. P. Guengerich and T. Shimada, *Chem. Res. Toxicol*., 4 (1991) 391.
19. L. Borek-Dohalska, P. Hodek, M. Sulc M. and M. Stiborova, *Chem.-Biol. Interact.*, 138 (2001) 85.
20. P. Strittmatter and S. F. Velick, *J. Biol. Chem.*, 221 (1956) 253.
21. R. W. Estabrook and J. Werringloer, *Methods Enzymol.*, 52 (1978) 212.
22. D. Aimova and M. Stiborova, *Biomed. Pap. Med. Fac. Univ. Palacky Olomouc Czech Repub.*, 149 (2005) 437.
23. C. Y. Chang and A. Puga, *Mol. Cell. Biol.*, 18 (1998) 525.
24. A. Ueda, H. K. Hamadeh, H. K. Webb, Y. Yamamoto, T. Suevoshi, C. A. Afshari, J. M. Lehmann and M. Negishi, *Mol. Pharmacol.*, 61 (2002) 1.
25. X. Ma, C. Cheung, K. W. Krausz, Y, M, Shah, T. Wang, J. R. Idle and F. J. Gonzalez, *Drug Metab. Dispos.*, 36 (2008) 2506.
26. D. Hynek, L. Krejcova, O. Zitka, V. Adam, L. Trnkova, J. Sochor, M. Stiborova, T. Eckschlager, J. Hubalek and R. Kizek, *Int. J. Electrochem. Sci.*, 7 (2012) 34.
27. D. Dospivova, K. Smerkova, M. Ryvolova, D. Hynek, V. Adam, P. Kopel, M. Stiborova, T. Eckschlager, J. Hubalek and R. Kizek, *Int. J. Electrochem. Sci.*, 7 (2012) 3072.

# *Příloha 2*

Marie Stiborová, Jitka Poljaková, **Iveta Mrízová**, Lucie Bořek-Dohalská, Tomáš Eckschlager, Vojtěch Adam, René Kizek, Eva Frei

**EXRESSION LEVELS OF ENZYMES METABOLIZING AN ANTICANCER DRUG ELLIPTICINE DETERMINED BY ELECTROMIGRATION ASSAYS INFLUENCE CYTOTOXICITY TO CANCER CELL – A COMPARATIVE STUDY**

*Int. J. Electrochem. Sci.* 9, 5675-5689, 2014

$IF_{2014} = 1.5$

*Int. J. Electrochem. Sci.*, 9 **(2014)** 5675 - 5689

International Journal of
ELECTROCHEMICAL
SCIENCE
www.electrochemsci.org

# Expression Levels of Enzymes Metabolizing an Anticancer Drug Ellipticine Determined by Electromigration Assays Influence its Cytotoxicity to Cancer Cells - A Comparative Study

*Marie Stiborova*[1,*], *Jitka Poljakova*[1], *Iveta Mrizova*[1], *Lucie Borek-Dohalska*[1], *Tomas Eckschlager*[2], *Vojtech Adam*[3,4], *Rene Kizek*[3,4], *Eva Frei*[5]

[1] Department of Biochemistry, Faculty of Science, Charles University, Albertov 2030, CZ-128 40 Prague 2, Czech Republic
[2] Department of Pediatric Hematology and Oncology, 2nd Medical School, Charles University and University Hospital Motol, V Uvalu 84, CZ-150 06 Prague 5, Czech Republic
[3] Department of Chemistry and Biochemistry, Faculty of Agronomy, Mendel University in Brno, Zemedelska 1, CZ-613 00 Brno, Czech Republic
[4] Central European Institute of Technology, Brno University of Technology, Technicka 3058/10, CZ-616 00 Brno, Czech Republic
[5] Division of Preventive Oncology, National Center for Tumor Diseases, German Cancer Research Center (DKFZ), Im Neuenheimer Feld 280, D-69 120 Heidelberg, Germany
[*]E-mail: stiborov@natur.cuni.cz

*Received:* 27 May 2014 / *Accepted:* 23 June 2014 / *Published:* 16 July 2014

The antineoplastic alkaloid ellipticine is a prodrug, of which the pharmacological efficiency is dependent on its cytochrome P450 (CYP)- and/or peroxidase-mediated activation to 12-hydroxy- and 13-hydroxyellipticine, which are both the metabolites forming DNA adducts in target tissues. Using the method of Western blotting, the expression of CYP1A1, 1B1, 3A4, lactoperoxidase, thyroid peroxidase, cyclooxygenase-1 and cytochrome $b_5$, the enzymes that catalyze and/or influence ellipticine metabolism, was investigated in several cancer cells sensitive to ellipticine (HL-60 promyelocytic leukemia and T-cell leukemia CCRF-CEM cells, glioblastoma U87MG cells, thyroid cancer BHT-101, B-CPAP and 8505-C cells, neuroblastoma UKF-NB-3 and UKF-NB-4 cell lines and breast adenocarcinoma MCF-7 cells). The findings summarized from several former studies reviewed in this study, together with new results indicate that, depending on individual cells, cytotoxicity of ellipticine, which is mediated by formation of covalent DNA adducts to these cancer cells, is influenced by expression levels of these CYP and peroxidase enzymes in the tested cancer cells. Furthermore, a potency of ellipticine to induce the enzymes dictating activation of ellipticine to form DNA adducts in studied cancer cells determines an increase in cytotoxicity of ellipticine to these tumor cells.

**Keywords:** Ellipticine; Cancer Cells; Cytotoxicity; Cytochromes P450; Peroxidases; Protein Expression; Western Blotting; Metabolism; DNA Adducts

## 1. INTRODUCTION

Ellipticine (5,11-dimethyl-6*H*-pyrido[4,3-*b*]carbazole, Fig. 1) and its derivatives are efficient anticancer compounds that function through multiple mechanisms participating in cell cycle arrest and initiation of apoptosis (for a summary see [1-6]). Ellipticine was found (i) to arrest cell cycle progression due to modulation of levels of cyclinB1 and Cdc2, and phosphorylation of Cdc2 in human mammary adenocarcinoma MCF-7 cells, (ii) to initiate apoptosis due to formation of toxic free radicals, stimulation of the Fas/Fas ligand system and modulation of proteins of Bcl-2 family in several tumor cell lines, and (iii) to induce the mitochondria-dependent apoptotic processes (for a summary see [3,4]). The predominant mechanisms of ellipticine's biological effects were suggested to be (i) intercalation into DNA [5-7] and (ii) inhibition of topoisomerase II [3-6]. Further, we showed that this antitumor agent forms covalent DNA adducts after its enzymatic activation with cytochromes P450 (CYP) and peroxidases [1-4,8-13], suggesting an additional DNA-damaging effect of ellipticine.

Of the CYP enzymes investigated, human CYP3A4 followed by CYP1A1 and 1B1 are the most active enzymes oxidizing ellipticine to 12-hydroxy- and 13-hydroxyellipticine, the reactive metabolites that dissociate to ellipticine-12-ylium and ellipticine-13-ylium, which bind to DNA [3,7,9-11]. The CYP1A isoforms also efficiently form the other ellipticine metabolites, 7-hydroxy- and 9-hydroxyellipticine, which are the detoxification products (Fig. 1). Recently, we found that cytochrome $b_5$ alters the ratio of ellipticine metabolites formed by CYP1A1, 1A2 and 3A4. While the amounts of the detoxification metabolites (7-hydroxy- and 9-hydroxyellipticine) were either decreased or not changed with added cytochrome $b_5$, 12-hydroxy-, 13-hydroxyellipticine and ellipticine $N^2$-oxide increased considerably. The change in amounts of metabolites resulted in an increased formation of covalent ellipticine-DNA adducts, one of the DNA-damaging mechanisms of ellipticine antitumor action [11,12]. In addition, we observed that levels of the DNA adduct formed by 13-hydroxyellipticine also increased if this ellipticine metabolite was conjugated with sulfate or acetate by human sulfotransferases 1A1, 1A2, 1A3 and 2A1, or *N,O*-acetyltransferases 1 and 2 [11-14] as it is shown in Fig. 1.

The same ellipticine-derived DNA adducts that were found in *in-vitro* incubations of ellipticine with DNA and enzymes activating this drug, were generated also *in vivo*, in several tissues of mice and rats exposed to ellipticine. In both animal models, ellipticine-DNA adduct formation was mediated mainly by CYP1A and 3A enzymes, but a role of peroxidases in several organs has been proved [15-17]. Therefore, expression levels of CYP and peroxidase enzymes metabolizing ellipticine seem to be crucial for antitumor, cytostatic and genotoxic activities of this drug in individual tissues. The ellipticine-DNA adducts were also found in several cancer cell lines and in DNA of rat mammary adenocarcinoma *in vivo* [3,19-25]. In this study, the utilizing the findings from several former studies [19-25] as well as new results found in this work, we evaluated whether cytotoxicity of ellipticine to cancer cells is dependent on formation of covalent ellipticine-DNA adducts and whether the expression of the enzymes metabolizing ellipticine *in vitro* and *in vivo* regulates their levels in cancer cells as well as the ellipticine cytotoxicity to these cells. The method of Western blotting determined the enzyme protein expression levels, whereas the $^{32}$P-postlabeling method detected and quantified DNA adducts formed by ellipticine [1-3,25-29].

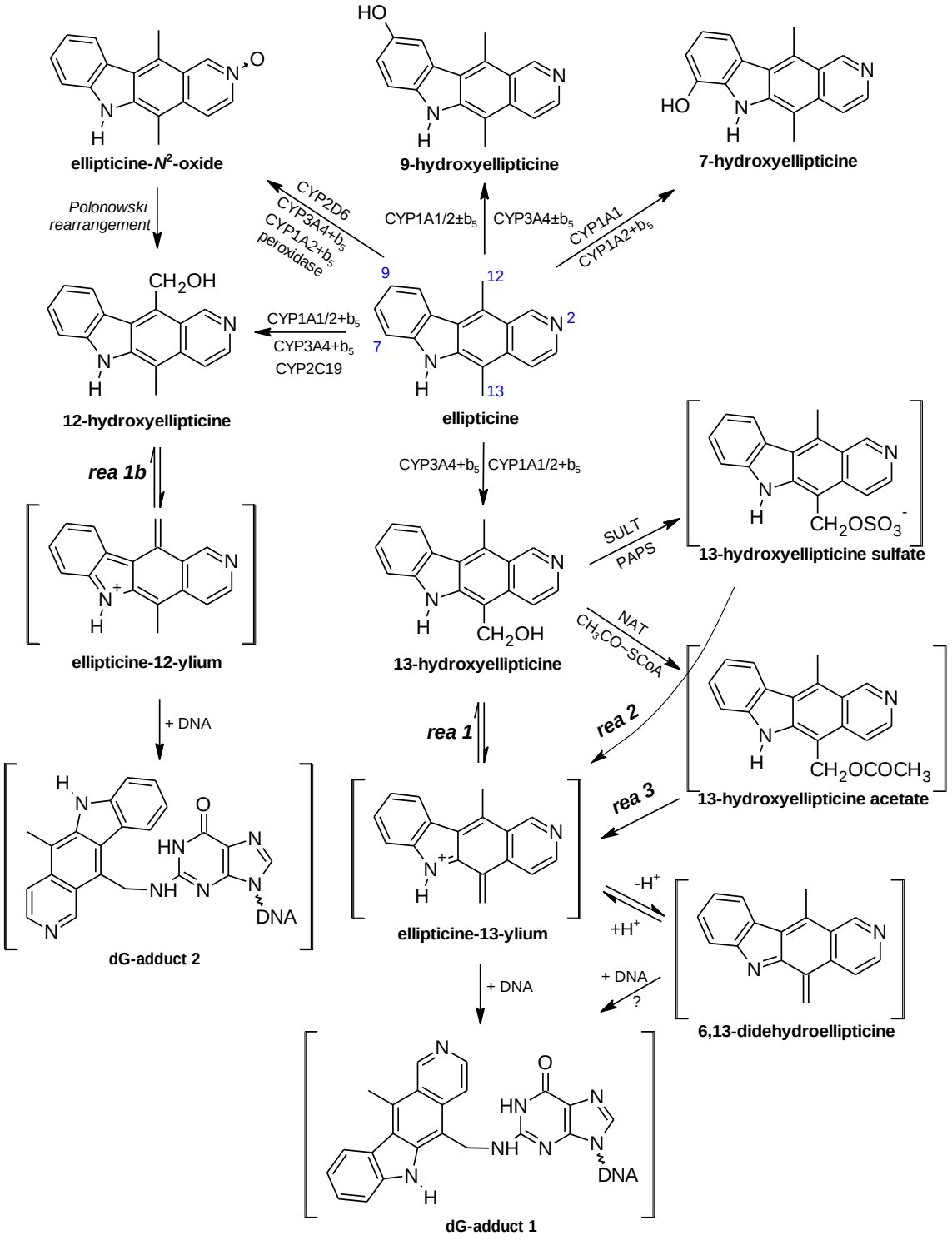


**Figure 1.** Scheme of ellipticine metabolism catalyzed by CYPs showing the identified metabolites and those proposed to form DNA adducts. The compounds showed in brackets were not detected under the experimental conditions and/or not yet structurally characterized. The CYP enzymes predominantly oxidizing ellipticine shown in the figure were identified in our previous studies [8,11,12]. Rea 1, 2 and 3 are reactions leading to ellipticine-13-ylium from 13-hydroxyellipticine, 13-hydroxyellipticine sulfate and 13-hydroxyellipticine acetate, respectively.

## 2. EXPERIMENTAL PART

### *2.1 Chemicals and material*

Ellipticine was from Sigma Chemical Co. (St. Louis, MO, USA). Enzymes and chemicals for the $^{32}$P-postlabeling assay were obtained from sources described [1]. All these and other chemicals used in the experiments were of analytical purity or better. 12-Hydroxy- and 13-hydroxyellipticine were isolated from multiple high performance liquid chromatography (HPLC) runs of ethyl acetate extracts of incubations containing ellipticine and human and/or rat hepatic microsomes as described [8].

### *2.2 Cell cultures*

Several cancer cell lines were utilized in studies investigating cytotoxicity of ellipticine [19-25]. Namely, the CCRF-CEM, a T lymphoblastoid cell line, was kindly provided by J.J. McGuire, Roswell Park Cancer Institute, (Buffalo, NY, USA) and HL-60 cells (a promyelotic line) were from the collection of cell lines of the Department of Pediatric Hematology and Oncology, 2nd Medical School, Charles University and University Hospital Motol (Prague, Czech Republic). HL-60 cells were cultivated in Iscove's modified Dulbecco's medium (IMDM, Biochrom AG, Berlin, Germany), high-glucose type, supplemented with 4 mM L-glutamine, 10% fetal calf serum (PAA Laboratories, Pasching, Austria), 100 units (U) per ml of penicillin and 100 μg/ ml streptomycin (PAA,Vienna, Austria) and 0.3% (*w*/*v*) $NaHCO_3$ at 37°C, 5% $CO_2$ and 95% atmospheric humidity. CCRF-CEM cells were cultivated in RPMI 1640 medium (Biochrom AG, Berlin, Germany) supplemented with 2 mM L-glutamine, 10% fetal calf serum (PAA Laboratories, Pasching, Austria) and 0.3% (*w*/*v*) $NaHCO_3$ at 37 °C, 5% $CO_2$ and 95% atmospheric humidity [20].

The MCF-7 cell line was from the collection of cell lines of the German Cancer Research Center Heidelberg, Germany). MCF-7 cells were cultivated in Dulbecco's modified Eagle's medium (DMEM, Biochrom AG, Berlin, Germany), high-glucose type (DMEM with 4.5 g D-glucose/l), supplemented with 4 mM L-glutamine, 25 mM HEPES Sigma, St. Louis, MO, U.S.A.), 5% fetal calf serum (Biochrom AG, Berlin, Germany) at 37 °C, 5% $CO_2$ and 95% atmospheric humidity [19].

The U87MG cell line was purchased from ATCC (Manassas, VA, USA). Cells were cultured in Eagle's MEM supplemented with 10% heat-inactivated fetal bovine serum (FBS), 0.6 mg/mL glutamine, 200 international unit (IU)/ml penicillin, 200 IU/ml streptomycin, and 0.1 mg/ml gentamicin (PAA Laboratories, Pasching, Austria) in humidified 5% $CO_2$ at 37 °C [23].

The UKF-NB-3 and UKF-NB-4 neuroblastoma cell lines, established from bone marrow metastases of high risk neuroblastoma, were a gift of Prof. J. Cinatl, Jr. (J. W. Goethe University, Frankfurt, Germany). The cell line UKF-NB-4 was established from chemoresistant recurrence. The cell lines used were derived from high risk neuroblastoma with MYCN amplification, del1p and aneuploidy. Cells were grown at 37°C and 5% $CO_2$ in Iscove's modified Dulbecco's medium (IMDM) (KlinLab Ltd, Prague, Czech Republic), supplemented with 10% fetal calf serum, 2 mM L-glutamine, 100 units/ml of penicilline and 100 μg/ml streptomycine (PAA Laboratories, Pasching, Austria) [22].

The human thyroid cancer cell lines BHT-101 and B-CPAP were purchased from the Leibniz Institute DSMZ German Collection of Microorganisms and Cell Cultures (Braunschweigh, Germany) and 8505-C cells from the European Collection of Cell Cultures (ECACC; Salisbury, UK). Cells were grown at 37 °C and 5 % $CO_2$ in Iscove's modified Dulbecco's medium (IMDM) (KlinLab Ltd, Prague, Czech Republic), supplemented with 10 % fetal calf serum, 2 mM L-glutamine, 100 units/ml of penicillin and 100 μg/ml streptomycine (PAA Laboratories, Pasching, Austria). All cells were grown at 37 °C in an atmosphere of ambient air with 5 % $CO_2$ (74% $N_2$, 20 % $O_2$) [25].

*2.3 MTT assay*

The cytotoxicity of ellipticine was determined by MTT test. For a dose-response curve, solution of ellipticine in dimethyl sulfoxide (DMSO, 1 mM) was dissolved in culture medium to final concentrations of 0 – 10 μM. MCF-7 cells were, in another experiment, also cultivated in the presence of 0.1 μM ellipticine for 72 h and these cells were thereafter treated with 0 – 10 μMellipticine. Cells in exponential growth were seeded at 1 x $10^4$ per well in a 96-well microplate. After incubation (48 hours) at 37 °C in 5% $CO_2$ saturated atmosphere the MTT solution (2 mg/ml PBS) was added, the microplates were incubated for 4 hours and cells lysed in 50% *N*,*N*-dimethylformamide containing 20% of sodium dodecyl sulfate (SDS), pH 4.5. The absorbance at 570 nm was measured for each well by multiwell ELISA reader Versamax (Molecular devices, CA, USA). The mean absorbance of medium controls was subtracted as a background. The viability of control cells was taken as 100% and the values of treated cells were calculated as a percentage of control. The $IC_{50}$ values were calculated from at least 3 independent experiments using linear regression of the dose-log response curves by SOFTmaxPro.

*2.4 Estimation of contents of enzymes biotransforming ellipticine in cancer cells*

To determine the expression of enzymes metabolizing ellipticine [*i.e.*, CYP1A1, 1B1, 2B, 2E1 and 3A4, cytochrome $b_5$, lactoperoxidase (LPO), thyroid peroxidase (TPO) and cyclooxygenase (COX)-1 and -2 proteins], cell pellets were resuspended in 25 mM Tris-HCl buffer pH 7.6 containing 150 mM NaCl, 1% detergent NP-40 (Sigma, St. Louis, MO, USA), 1% sodium deoxycholate, 0.1 % SDS and with solution of COMPLETE (protease inhibitor cocktail tablet, Roche, Basel, Switzerland) at concentration described by the provider. The samples were incubated for 60 min on ice and centrifuged for 20 min at 14 000 g and 4 °C. Supernatant was used for additional analysis. Protein concentrations were assessed using the DC protein assay (Bio-Rad, Hercules, CA, USA) with serum albumin as a standard and 10-75 μM of extracted proteins were subjected to sodium dodecyl sulfate-polyacrylamide gel electrophoresis (SDS-PAGE) on a 11% gel for analysis of CYP1A1, 1B1, 2B, 2E1 and 3A4, LPO, TPO and COX-1 and -2 protein expression, and a 17% gel for analysis of cytochrome $b_5$ protein expression [20-29]. After migration, proteins were transferred to a nitrocellulose membrane and incubated with 5% non-fat milk to block non-specific binding. The membranes were then exposed to specific rabbit polyclonal anti-cytochrome $b_5$ (1:750, Abcam, MA, USA), anti-CYP1A1 (1:1000,

Millipore, MA, USA), anti-CYP1B1 (1:500, Abcam, MA, USA), anti-CYP3A4 (1:5000, AbD Serotec, Oxford, UK), anti-COX-1 (1:1000, Abcam, MA, USA) antibodies, to the anti-CYP2B4-, CYP2E1-, anti-LPO- and anti-COX-2-chicken polyclonal antibodies prepared as described [30], and to specific mouse monoclonal anti-TPO (2.5 □g/ml, Abcam, MA, USA) antibody overnight at 4 $^{o}$C. Membranes were washed with distilled water and exposed to peroxidase-conjugated anti-IgG secondary antibodies (1:3000, Bio-Rad, Hercules, CA, USA), and the antigen-antibody complex was visualized by enhanced chemiluminiscence's detection system according to the manufacturer's instructions (Immun-Star HRP Substrate, Bio-Rad, Hercules, CA, USA) for thyroid cancer cells and by an alkaline phosphatase-conjugated rabbit anti-chicken IgG antibody and 5-bromo-4-chloro-3-indolylphosphate/nitrobluetetrazolium as dye for leukemia, glioblastoma, neuroblastoma and breast adenocarcinoma cells. Antibodies against glyceraldehyde-P-dehydrogenase (GAPDH) or actin (1:1000, Sigma, St. Louis, MO, USA) were used as loading controls [20-25].

### *2.5 Estimation of MPO content in HL-60 and CCRF-CEM cells*

MPO was detected by flow cytometry using anti-human MPO-FITC antibody (Immunotech, Marseille, France, cat. no. 1874) as shown in our previous work [20]. Cultivation was performed in 12-well plates, three samples from every well were prepared and two wells measured. Cells were permeabilized with Fix and Perm kit (Caltag Laboratories, Burlingame, CA, USA, cat. no. GAS-004), according to the recommendation of a producer. The fluorescence intensity of at least 10,000 cells was measured by FACSCalibur flow cytometer (Becton Dickinson Immunocytometry Systems, San Jose, CA, USA) equipped with 488 nm laser and list mode data were analyzed with the CellQuest software. Expression was evaluated as mean intensity of fluorescence. The fluorescence measurements were calibrated for each run by FITC-conjugated bead standards (DAKO cat. no. K0110). Results were expressed as mean of six determinations ± standard deviation [20].

### *2.6 Treatment of cancer cells with ellipticine for DNA adduct analyses*

Cell lines were seeded 24 h prior to treatment with ellipticine at a density of 1 x $10^5$ cells/ml in two 75 $cm^2$ culture flasks in a total volume of 20 ml of IMDM. Ellipticine was dissolved in 20 μM of DMSO, the final concentration was 0, 0.1, 1, 5 or 10 μM. After 24 h the cells were harvested after trypsinizing by centrifugation at 2000 x g for 3 min and two washing steps with 5 ml of PBS yielded a cell pellet, which was stored at -20 ºC until DNA isolation. DNA was isolated and labeled as described in the next section.

### *2.7 DNA isolation and $^{32}$P-postlabeling of DNA adducts*

DNA from cells was isolated by the phenol-chloroform extraction as described [19-25,31,32]. $^{32}$P-postlabeling analyses were performed using nuclease P1 enrichment as described previously [1].

Calf thymus DNA incubated with 13-hydroxy- and 12-hydroxyellipticine [8,9], and liver DNA of rats treated with ellipticine [3,13,15] were used to compare DNA adduct spot patterns.

### *2.8 Statistical analyses*

For statistical data analysis we used Student's *t*-test. All *P*-values are two-tailed and considered significant at the 0.05 level.

## 3. RESULTS

### *3.1 Expression of CYP and peroxidase enzymes in human cancer cells*

Using the method of Western blotting, the expression of several CYP enzymes and peroxidases were analyzed in cancer cell lines sensitive to ellipticine (HL-60 promyelocytic leukemia and T-cell leukemia CCRF-CEM cells, glioblastoma U87MG cells, neuroblastoma UKF-NB-3 and UKF-NB-4 cell lines, thyroid cancer BHT-101, B-CPAP and 8505-C cells and breast adenocarcinoma MCF-7 cells).

Employing antibodies against COX-1 and LPO, expression of these enzymes was proved in HL-60 promyelocytic leukemia and T-cell leukemia CCRF-CEM cells [20]. Beside these peroxidases, expression of MPO protein was also found in HL-60 cells, but was proved by flow cytometry using an anti-human MPO-FITC antibody (FACS) [20]. In contrast to these peroxidases, Western blots with polyclonal antibodies raised against COX-2 and various CYPs (CYP1A1, 2B4, 2E1 and 3A4) showed that CYP1A1 only is expressed in HL-60 cells. In the case of a human CCRF-CEM cell line, no detectable expression of MPO was determined by FACS analysis. Western blot analyses of other peroxidases (COX-1 and -2) and of CYPs (CYP1A1, 2B4, 2E1 and 3A4) enzymes in CCRF-CEM cells revealed that COX-1 and low but detectable levels of CYP1A1 are expressed in these cells [20].

Using Western blot analysis with polyclonal antibodies raised against CYP1A1, 1B1 and 3A4, the protein expression of these enzymes was detected also in another cancer cell line sensitive to ellipticine, a U87MG glioblastoma cell line. Beside these CYP enzymes, peroxidases such as LPO and COX-1 were also found to be expressed in U87MG cells [23].

Because the expression of several CYP enzymes is known to be induced by ellipticine [22-25, 28,29], the question whether ellipticine might be capable of inducing CYP enzymes expressed in U87MG cells was investigated [23]. The Western blots with antibodies against CYP1A1, 1B1 and 3A4 showed that the expression of CYP1B1 and 3A4 was induced in U87MG cells treated with ellipticine . The expression of CYP1A1 was also increased, but to a lower extent. In contrast to induction of CYP enzymes by ellipticine, the protein expression levels of both peroxidases tested in this study, COX-1 and LPO, were not affected by ellipticine in U87MG cells [23].

In UKF-NB-3 and UKF-NB-4 cells, CYP1A1, 1B1 and 3A4 as well as peroxidases LPO and COX-1 were detectable by Western blotting [22]. In addition, low expression levels of cytochrome $b_5$, the protein playing an important role in CYP1A- and CYP3A4-mediated ellipticine metabolism

[11,12,32], were detected in both neuroblastoma cell lines [22]. In addition to analysis of the basal levels of these enzymes, the effect of ellipticine on expression of these proteins was also investigated. Similar to U87MG glioblastoma cells, ellipticine acts as an inducer of CYP1A1 and 3A4 in neuroblastoma cells, but expression of CYP1B1 as well as COX-1 and LPO were attenuated by treatment of these cells with ellipticine [22]. In the case of cytocrome $b_5$, its expression was induced by treatment of UKF-NB-3 cells with ellipticine, but not in UKF-NB-4 cells [22].

In thyroid cancer BHT-101, B-CPAP and 8505-C cells, expression patterns of CYP1A1, 1B1, 3A4, cytochrome $b_5$, COX-1 and peroxidase specifically expressed in thyroid cancer cells, thyroid peroxidase (TPO), were found to be quite complex [25]. The levels of CYP1A1 were high in all thyroid cancer cells and induced in B-CPAP and 8505-C cells by their treatment with ellipticine. In contrast, expression of TPO was so low that the influence of cell lineage or ellipticine exposure cannot be assessed. Expression levels of CYP1B1, COX-1 and cytochrome $b_5$ were different in the three thyroid cancer cell lines and attenuated by their exposure to ellipticine. Most conspicuous was the near complete absence of cytochrome $b_5$ in 8505-C cells and the highest induction of CYP3A4 by ellipticine in B-CPAP cells [25].

In human breast adenocarcinoma MCF-7 cells, only the expression of CYP1A1, 1B1 and 3A4 enzymes was analyzed in this work, whereas peroxidase expression was not tested. The expression of CYP1A1, 1B1 and 3A4 was proved by Western blot analysis (see Fig. 2 for expression of CYP1B1). Whereas no effect of pre-treatment of MCF-7 cells with ellipticine was found for CYP1A1 and 3A4 [data not shown], an increase in CYP1B1 expression was induced by this process. Moreover, levels of this enzyme increased by pre-treatment of MCF-7 cells with a low concentration of ellipticine (0.1 μM) prior to their exposure to 2.5 and 5 μM ellipticine. In addition, a longer period of cell exposition to ellipticine produced higher expression of CYP1B1 (Fig. 2).

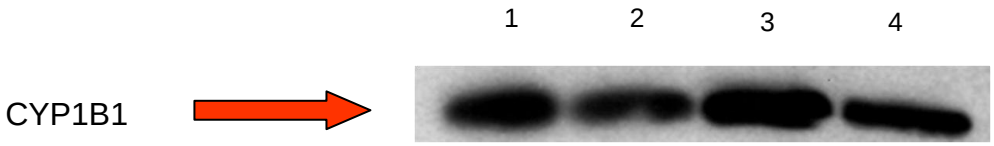


**Figure 2.** Expression of CYP1B1 in MCF-7 cells. Lane 1, cells pre-treated with 0.1 μM ellipticine for 72 h and then exposed to 2.5 μM ellipticine for 24 h, lane 2, cells exposed to 2.5 μM ellipticine only for 24 h, lane 3, cells pre-treated with 0.1 μM ellipticine for 72 h and then exposed to 5 μM ellipticine for 48 h, lane 4, cells exposed to 5 μM ellipticine only for 48 h.

### *3.2 Ellipticine-DNA adduct formation in cancer cells*

Treatment of tumor cells, in which CYP and/or peroxidase enzymes are expressed, with ellipticine resulted in the formation of the same ellipticine-derived DNA adducts that were formed by enzymatic activation of ellipticine *in vitro* and *in vivo* (see Figure 3 for adducts formed by ellipticine in MCF-7 cells, in rats *in vivo* and in DNA treated with 13-hydroxy- and 12-hydroxyellipticine) [3,4,8,9]. Two major ellipticine-DNA adducts (spots 1 and 2 in Figure 3) that are generated by 13-hydroxy- and

12-hydroxyellipticine (Figs. 3D and 3E), were formed in all tested cells [HL-60 promyelocytic leukemia and T-cell leukemia CCRF-CEM cells, glioblastoma U87MG cells, BHT-101, B-CPAP and 8505-C thyroid cancer cells, neuroblastoma UKF-NB-3 and UKF-NB-4 cell lines (data shown in [20-23,25]) and breast adenocarcinoma MCF-7 cells (Figs. 3A and 3B)] exposed to ellipticine. Moreover, two additional minor adducts (adducts spots 6 and 7 in Figure 3), but the structure of them is not known, are generated in several of tested cancer cells (Table 1). Levels of ellipticine-DNA adducts found in this work and the former studies [20-23,25] are shown in Table 1.

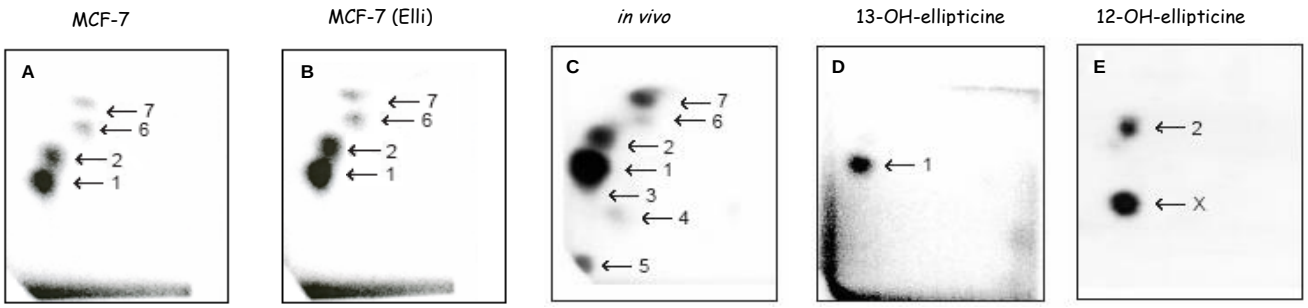


**Figure 3.** Autoradiographs of PEI-cellulose TLC maps of $^{32}$P-labeled digests of DNA isolated from MCF-7 (A), and from MCF-7 (Elli), the cells pre-treated with 0.1 μM ellipticine for 72 h (B), exposed to 5 μM ellipticine for 24 h, of liver DNA of rats treated with 40 mg ellipticine/kg body weight (C), from calf thymus DNA reacted with 13-hydroxyellipticine (D) and 12-hydroxyellipticine (E). Adduct spots 1-7 correspond to the ellipticine-derived DNA adducts. Besides adduct 2 formed by 12-hydroxyellipticine, another strong adduct (spot X in panel E), which was not found in any other activation systems or *in vivo* was generated. Analyses were performed by the nuclease P1 version of the $^{32}$P-postlabeling assay.

### *3.3. Cytotoxicity of ellipticine to human cancer cells*

As shown in our previous studies [20-23,25], the cytotoxicity of ellipticine to tested cancer cell lines, which were treated with the increasing concentrations of ellipticine, were measured with MTT assay. Ellipticine inhibited the growth of all cell lines tested in this and our former studies in a dose-dependent manner [20-23,25]. The $IC_{50}$ values for ellipticine calculated from the dose-log response curves are shown in Table 1. Neuroblastoma UKF-NB-4 and UKF-NB-3 and leukemia HL-60 cells were the most sensitive cells to ellipticine having the $IC_{50}$ values lower than 1 μM (see $IC_{50}$ values shown in Table 1). When we compared the sensitivity of additional cells to ellipticine, similar cytotoxicity of this agent was found to human breast adenocarcinoma MCF-7 cells and a glioblastoma U87MG cell line (the $IC_{50}$ values were app. 1 μM), whereas leukemia CCRF-CEM, and thyroid cancer BHT-101, 8505-C and B-CPAP cells were less sensitive. The $IC_{50}$ values for ellipticine in cancer cells (BHT-101 thyroid cancer cells and leukemia CCRF-CEM cells), which were less sensitive to ellipticine , were 10-times higher than in the most sensitive cells as neuroblastoma UFK-NB-3 and UKF-NB-4 cells (Table 1).

### *3.4. Induction of CYP1B1 increases ellipticine-DNA adduct formation and cytotoxicity of ellipticine in human breast adenocarcinoma MCF-7 cells*

In the present study, the induction of CYP1B1 in human breast adenocarcinoma MCF-7 cells mediated by their pre-treatment with ellipticine was investigated. Pretreatment of these cells with 0.1 μM ellipticine for 72 h resulted in an increase in formation of ellipticine-derived DNA adducts in these cells exposed thereafter to 2.5 and 5 μM ellipticine for 24 h (Table 2).

**Table 1.** DNA adduct formation by ellipticine and cytotoxicity of this agent in human cancer cell lines

| Cells | Levels of DNA adducts (RAL x $10^{-7}$)[a] | | | | | $IC_{50}$ (μM) |
|---|---|---|---|---|---|---|
| | Adduct 1 | Adduct 2 | Adduct 6 | Adduct 7 | Total | |
| HL-60 | 46.32 ± 4.30 | 21.18 ± 2.30 | n.d. | n.d. | 67.50 ± 6.23 | 0.64 ± 0.06 |
| CCRF-CEM | 9.40 ± 0.95 | 8.40 ± 0.79 | n.d | n.d | 17.80 ± 1.62 | 4.70 ± 0.48 |
| U87MG | 1.98 ± 0.15 | 3.42 ± 0.33 | n.d. | n.d. | 5.40 ± 0.53 | 1.48 ± 0.62 |
| UKF-NB-3 | 3.27 ± 0.32 | 5.01 ± 0.50 | n.d. | n.d. | 8.28 ± 0.80 | 0.44 ± 0.03 |
| UKF-NB-4 | 5.40 ± 0.56 | 6.50 ± 0.81 | 0.27 ± 0.03 | 0.37 ± 0.05 | 12.54 ± 1.51 | 0.49 ± 0.04 |
| BHT-101 | 3.90 ± 0.28 | 3.00 ± 0.50 | 0.10 ± 0.01 | 0.04 ± 0.01 | 7.04 ± 0.86 | 4.80 ± 2.50 |
| B-CPAP | 3.33 ± 0.31 | 4.18 ± 0.42 | 0.09 ± 0.01 | 0.03 ± 0.01 | 7.63 ± 0.76 | 2.80 ± 1.00 |
| 8505-C | 2.22 ± 0.56 | 1.81 ± 0.28 | 0.05 ± 0.01 | 0.01 ± 0.01 | 4.09 ± 0.45 | 3.60 ± 1.20 |
| MCF-7 | 3.72 ± 0.40 | 4.77 ± 0.50 | 0.81 ± 0.07 | n.d. | 9.30 ± 0.92 | 1.25 ± 0.13 |

Cancer cells were exposed to 10 μM ellipticine for 48 h. DNA adducts were analyzed by the nuclease P1 version of the $^{32}$P-postlabeling assay. [a]RAL, relative adduct labeling; averages and S.D. of three experiments. n.d. - not detected (the detection limit of RAL was $1/10^{10}$ nucleotides). $IC_{50}$ values were calculated from the linear regression of the dose-log response curves. Values are mean ± S.D. of at least 3 experiments. Data are taken from [19-23,25].

**Table 2.** DNA adduct formation by ellipticine and cytotoxicity of this agent in human MCF-7 cells

| Cells | Levels of DNA adducts (RAL x $10^{-7}$)[a] | | | | | $IC_{50}$ (μM) |
|---|---|---|---|---|---|---|
| | Adduct 1 | Adduct 2 | Adduct 6 | Adduct 7 | Total | |
| MCF-7 | | | | | | |
| + 2.5 μM ellipticine | 2.12 ± 0.21 | 1.38 ± 0.14 | 0.38 ± 0.04 | 0.23 ± 0.02 | 4.11 ± 0.41 | 1.25 ± 0.13 |
| + 5 μM ellipticine | 3.45 ± 0.35 | 1.59 ± 0.16 | 0.56 ± 0.06. | 0.45 ± 0.05 | 6.05 ± 0.61 | |
| MCF -7 (Elli) | | | | | | |
| + 2.5 μM ellipticine | 2.95 ± 0.30 | 1.43 ± 0.14 | 0.43 ± 0.04 | 0.23 ± 0.02 | 5.04 ± 0.50** | 0.70 ± 0.07*** |
| + 5 μM ellipticine | 6.37 ± 0.64 | 2.55 ± 0.26 | 0.76 ± 0.08 | 0.64 ± 0.06 | 10.30 ± 1.10*** | |

MCF-7 cells and MCF-7 (Elli) , the cells pre-treated with 0.1 μM ellipticine for 72 h, were exposed to 2.5 or 5 μM ellipticine for 24 h. DNA adducts were analyzed by the nuclease P1 version of the $^{32}$P-postlabeling assay. [a]RAL, relative adduct labeling; averages and S.D. of three experiments. n.d. - not detected (the detection limit of RAL was $1/10^{10}$ nucleotides). $IC_{50}$ values were calculated from the linear regression of the dose-log response curves. Values are mean ± S.D. of at least 3 experiments. Comparison was performed by *t*-test analysis; $^{**}P < 0.01$, $^{***}P < 0.001$, different from cells that were not pretreated with ellipticine.

In addition, the $IC_{50}$ values for ellipticine in MCF-7 cells indicate that their pretreatment with 0.1 μM ellipticine led to an increase in toxicity of ellipticine to these cells. The $IC_{50}$ value of ellipticine for the control (untreated) and the pretreated cells are 1.25 and 0.7 μM, respectively (Table 2). These results indicate that expression levels of this enzyme are responsible for the increase in formation of DNA adducts by ellipticine and cytotoxicity caused by this drug in these cells. Because no effect of pre-treatment of MCF-7 cells with ellipticine was found for CYP1A1 and 3A4, the CYP1B1 enzyme seems to play a crucial role determining formation of DNA adducts and cytotoxicity of ellipticine in these cells.

## 4. DISCUSSION

In this study, comparison of cytotoxicity of ellipticine and its relation to expression of the key enzymes catalyzing activation of ellipticine to metabolites forming covalent DNA adducts found in several human cancer cell lines (leukemia, glioblastoma, neuroblastoma, breast adenocarcinoma and thyroid cancer cells) in this and in the previous studies [19-23,25] was carried out. This study also presents the results showing the effects of induction of some of the enzymes metabolizing ellipticine on DNA adduct formation by ellipticine and its cytotoxicity. All these results helped us to shed more light on the mechanism of ellipticine toxic action to these cells.

The mode of antitumor, cytotoxic, mutagenic and genotoxic action of ellipticine is considered to be predominantly based on DNA damage such as intercalation into DNA, inhibition of topoisomerase II, and formation of covalent DNA adducts mediated by CYPs and peroxidases [1-6,13]. The intercalation of ellipticine into DNA and inhibition of topoisomerase II occur in all cell types irrespective of their metabolic capacity because of the general chemical properties of this drug and its affinity to DNA and topoisomerase II protein [5,6]. Hence, ellipticine should affect various cancer cells in a similar way. This is, however, not the case of cancer cells tested in this comparative study. As shown in Table 1 and Figure 4, cytotoxicity of ellipticine (expressed as the $IC_{50}$ values) differs in individual cells and corresponds to levels of ellipticine-derived DNA adducts in most cells. Generally, higher ellipticine-DNA adduct formation resulted in higher cytotoxicity of this drug to most of the tested cancer cells. This finding indicates that covalent modification of DNA by ellipticine plays an important role in toxicity of ellipticine to these cells.

As shown in this work, the toxic effects of ellipticine based on formation of covalent ellipticine-DNA adducts on several cancer cells are dependent on expression of CYP1A1, 1B1, 3A4 and peroxidases COX-1 and MPO in these cells. This is clearly seen in two leukemia cells tested, HL-60 and CCRF-CEM cells; high expression of one of the enzyme activating ellipticine, MPO, in HL-60 cells and the absence of this peroxidase in a CCRF-CEM cell line [20], resulted in quite different levels of ellipticine-derived DNA adducts and subsequently in ellipticine cytotoxicity in these cells. In addition, not only the basal levels of enzymes metabolizing ellipticine, but the induction effect of ellipticine on expression of several enzymes catalyzing its metabolism might be another factor determining DNA adduct formation by ellipticine and its cytotoxicity in several of the tested cancer cells. Indeed, in human UKF-NB-3 and UKF-NB-4 neuroblastoma cells [21,22], glioblastoma U87MG

[23] cells and adenocarcinoma MCF-7 cells (this work) that are very sensitive to ellipticine, CYP1A1, 3A4 and/or CYP1B1 were, depending on individual cells, induced by ellipticine. The CYP1A1 enzyme was also partially induced in B-CPAP and 8505-C thyroid cancer cell lines and CYP3A4 in BHT-101 and B-CPAP cells [25]. In contrast, exposure of cancer cells to ellipticine had either no (U87MG cells) or inhibition effects (UKF-NB-3, UKF-NB-4, and thyroid cancer cell lines) on expression of peroxidases COX-1 and/or LPO [23,25].

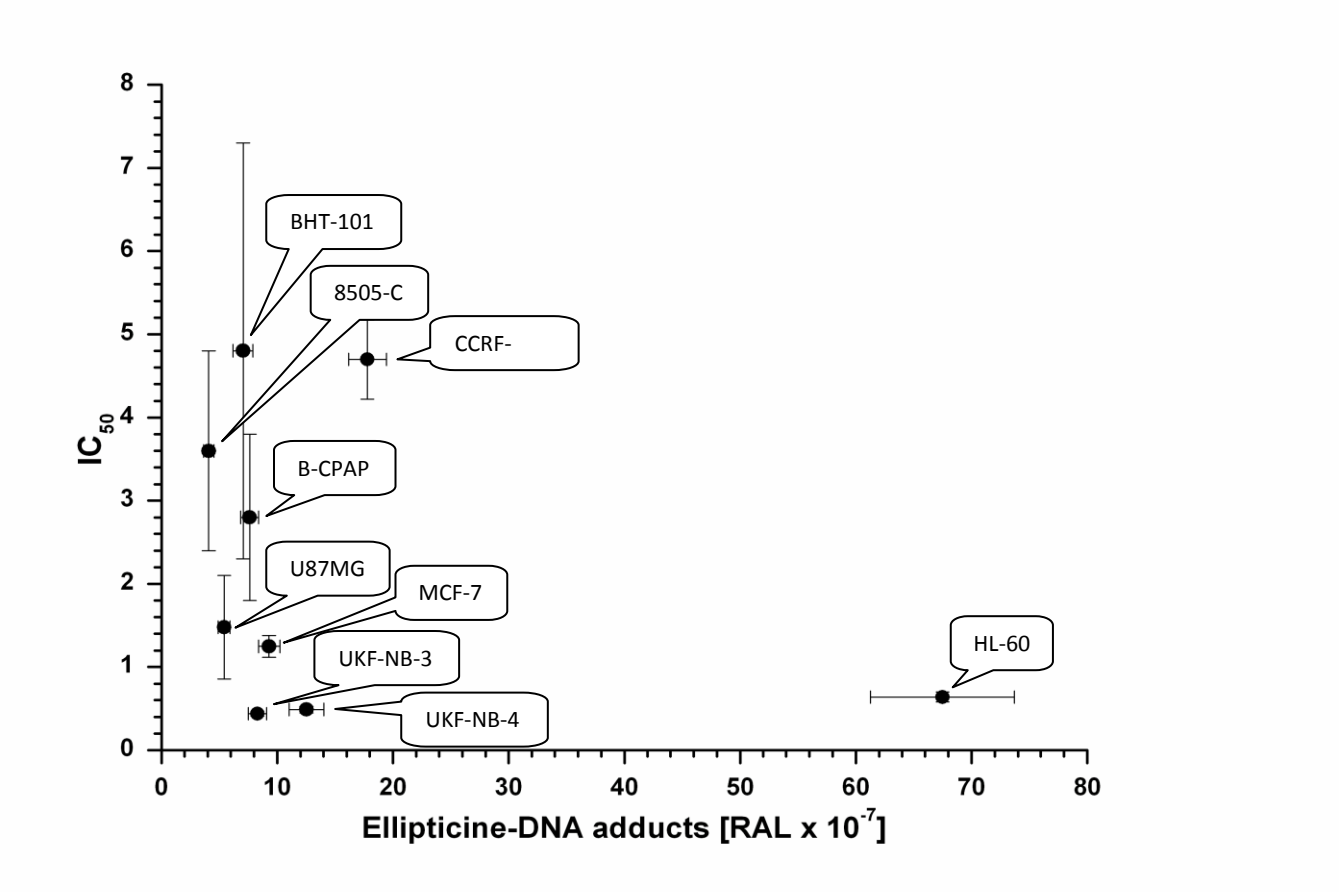


**Figure 4.** Relationship between the levels of ellipticine-derived DNA adducts and the $IC_{50}$ values for ellipticine in cancer cell lines.

The important effect of induction of enzymes metabolizing ellipticine by this drug on ellipticine cytotoxicity was unambiguously proved in this study, in MCF-7 cells, in which the CYP1B1 was induced by their pre-treatment with low concentrations of ellipticine (0.1 μM). Cytotoxicity of ellipticine in MCF-7, in which CYP1B1 expression was induced, was increased and correlated with higher levels of elllipticine-DNA adducts. Thus, these results indicate that the induction potency of ellipticine exerts concerted regulatory control of this drug on its own metabolic fate and pharmacological efficiency.

The results showed in the present comparative study suggest that ellipticine toxicity to most of the cancer cells tested in this work is dictated by formation of covalent ellipticine-DNA adducts mediated by enzymes catalyzing ellipticine activation in these cells. Nevertheless, this feature is not

absolute. This is, for example, not the case of the UKF-NB-3 cell line; lower levels of DNA adducts were found in these cells than in UKF-NB-4 cells, even though both neuroblastoma cells exhibit similar sensitivity to ellipticine. One of the reasons for this phenomenon might be different genetic programs of both neuroblastoma cells [33,34]. The UKF-NB-4 line was, namely, established from a recurrent disease. In addition, the mechanisms such as intercalation into DNA, inhibition of DNA topoisomerase II activity (for a review see [3-6,13]) or DNA damage caused by reactive oxygen species (ROS) generated during ellipticine oxidation [35,36], might also contribute to ellipticine cytotoxicity in UKF-NB-3 cells. Indeed, recently using two electrochemical methods, square wave voltametry [37,38] and capillary electrophoresis with laser-induced fluorescence [39], ellipticine as an DNA intercalator was found that might, to some extent, also participate in cytotoxicity of this drug in neuroblastoma UKF-NB-3 cells. Nevertheless, an actual contribution of DNA-damaging effects different from the covalent DNA modification by ellipticine, to ellipticine toxicity to cancer cells awaits further investigation.

## 5. CONCLUSIONS

The results of the present comparative study indicate that levels of protein expression of CYP1A1, 1B1, 3A4, lactoperoxidase, thyroid peroxidase and cyclooxygenase-1 enzymes that catalyze ellipticine metabolism in several cancer cells influence formation of covalent ellipticine-derived DNA adducts and sensitivity of these cells to ellipticine. The results found also demonstrate a potency of ellipticine to induce the enzymes dictating ellipticine activation to metabolites forming DNA adducts and this induction can lead to an increase in cytotoxicity of ellipticine in most studied cancer cells.

ACKNOWLEDGEMENTS
Financial support from GACR (grant P301/10/0356) and Charles University in Prague (UNCE 204025/2012) is highly acknowledged.

## References

1. M. Stiborova, C.A. Bieler, M. Wiessler and E. Frei, *Biochem. Pharmacol.*, 62 (2001) 1675.
2. M. Stiborova, M. Rupertova, H. H. Schmeiser and E. Frei, *Biomed. Pap. Med. Fac. Univ. Palacky Olomouc Czech Repub.*, 150 (2006) 13.
3. M. Stiborova, M. Rupertova and E. Frei, *Biochim. Biophys. Acta*, 1814 (2011) 175.
4. R. Kizek, V. Adam, J. Hrabeta, T. Eckschlager, S. Smutny, J. V. Burda, E. Frei and M. Stiborova, *Pharmacol. Ther.*, 133 (2012) 26.
5. C. Auclair, *Arch. Biochem. Biophys.*, 259 (1987) 1.
6. N. C. Garbett and D. E. Graves, *Curr. Med. Chem. Anti-Cancer Agents*, 4 (2004) 149.
7. K. Tmejova, L. Krejcova, D. Hynek, V. Adam, P. Babula, L. Trnkova, M. Stiborova, T. Eckschlager and R. Kizek, *Anti-Cancer Age. Med.*, 14 (2014), 331.
8. M. Stiborova, J. Sejbal, L. Borek-Dohalska, D. Aimova, J. Poljakova, K. Forsterova, M. Rupertova, J. Wiesner, J. Hudecek, M. Wiessler and E. Frei, *Cancer Res.*, 64 (2004) 8374.
9. M. Stiborova, J. Poljakova, H. Ryslava, M. Dracinsky, T. Eckschlager and E. Frei, *Int. J. Cancer*, 120 (2007) 243.

10. M. Stiborova, M. Rupertova, D. Aimova, H. Ryslava and E. Frei, *Toxicology*, 236 (2007) 50.
11. M. Stiborova, R. Indra, M. Moserova, V. Cerna, M. Rupertova, V. Martinek, T. Eckschlager, R. Kizek and E. Frei, *Chem. Res. Toxicol.*, 25 (2012) 1075.
12. V. Kotrbova, B. Mrazova, M. Moserova, V. Martinek, P. Hodek, J. Hudecek, E. Frei and M. Stiborova, *Biochem. Pharmacol.*, 82 (2011) 669.
13. M. Stiborova and E. Frei, *Current Med. Chem.*, 21 (2014) 575.
14. M. Moserova, V. Kotrbova, M. Rupertova, K. Naiman, J. Hudecek, P. Hodek, E. Frei and M Stiborova, *Neuro Endocrinol. Lett.*, 29 (2008) 728.
15. M. Stiborova, A. Breuer, D. Aimova, M. Stiborova-Rupertova, M. Wiessler and E. Frei, *Int J Cancer* 107 (2003) 885.
16. M. Stiborova, M. Rupertova, D. Aimova, H. Ryslava and E. Frei, *Toxicology*, 236 (2007) 50.
17. M. Stiborova, V.M. Arlt, C.J. Henderson, C.R. Wolf, V. Kotrbova, M. Moserova, J. Hudecek, D.H. Philips and E. Frei, *Toxicol. Appl. Pharmacol.*, 226 (2008) 318.
18. M. Stiborova, M. Moserova, B. Mrazova, V. Kotrbova and E. Frei, *Neuro Endocrinol. Lett.*, 31 (Suppl. 2) (2010) 26.
19. L. Borek-Dohalska, E. Frei and M. Stiborová, *Collect. Czech. Chem. Commun.*, 69 (2004) 603.
20. J. Poljakova, E. Frei, J.E. Gomez, D. Aimova, T. Eckschlager, J. Hrabeta and M. Stiborova, *Cancer Lett.*, 252 (2007) 270.
21. J. Poljakova, T. Eckschlager, J. Hrabeta, J. Hrebackova, S. Smutny, E. Frei E, V. Martínek, R. Kizek and M.Stiborová, *Biochem Pharmacol.*, **77** (2009) 1466.
22. J. Poljakova, J. Hrebackova, M. Dvorakova, M. Moserova, T. Eckschlager, J. Hrabeta, M. Göttlicherova, B. Kopejtkova, E. Frei, R. Kizek and M. Stiborova, *Neuro Endocrinol. Lett.*, 32, Suppl. 1 (2011) 101.
23. E. Martinkova, M. Dontenwill, E. Frei and M. Stiborova, *Neuro Endocrinol. Lett.*, 30, Suppl. 1 (2009) 60.
24. L. Bořek-Dohalská., J. Poljaková, M. Rupertová, E. Frei and M. Stiborová, *Interdisc. Toxicol.*, 2 (2009), 94.
25. J. Poljakova, T. Eckschlager, R. Kizek, E. Frei and M. Stiborová, *Int. J. Electrochem. Sci.*, 8 (2013) 1573.
26. M. Stiborova, V. Martinek, H. Rydlova, P. Hodek and E. Frei, *Cancer Res.*, 62 (2002) 5678.
27. M. Stiborova, V. Martinek, H. Rydlova, T. Koblas and P. Hodek, *Cancer Lett*. 220 (2005) 145.
28. D. Aimova, L. Svobodova, V. Kotrbova, B. Mrazova, P. Hodek, J. Hudecek, R. Vaclavikova, E. Frei and M. Stiborova, *Drug Metab. Dispos.* 35 (2007) 1926.
29. I. Vranová, M. Moserová, P. Hodek, R. Kizek, E. Frei and M Stiborová, *Int. J. Electrochem. Sci.*, 8 (2013) 1586.
30. P. Hodek, P. Trefil, J. Šimůnek, J. Hudeček and M Stiborova, *Int. J. Electrochem. Sci.*, 8 (2013) 113.
31. E. Frei, C.A. Bieler, V.M. Arlt, M. Wiessler and M Stiborová, *Biochem. Pharmacol.*, 64 (2002) 289.
32. M. Stiborová, J. Poljakova, E. Martínková, J. Ulrichová, V. Šimánek, Z. Dvořák and E. Frei, *Toxicology*, 302 (2012), 233.
33. J. Cinatl Jr, J. Cinatl, R. Kotchetkov, J.U. Vogel, B.G. Woodcock,, J. Matousek J, P. Pouckova and B. Kornhuber, *Int. J. Oncol* ., 15 (1999) 1001.
34. J. Bedrnicek, A. Vicha, M. Jarosova, M. Holzerova, J. Cinatl Jr, M. Michaelis, J. Cinatl and T. Ecschlager, *Neoplasma* 52: (2005) 415.
35. J.Y. Kim, S.G. Lee, J.Y. Chung, Y.J. Kim, J.E. Park, H. Koh, M.S. Han, Y.C. Park, Y.H. Yoo and J.M. Kim, *Toxicology,* 289 (2011) 91.
36. M. Pohanka. J. Sochor, B. Ruttkay-Nedecký, N. Cerii, V. Adam, J. Hubálek, M. Stiborová, T. Eckschlager and R. Kízek, *J. Appl. Biomed.*, 10 (2012) 155.

37. D. Huska, V. Adam,, S. Krizkova, J. Hrabeta, T. Eckschlager, M. Stiborova and R. Kizek, *Chim. Oggi-Chem. Today*, 28 (5, Suppl. S) (2010) 15.
38. D. Huska, V. Adam, J. Hubalek, L. Trnkova,, T. Eckschlager, M. Stiborova, I. Provaznik and R. Kizek, *Chim. Oggi-Chem. Today*, 28 (5, Suppl. S) (2010) 18.
39. M. Ryvolova, J. Chomoucka, J. Drbohlavova, P. Kopel, P. Babula, H. Hynek, V. Adam, T. Eckschlager, J. Hubalek, M. Stiborova, J. Kaiser and R. Kizek, *Sensors*, 12 (2012) 14792.

# *Příloha 3*

Marie Stiborová, Věra Černá, Michaela Moserová, **Iveta Mrízová**, Volker M. Arlt, Eva Frei

**THE ANTICANCER DRUG ELLIPTICINE ACTIVATED WITH CYTOCHROME P450 MEDIATES DNA DAMAGE DERMINING ITS PHARMACOLOGICAL EFFICIENCIES: STUDIES WITH RATS, HEPATIC CYTOCHROME P450 REDUCTASE NULL (HRN$^{TM}$) MICE AND PURE ENZYMES**

*Int. J. Mol. Sci.* 16, 284-306, 2015

$IF_{2014}$ = 2.862

*Int. J. Mol. Sci.* **2015**, *16*, 284-306; doi:10.3390/ijms16010284

OPEN ACCESS
International Journal of
**Molecular Sciences**
**ISSN 1422-0067**
www.mdpi.com/journal/ijms

*Review*

# The Anticancer Drug Ellipticine Activated with Cytochrome P450 Mediates DNA Damage Determining Its Pharmacological Efficiencies: Studies with Rats, Hepatic Cytochrome P450 Reductase Null (HRN™) Mice and Pure Enzymes

**Marie Stiborová [1,*], Věra Černá [1], Michaela Moserová [1], Iveta Mrízová [1], Volker M. Arlt [2] and Eva Frei [3]**

[1] Department of Biochemistry, Faculty of Science, Charles University, Hlavova 2030, CZ-12843 Prague 2, Czech Republic; E-Mails: vera.cerna@natur.cuni.cz (V.Č.); michaela.moserova@natur.cuni.cz (M.M.); iveta.vranova@natur.cuni.cz (I.M.)

[2] Analytical and Environmental Sciences Division, MRC-PHE Centre for Environmental & Health, King's College London, 150 Stamford Street, London SE1 9NH, UK; E-Mail: volker.arlt@kcl.ac.uk

[3] Division of Preventive Oncology, National Center for Tumor Diseases, German Cancer Research Center (DKFZ), Im Neuenheimer Feld 280, 69120 Heidelberg, Germany, E-Mail: eva.frei@t-on line.de

* Author to whom correspondence should be addressed; E-Mail: stiborov@natur.cuni.cz; Tel.: +420-221-951-285; Fax: +420-221-951-283.

Academic Editor: Guillermo T. Sáez

*Received: 19 October 2014 / Accepted: 17 December 2014 / Published: 25 December 2014*

---

**Abstract:** Ellipticine is a DNA-damaging agent acting as a prodrug whose pharmacological efficiencies and genotoxic side effects are dictated by activation with cytochrome P450 (CYP). Over the last decade we have gained extensive experience in using pure enzymes and various animal models that helped to identify CYPs metabolizing ellipticine. In this review we focus on comparison between the *in vitro* and *in vivo* studies and show a necessity of both approaches to obtain valid information on CYP enzymes contributing to ellipticine metabolism. Discrepancies were found between the CYP enzymes activating ellipticine to 13-hydroxy- and 12-hydroxyellipticine generating covalent DNA adducts and those detoxifying this drug to 9-hydroxy- and 7-hydroellipticine *in vitro* and *in vivo*. *In vivo*, formation of ellipticine-DNA adducts is dependent not only on expression levels of CYP3A, catalyzing ellipticine activation *in vitro*, but also on those of CYP1A that oxidize ellipticine *in vitro* mainly to the detoxification products. The finding showing that cytochrome $b_5$ alters the ratio of ellipticine metabolites generated by

CYP1A1/2 and 3A4 explained this paradox. Whereas the detoxification of ellipticine by CYP1A and 3A is either decreased or not changed by cytochrome $b_5$, activation leading to ellipticine-DNA adducts increased considerably. We show that (I) the pharmacological effects of ellipticine mediated by covalent ellipticine-derived DNA adducts are dictated by expression levels of CYP1A, 3A and cytochrome $b_5$, and its own potency to induce these enzymes in tumor tissues, (II) animal models, where levels of CYPs are either knocked out or induced are appropriate to identify CYPs metabolizing ellipticine *in vivo*, and (III) extrapolation from *in vitro* data to the situation *in vivo* is not always possible, confirming the need for these animal models.

**Keywords:** anticancer drug ellipticine; cytochrome P450 mediated DNA-damage; covalent DNA adducts; enzymes metabolizing ellipticine *in vitro* and *in vivo*

## 1. Introduction

A plant alkaloid ellipticine (5,11-dimethyl-6H-pyrido[4,3-b]carbazole, Figure 1) found in several Apocynaceae plants and its derivatives are efficient anticancer compounds that function through multiple mechanisms participating in cell cycle arrest and the initiation of apoptosis (for a summary see: [1–6]). Ellipticine was found (I) to arrest cell cycle progression due to modulation of levels of cyclinB1 and Cdc2, and phosphorylation of Cdc2 in human mammary adenocarcinoma MCF-7 cells [7]; (II) to initiate apoptosis by several mechanisms such as formation of reactive oxygen species (ROS) inducing DNA damage, the activation of mitogen-activated protein kinases (MAPKs), release of cytochrome *c* and apoptosis-inducing factor (AIF) from the mitochondrial membrane, caspase activation as well as a caspase-independent pathway [8,9], triggering of Fas/Fas ligand pathway and modulation of proteins of the Bcl-2 family in several tumor cell lines [10]; (III) to disrupt mitochondrial function and (IV) to cause the apoptotic signaling that is amplified by cross-talk between the Fas death receptor and the mitochondrial apoptotic pathway (for a summary see: [3,4,7–10]).

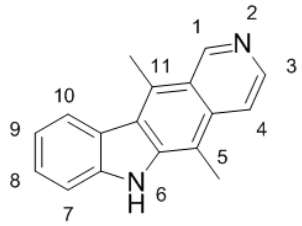


**Figure 1.** Ellipticine. Numbers 1–11 indicate locations of carbon and nitrogen atoms in the ellipticine molecule.

Several studies also demonstrated that the p53 tumor suppressor protein is involved in ellipticine-mediated induction of cell cycle arrest and apoptosis [9–20]. Ellipticine inhibits p53 protein phosphorylation by a selective inhibition of CDK2 kinase in Lewis lung carcinoma and the human colon cancer cell line SW480 [11], and this effect on p53 correlated with cytotoxic activity of ellipticine [11]. Treatment of Saos 2 cells transfected with mutant p53 with ellipticine restored the

transactivation function of p53, resulting in the induction of p53-responsive $p21^{Waf1}$ and *MDM2* genes at protein levels and activation of a p53-responsive luciferase reporter [15]. The results found in the study of Sugikawa and coworkers [15] indicate that ellipticine induces a shift of mutant p53 conformation towards wild-type and this activity is not caused by its function as an inhibitor of topoisomerase II, which is one of the DNA-damaging effects of ellipticine (for a summary see [1–6]). More importantly, ellipticine can even activate mutant p53 and induces $p21^{Waf1}$ and *MDM2* gene expression *in vivo*, in nude mouse tumor xenografts [16]. Moreover, Wang *et al.* [19] demonstrate that in mutant-p53 lymphoma cells, ellipticine-mediated reactivation of mutant p53 sensitizes these cells to treatment with further DNA-damaging drugs (*i.e.*, doxorubicin).

Ellipticine elevated the nuclear localization of endogenous p53 and exogenous mutant p53 in HCT116 colon cancer cells leading to transactivation of the p21 promoter. Nuclear localization of p53 is frequently the consequence of a genotoxic stress by compounds inducing DNA damage (*i.e.*, inhibitors of topoisomerase II) [21]. The ellipticine-mediated abundance of nuclear p53 was not associated with an increase in DNA double strand breaks. Therefore, this effect of ellipticine seems not to be dependent on the mechanism mediated by topoisomerase II inhibition, but on another genotoxic stress [22]. Further, ellipticine induced nuclear translocalization of p53 and of the serine/threonine kinase Akt (an enzyme providing a survival signal protecting cells from stress-induced apoptosis) and recruitment of autophagosomes in human non-small cell lung cancer (NSCLC) epithelial cells A549 [18]. Akt-related cell death also occurred in p53-deficient cells with stable expression of exogenous p53. Hence, as a DNA-damaging agent, ellipticine is a regulator in autophagy-related cell death by cooperation of p53 and Akt [18]. Ellipticine also activates the p53 pathway in glioblastoma cells; its impact on these cancer cells depends on the p53 status [14]. In a U87MG glioblastoma cell line expressing wild-type p53, ellipticine provoked an early G0/G1 cell cycle arrest, whereas in a U373 cell line expressing a p53 mutant it induced arrest in S and G2/M phases of the cell cycle [14].

All studies investigating the mechanism of ellipticine antitumor action indicate complex pathways leading to cancer cell death by this drug. Chemotherapy-induced cell cycle arrest and induction of apoptosis were shown to frequently result from DNA damage caused by exposure to a variety of chemotherapeutics including ellipticine. In addition, genotoxic stress as a result of multiple DNA-damage increases levels of nuclear p53 [21,22], the tumor suppressor protein shown to be involved in ellipticine-mediated induction of cell cycle arrest and apoptosis [10–16]. These findings suggest that DNA damage by ellipticine is crucial for its cytotoxic effects.

## 2. DNA-Damaging Mechanisms of Ellipticine Cytotoxicity to Cancer Cells

The most important DNA-damaging mechanisms of ellipticine were considered to be intercalation into DNA [5,23–26] and inhibition of DNA topoisomerase II activity [5,27,28]. Recently, Andrews and co-workers [29] demonstrated, however, that ellipticine and some of its derivatives are potent and specific inhibitors of RNA polymerase I (Pol-I) transcription and that this Pol-I inhibition occurs by a p53- and topoisomerase II-independent mechanism. They found that the drug influences the assembly and stability of preinitiation complexes by targeting the interaction between promoter recognition essential transcription factor SL1 and the rRNA promoter. In addition, Ghosh *et al.* [30] showed that along with DNA intercalation and/or topoisomerase II inhibition, interaction with the

telomeric DNA region and the resultant inhibition of telomerase activity might be an additional mode of action of ellipticine. Moreover, we showed that this antitumor agent also causes damage to the structural integrity of DNA through covalent binding, by forming covalent DNA adducts after its enzymatic activation with cytochrome P450 (CYP) or peroxidases [1–4,31–40]. Cytotoxicity of ellipticine in cells of several cancer lines sensitive to this drug such as HL-60 promyelocytic leukemia, T-cell leukemia CCRF-CEM, glioblastoma U87MG, neuroblastoma UKF-NB-3 and UKF-NB-4, thyroid cancer BHT-101, B-CPAP and 8505-C and breast adenocarcinoma MCF-7 corresponded to levels of ellipticine-derived DNA adducts generated after its enzymatic activation in most of these cell lines [41]. This indicates that covalent binding to DNA of reactive species generated by enzymatic bioactivation of ellipticine is one of the most important mechanisms responsible for ellipticine cytotoxicity in these cancer cells. The formation of ellipticine-DNA adducts ultimately forces cancer cells to initiate cell death signaling [9]. Based on these results, we suggest that ellipticine acts as a prodrug, which is metabolically activated to reactive species forming covalent DNA adducts causing genotoxic stress. Therefore, information on which enzymes are involved in the metabolism of ellipticine is critical to identify the pharmacological effects of ellipticine. Several *in vitro* and *in vivo* approaches have been developed to study the role of specific CYP and peroxidase enzymes in ellipticine metabolism.

Over the past 10 years we have gained extensive experience in using the pure enzymes and the various animal models to study the ellipticine metabolism. During these studies, ellipticine was found to be oxidized by CYP and peroxidase enzymes to both electrophilic species forming covalent DNA adducts detected by $^{32}$P-postlabeling (Figure 2) and to detoxification metabolites [1–4,32–40,42–51]. Moreover, we characterized the reactions leading to their formation.

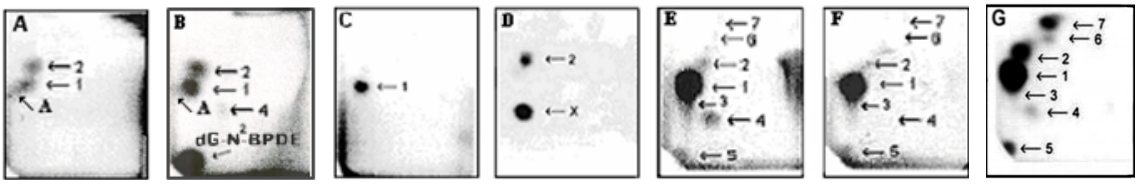


**Figure 2.** Autoradiographs of thin layer chromatography (TLC) maps of $^{32}$P-labeled digests of calf thymus DNA reacted with ellipticine activated by hepatic microsomes from wild-type (WT) mice (**A**), with those from Hepatic Cytochrome P450 Reductase Null (HRN) mice pre-treated with benzo[a]pyrene (BaP) (**B**), from calf thymus DNA reacted with 13-hydroxyellipticine (**C**) [31] or 12-hydroxyellipticine (**D**) [32] of DNA from livers of WT (**E**) and HRN (**F**) mice treated intraperitoneally (*i.p.*) with 10 mg ellipticine/kg body weight [48] and of DNA from liver of Wistar rats treated *i.p.* with 40 mg ellipticine per kilogram body weight (**G**) [33,37]. Analyses were performed by the nuclease P1 version of the $^{32}$P-postlabeling assay. Adduct spots 1–7 and A correspond to the ellipticine-derived DNA adducts. Besides adduct 2, another strong adduct (spot X in panel **D**), which was not found in any other activation systems or *in vivo* was generated by 12-hydroxyellipticine.

In this review we focus on comparison between the data found in the *in vitro* and *in vivo* studies investigating ellipticine metabolism and show a necessity of both approaches to obtain valid information on CYP enzymes participating in this process.

## 3. Metabolism of Ellipticine by Cytochromes P450 (CYPs), Peroxidases and Conjugation Enzymes *in Vitro*

Utilizing numerous *in vitro* systems such as subcellular microsomal fractions and cells in culture expressing CYPs, isolated CYPs reconstituted with other components of the mixed-function-oxidase system [NADPH:CYP reductase (POR), cytochrome $b_5$], and recombinant CYPs, human, rat, rabbit, and mouse CYP enzymes were found to oxidize ellipticine. Ellipticine is oxidized to five metabolites, 7-hydroxy-, 9-hydroxy-, 12-hydroxy-, 13-hydroxyellipticine, and ellipticine $N^2$-oxide (Figure 3), and at least two major ellipticine DNA-adducts were generated by these enzymatic systems [3,31,33–36,38–40,48,49]. 7-Hydroxy- and 9-hydroxyellipticine are efficiently excreted by experimental animals and considered to be the detoxification products of ellipticine [52,53]. But 9-hydroxyellipticine is also an efficient inhibitor of Pol-I transcription *in vitro* with $IC_{50}$ values in cells in the nanomolar range [29], intercalates into DNA, and inhibits topoisomerase II activity [54–56]. It is therefore a pharmacologically important metabolite. 13-Hydroxy- and 12-hydroxyellipticine are the active metabolites, which spontaneously form ellipticine-13-ylium and ellipticine-12-ylium, which reacts with DNA to produce two major deoxyguanosine adducts (see adduct spots 1 and 2 in Figure 2 and the proposed structures of these DNA adducts in Figure 3) [2–4,31,32,34–36,39,40,49]. In addition, ellipticine $N^2$-oxide is also considered a potent active ellipticine metabolite, since it converts to 12-hydroxyellipticine [31], by the Polonowski rearrangement [57] (Figure 3). All these results suggest that the enzymes activating or detoxifying ellipticine are crucial for its pharmacological effects. Thus, the identification of enzymes necessary for ellipticine metabolism is of great importance.

Using a variety of human recombinant CYPs, inhibitors of these enzymes in human hepatic microsomes and correlation analyses, the roles of individual CYPs in the formation of ellipticine metabolites was identified [31,34,35,40]. Human recombinant CYP1A1 and 1A2, followed by CYP1B1, are most effective in formation of 7-hydroxy- and 9-hydroxyellipticine detoxifying ellipticine (Figure 3) [31]. The active metabolite, 13-hydroxyellipticine, forming the ellipticine-DNA adduct 1 (Figure 2C), is generated predominantly by CYP3A4. Oxidation of ellipticine to another activation metabolite, 12-hydroxyellipticine, generating DNA adduct 2 (Figure 2D) is also catalyzed by CYP3A4, but more efficiently by CYP2C19. The $N^2$-oxide of ellipticine is generated mainly by CYP2D6 beside CYP3A4 [31,34,35,39]. These results demonstrate that CYP3A4 is the most effective enzyme leading to ellipticine-DNA adducts 1 and 2, while adduct 2 is also generated by CYP2C19 and 2D6. Moreover, orthologous CYP enzymes of rats and mice catalyze formation of these metabolites and DNA adducts [1–4,36,38]. This indicates that these animals might be suitable models mimicking the fate of ellipticine in human.

Recently, we could show that levels of the DNA adduct formed by 13-hydroxyellipticine increased if this ellipticine metabolite was conjugated with sulfate or acetate by human sulfotransferases 1A1, 1A2, 1A3 and 2A1, or *N*,*O*-acetyltransferases 1 and 2 (Figure 3) [34,58].

Besides CYP enzymes, peroxidases are able to oxidize ellipticine to metabolites generating covalent DNA adducts. Human myeloperoxidase, bovine lactoperoxidase, ovine cyclooxygenase (COX)-1, human COX-2 and plant horseradish peroxidase oxidize ellipticine *in vitro* to form up to four DNA adducts [32]. Even though mechanisms of oxidation of ellipticine by peroxidases and CYPs are different, two of the DNA adducts formed during oxidation of ellipticine by peroxidases are identical to those

produced by 13-hydroxy- and 12-hydroxyellipticine generated by CYPs [32]. Ellipticine oxidation to 6,13-didehydroellipticine (the ellipticine methylene-imine) and ellipticine $N^2$-oxide [32,59] explain the mechanisms of peroxidase-mediated formation of DNA adducts identical to those formed by CYPs (Figure 4). The two minor DNA adducts that are formed by peroxidases (spots 6 and 7 in Figure 2) [32], are also generated after ellipticine activation with hepatic microsomes from humans [31,60], rats [1,38,60], rabbits [1,39], and mice [48,61], and in several organs of mice (Figure 2E,F) and rats (Figure 2G) treated with ellipticine [33,37,48].

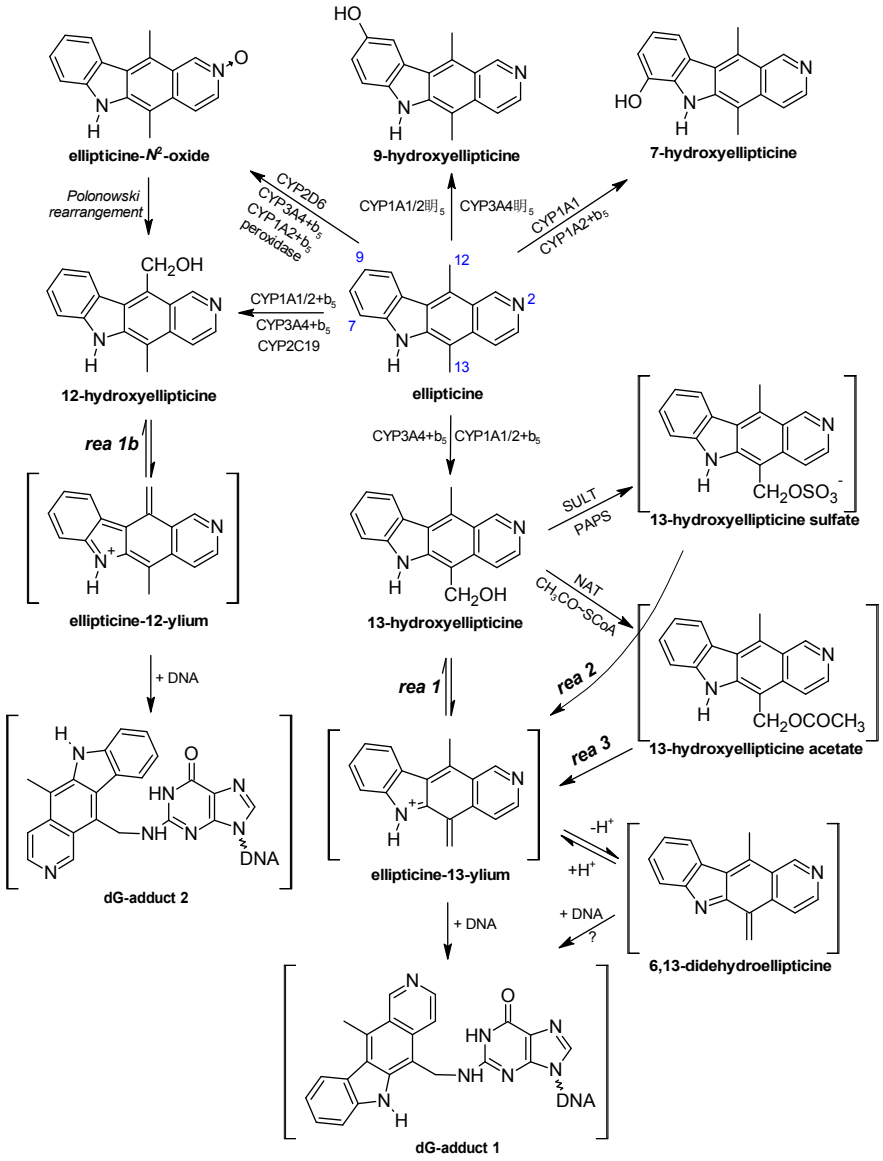


**Figure 3.** Ellipticine metabolism by CYPs showing the identified metabolites and those proposed to form DNA adducts. The compounds shown in brackets were not detected under the experimental conditions and/or are not yet structurally characterized. The CYP enzymes predominantly oxidizing ellipticine shown were identified in our previous studies [31,34,35,38,39]. Reactions 1, 2 and 3 lead to ellipticine-13-ylium from 13-hydroxyellipticine, 13-hydroxyellipticine sulfate and 13-hydroxyellipticine acetate, respectively, and rea 1b to ellipticine 12-ylium. ? indicates that the mechanisms of this reaction are not known.

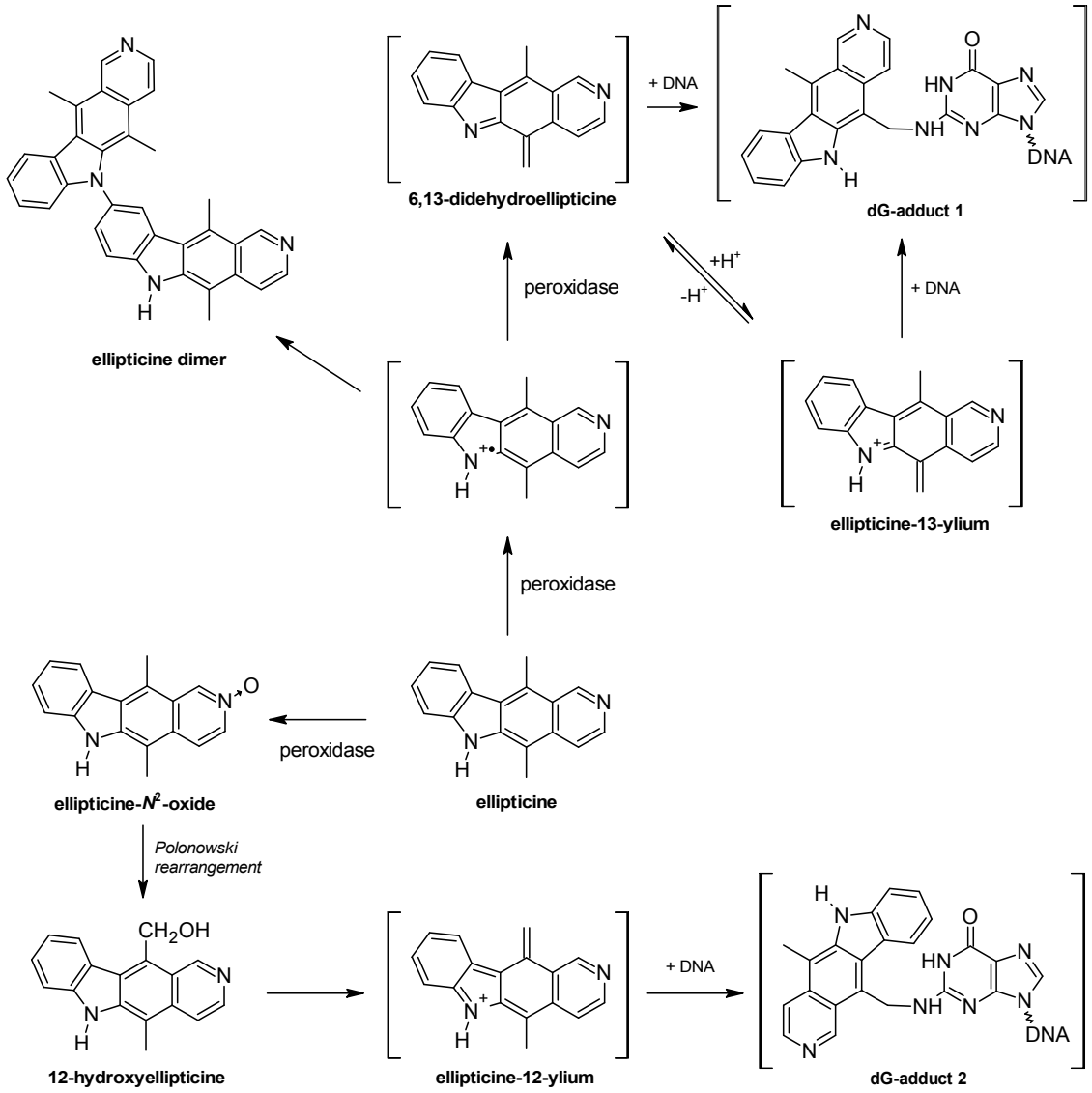


**Figure 4.** Oxidation of ellipticine by peroxidases showing the characterized metabolites and those proposed to form DNA adducts. The compounds shown in brackets were not detected under the experimental conditions and are the electrophilic metabolites postulated as ultimate arylating species or the postulated $N^2$-deoxyguanosine adducts (adapted from reference [32]).

## 4. Oxidation of Ellipticine by CYP Enzymes *in Vivo*

In order to extrapolate from the *in vitro* data to the *in vivo* situation, additional factors have to be considered such as route of administration, absorption, renal clearance, and tissue-specific expression of enzymes metabolizing ellipticine. To identify CYP enzymes responsible for activation of ellipticine *in vivo*, several animal models were used: (I) wild-type (WT) and Hepatic P450 Reductase Null (HRN) mice; (II) the same mouse models, in which expression of enzymes of the mixed-function oxidase system was induced by benzo[a]pyrene (BaP); and (III) Wistar rats. The data obtained with these animal models revealed a paradox: namely, that CYP1A enzymes appear to be more important for activation of ellipticine *in vivo*, despite being involved in its metabolic detoxification *in vitro*.

### *4.1. Utilization of Wild-Type (WT) and Hepatic P450 Reductase Null (HRN) Mice to Identify Enzymes Metabolizing Ellipticine in Vivo*

In HRN mice, POR, the most important electron donor to mouse CYPs, is deleted specifically in hepatocytes. This model was developed by Henderson *et al.* [62] to evaluate the role of both hepatic POR and CYPs in xenobiotic metabolism. Deletion of this enzyme results not only in the loss of essentially all hepatic CYP function, but also in the lack of direct reduction of xenobiotics by POR, an additional property of this enzyme. This mouse model has been used successfully to investigate the role of hepatic *versus* extra-hepatic CYP-catalyzed metabolism and the disposition of several carcinogens and drugs including ellipticine [48,62–69].

Using WT and HRN mouse lines, hepatic CYPs were demonstrated to be important in ellipticine-derived DNA adduct formation also *in vivo*, because up to seven ellipticine-specific DNA adducts were observed in liver, lung, kidney, spleen, colon and bladder (see Figure 2E,F for liver of WT and HRN mice). Deoxyguanosine adduct spots 1 and 2 derived from 13-hydroxy- and 12-hydroxyellipticine, respectively (Figures 2 and 3), were the predominant adducts in all mouse tissues examined.

The finding that ellipticine-DNA adducts are formed in all organs tested in these animals suggest that ellipticine or its metabolites are distributed via the blood stream to different organs and that these tissues may have the metabolic capacity to oxidatively activate ellipticine. As found by Chadwick and co-workers [52,53] ellipticine is very rapidly distributed from the blood, and its excretion is essentially complete by 24 h in several species including mice, rats, dogs, and monkeys. The rate of ellipticine elimination from blood was found to reflect the rate of metabolism of this drug [52]. The main organ responsible for its biotransformation was found to be the liver, forming predominantly 9-hydroxyellipticine, which is excreted mainly in bile as its glucuronide or sulfate conjugate [52,53]. Other *in vivo* pathways involving hydroxylation at as yet unknown positions in the molecule have also been found [52,53]. As mentioned above, in *in vitro* experiments, ellipticine is oxidized by CYPs in hepatic microsomes from a variety of species, including humans, rats, rabbits and mice [31,39,48,49,60,61] to several hydroxylated derivatives, with 9-hydroxy-, 12-hydroxy- and 13-hydroxyellipticine as the major metabolites in most species. However, because 13-hydroxy- and 12-hydroxyellipticine are reactive and have been found to form the two major ellipticine-DNA adducts [31,32,39,47], they will not be easily detectable *in vivo*. In addition, in these early studies radioactively labelled ellipticine was found to be deposited in a number of organs with the highest levels in the liver, followed by kidney, lung, intestine and spleen, and was located primarily in the nuclear fraction [52]. Our more recent data would suggest that covalent binding of ellipticine to DNA can explain this localization [32,33,48].

The levels of ellipticine-DNA adducts in the livers of HRN mice were lower (by up to 65%) than those in WT mice, demonstrating that CYP enzyme activity is important for the oxidative activation of ellipticine to metabolites generating these adducts. Whereas hepatic CYP-mediated ellipticine DNA binding was reduced in HRN mice, adduct levels in extrahepatic organs were up to 4.7-fold higher (Figure 5).

These tissues therefore have the metabolic capacity to oxidize ellipticine and, more importantly, the same reactive species forming DNA adducts are produced as in the liver, probably by both CYP catalysis and maybe peroxidases.

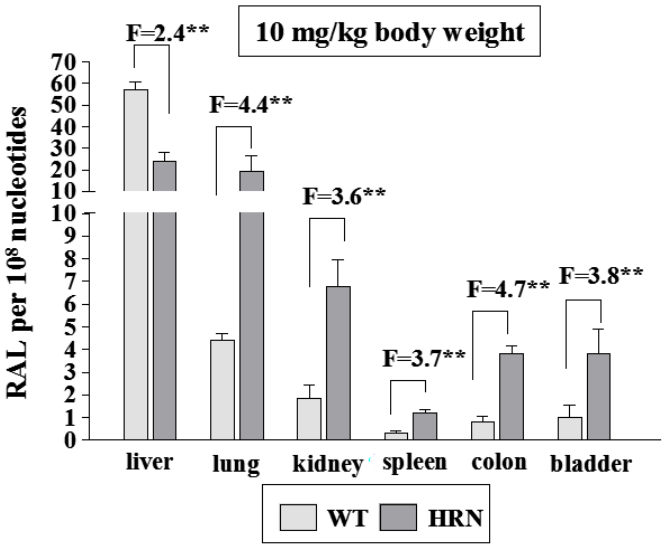


**Figure 5.** Total levels of ellipticine-DNA adducts determined and quantified by $^{32}$P-postlabelling analysis of DNA isolated from organs of HRN and WT mice treated *i.p.* with 10 mg ellipticine/kg body weight. F = fold higher and/or lower DNA adducts in HRN than WT mice. Columns, mean; bars, SD ($n$ = 3); each DNA sample was analysed twice. ** $p < 0.01$. RAL, relative adduct labeling.

Experiments utilizing *ex vivo* incubations of ellipticine with hepatic microsomes of WT and HRN mice and those of these mice exposed to BaP, as well as employing inhibitors of the most important CYP enzymes catalyzing detoxification and activation of ellipticine *in vitro*, CYP1A and 3A, respectively, helped to resolve which of these CYPs play a role in the mouse models. As expected, treatment of WT and HRN mice with BaP significantly induced expression of CYP1A, predominantly of CYP1A1 in liver (up to 175-fold), both at the transcriptional and translation levels [61,65]. This carcinogen also increased the expression of POR protein and its enzymatic activity in livers of these mouse models, but to a much lower extent, up to 2.9-fold. More interestingly, exposure of WT and HRN mice to BaP was also found to result in an increased expression of cytochrome $b_5$, a protein of the microsomal mixed-function-oxidase system, in livers of these mice [66].

In the presence of NADPH, a cofactor of POR- and CYP-dependent enzyme systems, the *ex vivo* incubations with ellipticine, DNA and hepatic microsomes of untreated (control) WT and HRN mice and mice treated with BaP led to activation of this drug to ellipticine-derived DNA adducts (Figures 2A,B and 6), confirming the role of CYPs in ellipticine activation. Arachidonic acid, a cofactor for COX-dependent oxidation [48,64,70–72], also mediated formation of ellipticine-DNA adducts 1 and 2 in hepatic microsomes of all mice used. This suggests that COX also activates ellipticine in mouse liver [48,61], but arachidonic acid as a cofactor was much less effective than NADPH (Figure 6).

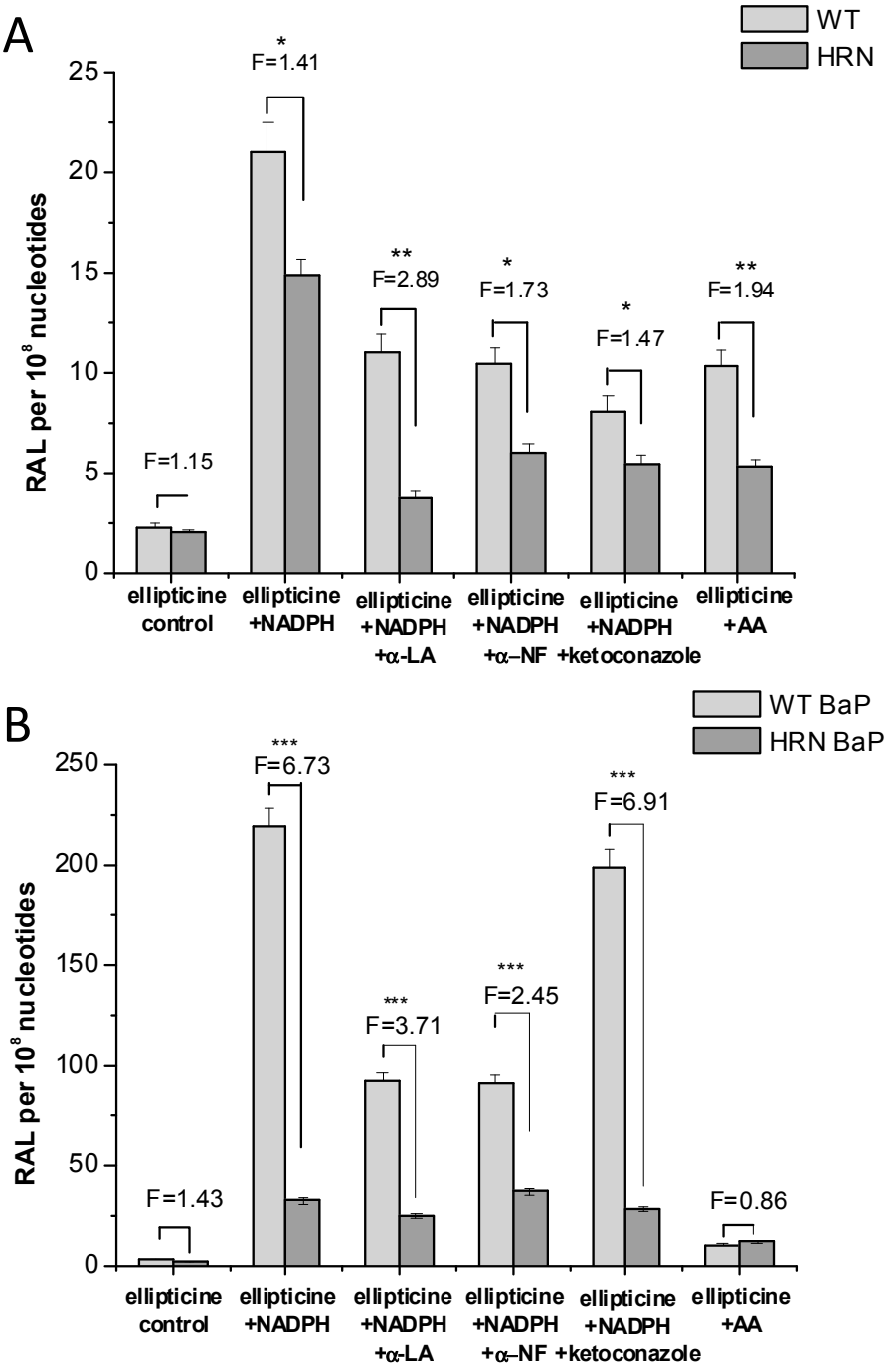


**Figure 6.** DNA adduct formation by ellipticine activated with microsomes isolated from livers of untreated Hepatic Cytochrome P450 Reductase Null (HRN) or wild-type (WT) mice (**A**) and from mice treated with BaP (**B**) as determined by $^{32}$P-postlabeling. F = fold higher DNA adducts levels in microsomes from WT mice compared to HRN mice. Columns: Mean RAL (relative adduct labeling) ± standard deviations (SD) shown represents total levels of DNA adducts of four determinations (duplicate analyses of two independent *in vitro* incubations). Values significantly different from HRN mice: * $p < 0.05$, ** $p < 0.01$, *** $p < 0.001$. Control = without cofactor; AA = arachidonic acid; α-NF = α-naphthoflavone; α-LA = α-lipoic acid.

Surprisingly, levels of ellipticine-derived DNA adducts formed in the *ex vivo* incubations of HRN mice liver microsomes with NADPH were only 1.4-fold lower than amounts formed by hepatic microsomes from WT mice (Figure 6), even though POR expression in livers of HRN mice was two orders of magnitude lower. This finding indicates that ellipticine activation should be at least partially catalyzed also by enzymes with POR-independent activity [48]. Beside peroxidases that were found to activate ellipticine [32], the CYP2S1 enzyme, which is abundantly expressed in several tissues [73–76], might be such an enzyme, because it catalyzes the oxidation of compounds having polycyclic aromatic structures similar to ellipticine without participation of POR [75,76]. Whereas a role of a COX peroxidase in hepatic microsomes of WT and HRN mice was proven (see Figure 6) [48,61], the participation of CYP2S1 in ellipticine activation awaits further examination. Therefore, the human recombinant CYP2S1 enzyme heterologously expressed in *Escherichia coli* was prepared in our laboratory [77] and will be utilized to investigate efficiency of this CYP in ellipticine oxidation in an additional study.

At least two adducts (spots 1 and 2 in Figure 2A,B), which were identical to those generated *in vivo* in mice treated with ellipticine (Figure 2E,F) were formed by mouse hepatic microsomes. Furthermore, ellipticine-derived DNA adduct, spot A, was found as a minor adduct (Figure 2A), predominantly in microsomes isolated from HRN mice [48]. In incubations containing hepatic microsomes of WT and HRN mice treated with BaP, an additional adduct spot, corresponding to the 10-(deoxyguanosin-$N^2$-yl)-7,8,9-trihydroxy-7,8,9,10-tetrahydrobenzo[*a*]pyrene (dG-$N^2$-BPDE) adduct of BaP-7,8-dihydrodiol-9,10-epoxide with DNA *in vitro* and *in vivo* [65,78] was also detected (Figure 2B). This finding indicates that residual BaP is present in microsomes isolated from livers of WT and HRN mice treated with BaP, and is activated by CYP1A1 in combination with microsomal epoxide hydrolase to form this adduct.

Ketoconazole, a selective inhibitor of CYP3A [79,80], inhibited formation of ellipticine-DNA adducts in hepatic microsomes of untreated (control) WT and HRN mice, by ~60% (Figure 6A), confirming a role of CYP3A in ellipticine activation in mouse liver. However, the effect of this inhibitor was much lower in hepatic microsomes of BaP-treated WT and HRN mice, only by ~10% (Figure 6B). In mice exposed to BaP the contribution of CYP3A is much lower, because of the massive CYP1A induction by BaP. Surprisingly, this increased level of CYP1A, the enzymes that mainly detoxify ellipticine *in vitro*, led to higher amounts of ellipticine-DNA adducts formed (Figure 6), predominantly of adduct 1 [61]. Moreover, a selective inhibitor of CYP1A activities, α-naphthoflavone (α-NF) [79], inhibited formation of ellipticine-DNA adducts in all mice except HRN mice exposed to BaP (Figure 6). Induction of CYP1A in HRN mice by BaP also resulted in increased levels of ellipticine-DNA adducts, but α-NF caused an increase rather than a decrease in formation of ellipticine-DNA adducts (Figure 6). Therefore, here the BaP induced CYP1A enzymes seem to increase ellipticine detoxification.

Ellipticine metabolites formed in hepatic microsomes from all mouse lines used in previous studies [48,61] were analogous; 9-hydroxy-, 12-hydroxy-, 13-hydroxy, 7-hydroxyellipticine and $N^2$-oxide of ellipticine were formed (Figure 7). However, the patterns of individual metabolites in WT and HRN mice, either control (untreated) or treated with BaP, were different. In incubations with HRN microsomes from untreated mice, 9-hydroxyellipticine levels were only one sixth, while the amounts of 13-hydroxy- and 12-hydroxyellipticine, were about one half of the levels in incubations with WT microsomes.

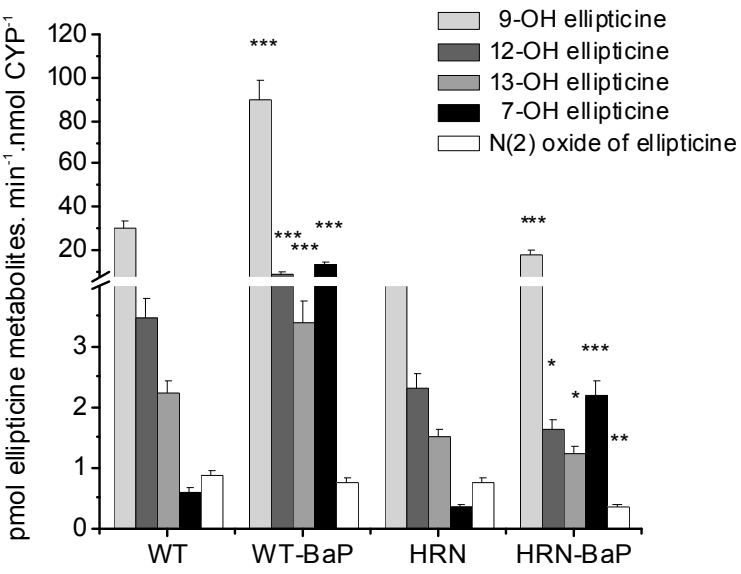


**Figure 7.** Levels of ellipticine metabolites formed by hepatic microsomes (0.2 mg protein) of Hepatic Cytochrome P450 Reductase Null (HRN) and wild-type (WT) mice from 10 μM ellipticine and by hepatic microsomes of HRN and WT mice pre-treated with BaP. Levels of ellipticine metabolites were determined by high performance liquid chromatography (HPLC) [31,60] and are averages ± standard deviations of triplicate incubations. Values significantly different from untreated mice: * $p < 0.05$, ** $p < 0.01$, *** $p < 0.001$.

Exposure of mice to BaP induced CYP1A and resulted, as expected, in an increase in formation of 9-hydroxy- and 7-hydroxyellipticine (Figure 7). This result is consistent with previous studies where CYP1A1 and 1A2 were the major enzymes forming these metabolites [31,35,40]. Treatment of WT mice with BaP, however, also resulted in up to 2.5-fold higher levels of 13-hydroxy- and 12-hydroxyellipticine (Figure 7), the metabolites that were found to be formed *in vitro* mainly by CYP3A, and much less efficiently by CYP1A1 [31,39]. Hence not only CYP3A, but also CYP1A expressed in mouse liver are important for activation of ellipticine to ellipticine-DNA adducts in WT mice only, while in HRN mice the detoxification only is induced by BaP explaining the DNA adduct levels. These findings show that in contrast to the pure *in vitro* CYP systems (CYPs reconstituted with POR), CYP1A enzymes are responsible for ellipticine activation to form DNA adducts in mouse liver [48,61].

### *4.2. Ellipticine Metabolism in Wistar Rats*

In order to further identify CYP enzymes responsible for activation and detoxification of ellipticine *in vivo*, Wistar rats were used. Also in this animal model, ellipticine treatment resulted in ellipticine-derived DNA adduct generation in several healthy organs (liver, kidney, lung, spleen, breast, heart and brain) (see Figure 2G for rat liver) [3,33,37] and in DNA of mammary adenocarcinoma [3]. The levels of ellipticine-derived DNA adducts generated in these adenocarcinomas were almost 2-fold higher than in normal healthy mammary tissue. This finding indicates that other CYPs such as CYP1B1, able to activate ellipticine may be expressed at higher levels in this adenocarcinoma [41]

than in peritumoral tissues. Indeed, we [41], and others [81–83] previously showed CYP1B1 to be a typical CYP expressed in breast cancer.

Genotoxic side effects of ellipticine in healthy organs of experimental animals *in vivo* may of course also be determined by expression levels of CYP enzymes activating ellipticine in these tissues [33,37,48]. Indeed, several studies have found a positive correlation between DNA adduct levels of carcinogens or genotoxic agents, their persistence and their mutagenicity and/or tumorigenicity [84–88]. To better understand the role of ellipticine-DNA adducts in genotoxic side effects in healthy tissues, we have analyzed the persistence of ellipticine-DNA adducts in liver, lung, kidney, spleen, heart, and brain of rats to model the bioactivation of ellipticine in humans treated with ellipticine [33]. Only very low levels of adducts persisted only in some tissues. In addition, not all ellipticine-DNA adducts persist in the tissues analyzed in the study (only adducts 1, 2, 4, and 5) [33]. This finding demonstrates that healthy tissues of rats treated with ellipticine possess effective DNA repair systems to remove certain lesions and suggests a relatively low impact of the genotoxic side effects of ellipticine during cancer treatment in humans.

Also in rats, formation of ellipticine-DNA adduct 1 is dependent not only on levels of CYP3A, but also on those of CYP1A1. The levels of ellipticine DNA adduct 1 in analyzed organs correlated not only with expression levels of CYP3A, but also with those of CYP1A1 in the same organs, which again does not correspond to the situation *in vitro*. As outlined above, in the *in vitro* systems, CYP3A is mainly responsible for formation of ellipticine-DNA adducts and CYP1A predominantly oxidizes ellipticine to its detoxification metabolites [3,4,36]. *In-vitro* studies investigating the effect of cytochrome $b_5$ on the metabolism of ellipticine explained the discrepancies between CYP oxidation of ellipticine *in vitro* and *in vivo*, because this protein has a crucial role in directing individual CYP enzymes to ellipticine activation or detoxification. Moreover, the induced expression of cytochrome $b_5$ protein in liver of rats treated with ellipticine [35,51] suggests that cytochrome $b_5$ may modulate the CYP-mediated bioactivation and detoxification of ellipticine in this animal model *in vivo* as well.

Cytochrome $b_5$ is an important component of the microsomal mixed-function-oxidase system and can influence the metabolism of xenobiotics [69,78,89–95]. For more than four decades, the role of cytochrome $b_5$ in CYP catalysis has been controversial, and based entirely on *in vitro* data, which showed that cytochrome $b_5$ could inhibit or stimulate CYP activity depending on a number of variables including CYP isoenzyme, substrate and cytochrome $b_5$ concentration [89–94]. In order to investigate the role of cytochrome $b_5$ in ellipticine metabolism we conducted some *in vitro* experiments using human liver microsomes, hepatic microsomes from control and ellipticine-pretreated rats and reconstituted systems with human CYP1A1, CYP1A2, CYP3A4, POR, and cytochrome $b_5$ in different ratios [34,35,39,49,51,96]. We found that cytochrome $b_5$ alters the ratio of ellipticine metabolites generated by CYP1A1, 1A2, and 3A4. Whereas the amounts of the detoxification metabolites (7-hydroxy- and 9-hydroxyellipticine) are either decreased (CYP1A1/2) or not changed (CYP3A4) with cytochrome $b_5$ added to the reconstituted system, the amounts of the active metabolites, 12-hydroxy- and 13-hydroxyellipticine, increased considerably, leading to higher ellipticine-DNA adduct levels [34,35,39].

### *4.3. Studies with Human Microsomes and Cancer Cells*

Because in the studies described above with isolated enzymes the ratios of the various partners of CYP are generated experimentally, a more physiological model to identify human enzymes responsible for ellipticine activation was used, namely, human hepatic microsomes [31,39]. These microsomal fractions contain a mixture of human CYPs, POR, cytochrome $b_5$ and its reductase (NADH:cytochrome $b_5$ reductase). Thus, they comprise the essential components of the enzymatic system metabolizing drugs, mimicking well a situation in human liver, where a majority of drug metabolism occurs [78,95]. Human hepatic microsomes oxidize ellipticine mainly to 13-hydroxy- and 12-hydroxyellipticine, whereas 7-hydroxy-, 9-hydroxyellipticine and ellipticine $N^2$-oxide are generated at more than 10-fold lower amounts (see table 2 in [39]). Similar results were found in hepatic microsomes of rats [60]. As a consequence, high levels of both major ellipticine-DNA adducts are formed when DNA is added to the microsomal incubations. The amounts formed correlated with the activity of the major CYPs found previously to form the metabolites generating these DNA adducts (see above) [31,39].

All these results explained why the CYP1A enzymes are more important in ellipticine activation *in vivo*; their activity is modulated by cytochrome $b_5$. These results also demonstrated that not only the expression levels of CYP1A and 3A in several species including human, but also the amounts of expressed cytochrome $b_5$ dictate the oxidative activation and detoxification of ellipticine *in vivo*. Moreover, because ellipticine itself is capable of inducing expression of CYP1A (predominantly CYP1A1), POR, and cytochrome $b_5$ [51,96], it increases its own metabolism leading predominantly to activation of this drug to reactive species forming DNA adducts [34,35], thereby modulating its own pharmacological potential.

The ellipticine-derived DNA adducts formed by enzymatic activation of ellipticine *in vitro* and *in vivo* were also found in human tumor cells, in which CYP enzymes are expressed. The adducts were found in human adenocarcinoma MCF-7 [41], neuroblastoma IMR-32, UKF-NB-3, and UKF-NB-4 [43,44], glioblastoma U87MG [46], and BHT-101, B-CPAP and 8505-C thyroid cancer cells [45] exposed to ellipticine. Cytotoxicity of ellipticine corresponded to the amounts of ellipticine-DNA adducts formed in the specific cancer cells and depended on expression levels of CYP enzymes metabolizing ellipticine (CYP1A1, 1B1, and 3A4) and/or cytochrome $b_5$ in these cells [36,41,43–46]. High expression levels of cytochrome $b_5$ together with those of CYP1A1 and 3A4 lead to more ellipticine-DNA adducts and higher cytotoxicity of ellipticine predominantly in neuroblastoma UKF-NB-4, glioblastoma U87MG and thyroid cancer cells [14,36,41,43–45]. These findings again demonstrate the importance of expression of CYPs, but also of cytochrome $b_5$, in the tumor and normal tissue, because the ratios of these enzymes determine the pharmacological effects of ellipticine.

## 5. Conclusions

The data summarized in this review demonstrate that the DNA-damaging anticancer alkaloid ellipticine might be considered a prodrug, whose major mechanism of action is mediated by an enzymatic activation leading to formation of covalent DNA adducts in target tissues. These ellipticine-DNA adducts are formed in both healthy and tumor tissues and cells, but they do not persist

in healthy tissues. The data show that cytotoxic effects of ellipticine in tumor tissues are dictated by (I) levels of CYP expression (and/or peroxidase expression); (II) levels of cytochrome $b_5$ expression; and (III) its own potency to induce CYP1A1, CYP3A and cytochrome $b_5$ in tumor tissues and cells. The results also demonstrate that animal models, where levels of biotransformation enzymes either knocked out or induced, are appropriate tools to identify enzymes responsible for the metabolic activation and detoxification of ellipticine. They also demonstrate that extrapolation from *in vitro* data to the situation *in vivo* is not always possible, confirming the need for these animal models.

Even though the role of cytochrome $b_5$ in modulation of ellipticine metabolism *in vitro* was clearly shown, its effect *in vivo* is still quite enigmatic. Two mouse lines, one with a conditional hepatic deletion of cytochrome $b_5$ (HBN, Hepatic cytochrome $b_5$ Null) [97] and a double conditional mutant, HBRN (Hepatic cytochrome $b_5$/P450 Reductase Null), in which both enzymes are deleted specifically in the liver [98], which were recently developed in the laboratory of Wolf and coworkers [97,98], may help to resolve the role of cytochrome $b_5$ in CYP-mediated metabolism of ellipticine *in vivo*.

The results summarized in this review form the basis to further predict the susceptibility of human cancers to ellipticine and suggest this alkaloid for treatment in combination with CYP gene transfer (CYP-gene-directed enzyme-prodrug therapy) [99,100], which has the potential to provide efficient activation of ellipticine in target tumor tissue, thereby increasing the anticancer potential of this prodrug. Furthermore, two of the ellipticine metabolites formed by oxidation with CYPs in combination with cytochrome $b_5$, 13-hydroxy- and 12-hydroxyellipticine, are reactive enough to decompose spontaneously to the carbenium ions forming DNA adducts that are predominantly responsible for killing cancer cells. Both these ellipticine metabolites are, therefore, excellent candidates for tumor-specific targeting by appropriate derivatives, including their encapsulated forms into nanocarriers. Research into such targeted carrier systems for active ellipticine metabolites is a major research aim on the path to clinical application of ellipticine in tumor therapy.

## Acknowledgments

This work was supported by the Grant Agency of the Czech Republic (grant 14-18344S in panel P301) and Charles University (UNCE204025/2012). Work at King's College London was supported by the Cancer Research UK and the Wellcome Trust. Volker M Arlt is a member of the Wellcome-funded COMSIG (Causes of Mutational SIGnatures) consortium.

## Author Contributions

Conception and design: Marie Stiborová, Věra Černá, Michaela Moserová, Iveta Mrízová, Eva Frei. Analysis and interpretation of the data: Marie Stiborová, Volker M. Arlt, Eva Frei. Drafting of the article: Marie Stiborová, Eva Frei. Critical revision of the article for important intellectual content: Marie Stiborová, Volker M. Arlt, Eva Frei.

## Conflicts of Interest

The authors declare no conflict of interest.

## References


1. Stiborova, M.; Bieler, C.A.; Wiessler, M.; Frei, E. The anticancer agent ellipticine on activation by cytochrome P450 forms covalent DNA adducts. *Biochem. Pharmacol.* **2001**, *62*, 1675–1684.
2. Stiborova, M.; Rupertova, M.; Schmeiser, H.H.; Frei, E. Molecular mechanisms of antineoplastic action of an anticancer drug ellipticine. *Biomed. Pap. Med. Fac. Univ. Palacky Olomouc Czech Repub.* **2006**, *150*, 13–23.
3. Stiborova, M.; Rupertova, M.; Frei, E. Cytochrome P450- and peroxidase-mediated oxidation of anticancer alkaloid ellipticine dictates its anti-tumor efficiency. *Biochim. Biophys. Acta* **2011**, *1814*, 175–185.
4. Kizek, R.; Adam, V.; Hrabeta, J.; Eckschlager, T.; Smutny, S.; Burda, J.V.; Frei, E.; Stiborova, M. Anthracyclines and ellipticines as DNA-damaging anticancer drugs: Recent advances. *Pharmacol. Ther.* **2012**, *133*, 26–39.
5. Auclair, C. Multimodal action of antitumor agents on DNA: The ellipticine series. *Arch. Biochem. Biophys.* **1987**, *259*, 1–14.
6. Garbett, N.C.; Graves, D.E. Extending nature's leads: The anticancer agent ellipticine. *Curr. Med. Chem. Anti-Cancer Agents* **2004**, *4*, 149–172.
7. Kuo, P.L.; Hsu, Y.L.; Chang, C.H.; Lin, C.C. The antiproliferative inhibition of ellipticine in human breast mda-mb-231 cancer cells is through cell cycle arrest and apoptosis induction. *Anti-Cancer Drugs* **2005**, *16*, 789–795.
8. Russell, E.G.; O'Sullivan, E.C.; Miller, C.M.; Stanicka, J.; McCarthy, F.O.; Cotter, T.G. Ellipticine derivative induces potent cytostatic effect in acute myeloid leukaemia cells. *Investig. New Drugs* **2014**, *32*, 1113–1122.
9. Kim, J.Y.; Lee, S.G.; Chung, J.Y.; Kim, Y.J.; Park, J.E.; Koh, H.; Han, M.S.; Park, Y.C.; Yoo, Y.H.; Kim, J.M. Ellipticine induces apoptosis in human endometrial cancer cells: The potential involvement of reactive oxygen species and mitogen-activated protein kinases. *Toxicology* **2011**, *289*, 91–102.
10. Kuo, P.L.; Hsu, Y.L.; Chang, C.H.; Lin, C.C. The mechanism of ellipticine-induced apoptosis and cell cycle arrest in human breast MCF-7 cancer cells. *Cancer Lett.* **2005**, *223*, 293–301.
11. Ohashi, M.; Sugikawa, E.; Nakanishi, N. Inhibition of p53 protein phosphorylation by 9-hydroxyellipticine: A possible anticancer mechanism. *Jpn. J. Cancer Res.* **1995**, *86*, 819–829.
12. Shi, L.M.; Myers, T.G.; Fan, Y.; O'Conno, R.P.M.; Paull, K.D.; Friend, S.H.; Weinstein, J.N. Mining the National Cancer Institute Anticancer Drug Discovery Database: Cluster analysis of ellipticine analogs with p53-inverse and central nervous system-selective patterns of activity. *Mol. Pharmacol.* **1998**, *53*, 241–251.
13. Kuo, P.L.; Kuo, Y.C.; Hsu, Y.L.; Cho, C.Y.; Lin, C.C. Ellipticine induced apoptosis through p53-dependent pathway in human hepatocellular carcinoma HepG2 cells. *Life Sci.* **2006**, *78*, 2550–2557.
14. Martinkova, E.; Maglott, A.; Leger, D.Y.; Bonnet, D.; Stiborova, M.; Takeda, K.; Martin, S.; Dontenwill, M. α5β1 integrin antagonists reduce chemotherapy-induced premature senescence and facilitate apoptosis in human glioblastoma cells. *Int. J. Cancer* **2010**, *127*, 1240–1248.

15. Sugikawa, E.; Hosoi, T.; Yazaki, N.; Gamanuma, N.; Nakanishi, N.; Ohashi, M. Mutant p53 mediated induction of cell cycle arrest and apoptosis at G1 phase by 9-hydroxyellipticine. *Anticancer Res.* **1999**, *19*, 3099–3108.
16. Peng, Y.; Li, C.; Chen, L.; Sebti, S.; Chen, J. Rescue of mutant p53 transcription function by ellipticine. *Oncogene* **2003**, *22*, 4478–4487.
17. Savorani, C.; Manfé, V.; Biskup, E.; Gniadecki, R. Ellipticine induces apoptosis in T-cell lymphoma via oxidative DNA damage. *Leuk. Lymphoma* **2014**, *4*, 1–9.
18. Fang, K.; Chen, S.P.; Lin, C.W.; Cheng, W.C.; Huang, H.T. Ellipticine-induced apoptosis depends on Akt translocation and signaling in lung epithelial cancer cells. *Lung Cancer* **2009**, *63*, 227–234.
19. Wang, F.; Liu, J.; Robbins, D.; Morris, K.; Sit, A.; Liu, Y.Y.; Zhao, Y. Mutant p53 exhibits trivial effects on mitochondrial functions which can be reactivated by ellipticine in lymphoma cells. *Apoptosis* **2011**, *16*, 301–310.
20. Miller, C.M.; McCarthy, F.O. Isolation, biological activity and synthesis of the natural product ellipticine and related pyridocarbazoles. *RSC Adv.* **2012**, *2*, 8883–8918.
21. Fritsche, M.; Haessler, C.; Brandner, G. Induction of nuclear accumulation of the tumor-suppressor protein p53 by DNA-damaging agents. *Oncogene* **1993**, *8*, 307–318.
22. Xu, G.W.; Mawji, I.A.; Macrae, C.J.; Koch, C.A.; Datti, A.; Wrana, J.L.; Dennis, J.W.; Schimmer, A.D. A high-content chemical screen identifies ellipticine as a modulator of p53 nuclear localization. *Apoptosis* **2008**, *13*, 413–422.
23. Kohn, K.W.; Waring, M.J.; Glaubiger, D.; Friedman, C.A. Intercalative binding of ellipticine to DNA. *Cancer Res.* **1975**, *35*, 71–76.
24. Patel, N.; Bergman, J.; Gräslund, A. $^{1}$H-NMR studies of the interaction between a self-complementary deoxyoligonucleotide duplex and indolo[2,3-b]quinoxaline derivatives active against herpes virus. *Eur. J. Biochem.* **1991**, *197*, 597–604.
25. Chu, Y.; Hsu, M.T. Ellipticine increases the superhelical density of intracellular SV40 DNA by intercalation. *Nucleic Acids Res.* **1992**, *20*, 4033–4038.
26. Singh, M.P.; Hill, G.C.; Peoch, D.; Rayner, B.; Inabach, J.L.; Lown, J.W. High-field NMR and restrained molecular modeling studies on a DNA heteroduplex containing a modified apurinic abasic site in the form of covalently linked 9-aminoellipticine. *Biochemistry* **1994**, *33*, 10271–10285.
27. Belehradek, J., Jr.; Fermandjian, S. DNA-drug recognition and effects on topoisomerase II-mediated cytotoxicity. A three-mode binding model for ellipticine derivatives. *J. Biol. Chem.* **1991**, *266*, 1820–1829.
28. Froelich-Ammon, S.J.; Patchan, M.W.; Osheroff, N.; Thompson, R.B. Topoisomerase II binds to ellipticine in the absence or presence of DNA. Characterization of enzyme-drug interactions by fluorescence spectroscopy. *J. Biol. Chem.* **1995**, *270*, 14998–5004.
29. Andrews, W.J.; Panova, T.; Normand, C.; Gadal, O.; Tikhonova, I.G.; Panov, K.I. Old drug, new target: Ellipticines selectively inhibit RNA polymerase I transcription. *J. Biol. Chem.* **2013**, *288*, 4567–4582.
30. Ghosh, S.; Kar, A.; Chowdhury, S.; Dasgupta, D. Ellipticine binds to a human telomere sequence: An additional mode of action as a putative anticancer agent? *Biochemistry* **2013**, *52*, 4127–4137.

31. Stiborová, M.; Sejbal, J.; Borek-Dohalská, L.; Aimová, D.; Poljaková, J.; Forsterová, K.; Rupertová, M.; Wiesner, J.; Hudecek, J.; Wiessler, M.; *et al.* The anticancer drug ellipticine forms covalent DNA adducts, mediated by human cytochromes P450, through metabolism to 13-hydroxyellipticine and ellipticine $N^2$-oxide. *Cancer Res.* **2004**, *64*, 8374–8380.
32. Stiborová, M.; Poljaková, J.; Ryslavá, H.; Dracínský, M.; Eckschlager, T.; Frei, E. Mammalian peroxidases activate anticancer drug ellipticine to intermediates forming deoxyguanosine adducts in DNA identical to those found *in vivo* and generated from 12-hydroxyellipticine and 13-hydroxyellipticine. *Int. J. Cancer* **2007**, *120*, 243–251.
33. Stiborová, M.; Rupertová, M.; Aimová, D.; Ryslavá, H.; Frei, E. Formation and persistence of DNA adducts of anticancer drug ellipticine in rats. *Toxicology* **2007**, *236*, 50–60.
34. Stiborová, M.; Indra, R.; Moserová, M.; Cerná, V.; Rupertová, M.; Martínek, V.; Eckschlager, T.; Kizek, R.; Frei, E. Cytochrome $b_5$ increases cytochrome P450 3A4-mediated activation of anticancer drug ellipticine to 13-hydroxyellipticine whose covalent binding to DNA is elevated by sulfotransferases and *N,O*-acetyltransferases. *Chem. Res. Toxicol.* **2012**, *25*, 1075–1085.
35. Kotrbová, V.; Mrázová, B.; Moserová, M.; Martínek, V.; Hodek, P.; Hudeček, J.; Frei, E.; Stiborová, M. Cytochrome $b_5$ shifts oxidation of the anticancer drug ellipticine by cytochromes P450 1A1 and 1A2 from its detoxication to activation, thereby modulating its pharmacological efficacy. *Biochem. Pharmacol.* **2011**, *82*, 669–680.
36. Stiborova, M.; Frei, E. Ellipticines as DNA-targeted chemotherapeutics. *Curr. Med. Chem.* **2014**, *21*, 575–591.
37. Stiborová, M.; Breuer, A.; Aimová, D.; Stiborová-Rupertová, M.; Wiessler, M.; Frei, E. DNA adduct formation by the anticancer drug ellipticine in rats determined by $^{32}$P-postlabeling. *Int. J. Cancer* **2003**, *107*, 885–890.
38. Stiborová, M.; Stiborová-Rupertová, M.; Bořek-Dohalská, L.; Wiessler, M.; Frei, E. Rat microsomes activating the anticancer drug ellipticine to species covalently binding to deoxyguanosine in DNA are a suitable model mimicking ellipticine bioactivation in humans. *Chem. Res. Toxicol.* **2003**, *16*, 38–47.
39. Stiborová, M.; Poljakova, J.; Martínková, E.; Ulrichová, J.; Šimánek, V.; Dvořák, Z.; Frei, E. Ellipticine oxidation and DNA adduct formation in human hepatocytes is catalyzed by human cytochromes P450 and enhanced by cytochrome $b_5$. *Toxicology* **2012**, *302*, 233–241.
40. Kotrbová, V.; Aimová, D.; Březinová, A.; Janouchová, K.; Poljaková, J.; Hodek, P.; Frei, E.; Stiborová, M. Cytochromes P450 reconstituted with NADPH:P450 reductase mimic the activating and detoxicating metabolism of the anticancer drug ellipticine in microsomes. *Neuro Endocrinol. Lett.* **2006**, *27* (Suppl. 2), 18–20.
41. Stiborova, M.; Poljakova, J.; Mrizova, I.; Borek-Dohalska, L; Eckschlager, T.; Adam, V.; Kizek, R.; Frei, E. Expression levels of enzymes metabolizing an anticancer drug ellipticine determined by electromigration assays influence its cytotoxicity to cancer cells—A comparative study. *Int. J. Electrochem. Sci.* **2014**, *9*, 5675–5689.
42. Poljaková, J.; Frei, E.; Gomez, J.E.; Aimová, D.; Eckschlager, T.; Hraběta, J.; Stiborová, M. DNA adduct formation by the anticancer drug ellipticine in human leukemia HL-60 and CCRF-CEM cells. *Cancer Lett.* **2007**, *252*, 270–279.

43. Poljaková, J.; Eckschlager, T.; Hraběta, J.; Hřebačková, J.; Smutný, S.; Frei, E.; Martínek, V.; Kizek, R.; Stiborová, M. The mechanism of cytotoxicity and DNA adduct formation by the anticancer drug ellipticine in human neuroblastoma cells. *Biochem. Pharmacol.* **2009**, *77*, 1466–1479.
44. Poljakova, J.; Hrebackova, J.; Dvořákova, M.; Moserova, M.; Eckschlager, T.; Hrabeta, J.; Göttlicherova, M.; Kope Jtkova, B.; Frei, E.; Kizek, R.; *et al*. Anticancer agent ellipticine combined with histone deacetylase inhibitors, valproic acid and trichostatin A, is an effective DNA damage strategy in human neuroblastoma. *Neuro Endocrinol. Lett.* **2011**, *32* (Suppl. 1), 101–116.
45. Poljaková, J.; Eckschlager, T.; Kizek, R.; Frei, E.; Stiborová, M. Electrochemical determination of enzymes metabolizing ellipticine in thyroid cancer cells—A tool to explain the mechanism of ellipticine toxicity to these cells. *Int. J. Electrochem. Sci.* **2013**, *8*, 1573–1585.
46. Martinkova, E.; Dontenwill, M.; Frei, E.; Stiborová, M. Cytotoxicity of and DNA adduct formation by ellipticine in human U87MG glioblastoma cancer cells. *Neuro Endocrinol. Lett.* **2009**, *30* (Suppl. 1), 60–66.
47. Poljaková, J.; Dračínský, M.; Frei, E.; Hudeček, J., Stiborová, M. The effect of pH on peroxidase-mediated oxidation of and DNA-adduct formation by ellipticine. *Collect. Czech Chem. Commun.* **2006**, *71*, 1169–1185.
48. Stiborová, M.; Arlt, V.M.; Henderson, C.J.; Wolf, C.R.; Kotrbová, V.; Moserová, M.; Hudecek, J.; Phillips, D.H.; Frei, E. Role of hepatic cytochromes P450 in bioactivation of the anticancer drug ellipticine: Studies with the hepatic NADPH:Cytochrome P450 reductase null mouse. *Toxicol. Appl. Pharmacol.* **2008**, *226*, 318–327.
49. Stiborová, M.; Moserová, M.; Mrázová, B.; Kotrbová, V.; Frei, E. Role of cytochromes P450 and peroxidases in metabolism of the anticancer drug ellipticine: Additional evidence of their contribution to ellipticine activation in rat liver, lung and kidney. *Neuro Endocrinol. Lett.* **2010**, *31* (Suppl. 2), 26–35.
50. Stiborová, M.; Eckschlager, T.; Poljaková, J.; Hraběta, J.; Adam, V.; Kizek, R.; Frei, E. The synergistic effects of DNA-targeted chemotherapeutics and histone deacetylase inhibitors as therapeutic strategies for cancer treatment. *Curr. Med. Chem.* **2012**, *19*, 4218–4238.
51. Vranová, I.; Moserová, M.; Hodek, P.; Kizek, R.; Frei, E.; Stiborová, M. The anticancer drug ellipticine induces cytochromes P450 1A1, 1A2 and 3A, cytochrome $b_5$ and NADPH:Cytochrome P450 in rat liver, kidney and lung. *Int. J. Electrochem. Sci.* **2013**, *8*, 1586–1597.
52. Chadwick, M.; Silveira, D.M.; Platz, B.R.; Hayes, D. Comparative physiological disposition of ellipticine in several animal species after intravenous administration. *Drug Metab. Dispos.* **1978**, *6*, 528–541.
53. Branfam, A.R.; Bruni, R.J.; Reihold, V.N.; Silveira, D.M.; Chadwick, M.; Yesair, D.W. Characterization of metabolites of ellipticine in rat bile. *Drug Metab. Dispos.* **1978**, *6*, 542–548.
54. Ismail, M.A.; Sanders, K.J.; Fennell, G.C.; Latham, H.C.; Wormell, P.; Rodger, A. Spectroscopic studies of 9-hydroxyellipticine binding to DNA. *Biopolymers* **1998**, *46*, 127–143.

55. Fossé, P.; René, B.; le Bret, M.; Paoletti, C.; Saucier, J.M. Sequence requirements for mammalian topoisomerase II mediated DNA cleavage stimulated by an ellipticine derivative. *Nucleic Acids Res.* **1991**, *19*, 2861–2868.
56. Fossé, P.; René, B.; Charra, M.; Paoletti, C.; Saucier, J.M. Stimulation of topoisomerase II-mediated DNA cleavage by ellipticine derivatives: Structure-activity relationships. *Mol. Pharmacol.* **1992**, *42*, 590–595.
57. Hofle, G.; Glase, N.; Leibold, T.; Sefkow, M. Epothilone A–D and their thiazole-modified analogs as novel anticancer agents. *Pure Appl. Chem.* **1999**, *71*, 2019–2024.
58. Moserova, M.; Kotrbova, V.; Rupertova, M.; Naiman, K.; Hudecek, J.; Hodek, P.; Frei, E.; Stiborova, M. Isolation and partial characterization of the adduct formed by 13-hydroxyellipticine with deoxyguanosine in DNA. *Neuro Endocrinol. Lett.* **2008**, *29*, 728–732.
59. Martínek, V.; Sklenár, J.; Dracínsky, M.; Sulc, M.; Hofbauerová, K.; Bezouska, K.; Frei, E.; Stiborová, M. Glycosylation protects proteins against free radicals generated from toxic xenobiotics. *Toxicol. Sci.* **2010**, *117*, 59–74.
60. Stiborová, M.; Borek-Dohalská, L.; Aimová, D.; Kotrbová, V.; Kukacková, K.; Janouchová, K.; Rupertová, M.; Ryslavá, H.; Hudecek, J.; Frei, E. Oxidation pattern of the anticancer drug ellipticine by hepatic microsomes—Similarity between human and rat systems. *Gen. Physiol. Biophys.* **2006**, *25*, 245–261.
61. Stiborova, M.; Cerna, V.; Moserova, M.; Arlt, V.M.; Frei, E. The effect of benzo[a]pyrene on metabolic activation of anticancer drug ellipticine in mice. *Neuro Endocrinol. Lett.* **2013**, *34* (Suppl. 2), 43–54.
62. Henderson, C.J.; Otto, D.M.; Carrie, D.; Magnuson, M.A.; McLaren, A.W.; Rosewell, I.; Wolf, C.R. Inactivation of the hepatic cytochrome P450 system by conditional deletion of hepatic cytochrome P450 reductase. *J. Biol. Chem.* **2003**, *278*, 13480–13486.
63. Arlt, V.M.; Stiborova, M.; Henderson, C.J.; Osborne, M.R.; Bieler, C.A.; Frei, E.; Martinek, V.; Sopko, B.; Wolf, C.R.; Schmeiser, H.H.; *et al.* Environmental pollutant and potent mutagen 3-nitrobenzanthrone forms DNA adducts after reduction by NAD(P)H:quinone oxidoreductase and conjugation by acetyltransferases and sulfotransferases in human hepatic cytosols. *Cancer Res.* **2005**, *65*, 2644–2652.
64. Arlt, V.M.; Henderson, C.J.; Wolf, C.R.; Schmeiser, H.H.; Phillips, D.H.; Stiborova, M. Bioactivation of 3-aminobenzanthrone, a human metabolite of the environmental pollutant 3-nitrobenzanthrone: Evidence for DNA adduct formation mediated by cytochrome P450 enzymes and peroxidases. *Cancer Lett.* **2006**, *234*, 220–2231.
65. Arlt, V.M.; Stiborová, M.; Henderson, C.J.; Thiemann, M.; Frei, E.; Aimová, D.; Singh, R.; Gamboa da Costa, G.; Schmitz, O.J.; Farmer, P.B.; *et al.* Metabolic activation of benzo[a]pyrene *in vitro* by hepatic cytochrome P450 contrasts with detoxification *in vivo*: Experiments with hepatic cytochrome P450 reductase null mice. *Carcinogenesis* **2008**, *29*, 656–665.
66. Arlt, V.M.; Poirier, M.C.; Sykes, S.E.; John, K.; Moserova, M.; Stiborova, M.; Wolf, C.R.; Henderson, C.J.; Phillips, D.H. Exposure to benzo[a]pyrene of Hepatic Cytochrome P450 Reductase Null (HRN) and P450 Reductase Conditional Null (RCN) mice: Detection of benzo[a]pyrene diol epoxide-DNA adducts by immunohistochemistry and $^{32}$P-postlabelling. *Toxicol. Lett.* **2012**, *213*, 160–166.

67. Pass, G.J.; Carrie, D.; Boylan, M.; Lorimore, S.; Wright, E.; Houston, B.; Henderson, C.J.; Wolf, C.R. Role of hepatic cytochrome P450s in the pharmacokinetics and toxicity of cyclophosphamide: Studies with the hepatic cytochrome P450 reductase null mouse. *Cancer Res.* **2005**, *65*, 4211–4217.
68. Xiao, Y.; Ge, M.; Xue, X.; Wang, H.; Wu, X.; Li, L.; Liu, L.; Qi, X.; Zhang, Y.; Li, Y.; *et al.* Detoxication role of hepatic cytochrome P450s in the kidney toxicity induced by aristolochic acid. *Kidney Int.* **2008**, *73*, 1231–1239.
69. Levová, K.; Moserová, M.; Kotrbová, V.; Šulc, M.; Henderson, C.J.; Wolf, C.R.; Phillips, D.H.; Frei, E.; Schmeiser, H.H.; Mareš, J.; *et al.* Role of cytochromes P450 1A1/2 in detoxication and activation of carcinogenic aristolochic acid I: Studies with the hepatic NADPH:cytochrome P450 reductase null (HRN) mouse model. *Toxicol. Sci.* **2011**, *121*, 43–56.
70. Eling, T.E.; Thompson, D.C.; Foureman, G.L.; Curtis, J.F.; Hughes, M.F. Prostaglandin H synthase and xenobiotic oxidation. *Annu. Rev. Pharmacol. Toxicol.* **1990**, *30*, 1–45.
71. Eling, T.E.; Curtis, J.F. Xenobiotic metabolism by prostaglandin H synthase. *Pharm. Ther.* **1992**, *53*, 261–273.
72. Stiborova, M.; Frei, E.; Hodek, P.; Wiessler, M.; Schmeiser, H.H. Human hepatic and renal microsomes, cytochromes P450 1A1/2, NADPH:cytochrome P450 reductase and prostaglandin H synthase mediate the formation of aristolochic acid-DNA adducts found in patients with urothelial cancer. *Int. J. Cancer* **2005**, *113*, 189–197.
73. Downie, D.; McFadyen, M.C.; Rooney, P.H.; Cruickshank, M.E.; Parkin, D.E.; Miller, I.D.; Telfer, C.; Melvin, W.T.; Murray, G.I. Profiling cytochrome P450 expression in ovarian cancer: Identification of prognostic markers. *Clin. Cancer Res.* **2005**, *11*, 7369–7735.
74. Saarikoski, T.; Rivera, S.P.; Hankinson, O.; Husgafvel-Pursiainen, K. CYP2S1: A short review. *Toxicol. Appl. Pharmacol.* **2005**, *207*, 62–69.
75. Bui, P.H.; Hankinson, O. Functional characterization of human cytochrome P450 2S1 using a synthetic gene-expressed protein in *Escherichia coli*. *Mol. Pharmacol.* **2009**, *76*, 1031–1043.
76. Bui, P.H.; Hsu, E.L.; Hankinson, O. Fatty acid hydroperoxides support cytochrome P450 2S1-mediated bioactivation of benzo[a]pyrene-7,8-dihydrodiol. *Mol. Pharmacol.* **2009**, *76*, 1044–1052.
77. Mrizová, I.; Moserová, M.; Milichovsky, J.; Šulc, M.; Guengerich, F.P.; Stiborová, M. Heterologous expression of cytochrome P450 2S1 in *Escherichia coli*. *Interdisc. Toxicol.* **2014**, *7* (Suppl. 1), 66.
78. Stiborova, M.; Moserova, M.; Černá, V.; Indra, R.; Dračínský, M.; Šulc, M.; Henderson, C.J.; Wolf, C.R.; Schmeiser, H.H.; Phillips, D.H.; *et al.* Cytochrome $b_5$ and epoxide hydrolase contribute to benzo[*a*]pyrene-DNA adduct formation catalyzed by cytochrome P450 1A1 under low NADPH:P450 oxidoreductase conditions. *Toxicology* **2014**, *318*, 1–12.
79. Rendic, S.; DiCarlo, F.J. Human cytochrome P450 enzymes: A status report summarizing their reactions, substrates, inducers, and inhibitors. *Drug Metab. Rev.* **1997**, *29*, 413–480.
80. Ueng, Y.-F.; Kuwabara, T.; Chun, Y.-J.; Guengerich, F.P. Cooperativity in oxidation catalyzed by cytochrome P450 3A4. *Biochemistry* **1997**, *36*, 370–381.

81. Patterson, L.H.; McKeown, S.R.; Robson, T.; Gallagher, R.; Raleigh, S.M.; Orr, S. Antitumor prodrug development using cytochrome P450 (CYP) mediated activation. *Anti-Cancer Drug Des.* **1999**, *14*, 473–486.
82. Murray, G.I.; Melvin, W.T.; Burke, M. Cytochrome P450 expression in tumors. *J. Pathol*. **1995**, *176*, 323–324.
83. El-Rayes, B.F.; Ali, S.; Heilbrun, L.K.; Lababidi, S.; Bouwman, S.; Vischer, D.; Philip, P.A. Cytochrome P450 and glutathione transferase expression in human breast cancer. *Clin. Cancer Res.* **2003**, *9*, 1705–1709.
84. Godschalk, R.W.L.; Moonen, E.J.C.; Schilderman, P.A.E.L.; Broekmans, W.M.R.; Kleinjans, J.C.S.; van Schooten, F.J. Exposure-route-dependent DNA adduct formation by polycyclic aromatic hydrocarbons. *Carcinogenesis* **2000**, *21*, 87–92.
85. Poirier, M.C. Chemical-induced DNA damage and human cancer risk. *Nat. Rev.* **2004**, *4*, 630–637.
86. Randerath, K.; Haglund, R.E.; Phillips, D.H.; Reddy, M.V. $^{32}$P-post-labelling analysis of DNA adducts formed in the livers of animals treated with safrole, estragole and other naturally-occurring alkenylbenzenes. I. Adult female CD-1 mice. *Carcinogenesis* **1984**, *5*, 1613–1622.
87. Ross, J.A.; Nelson, G.B.; Wilson, K.H.; Rabinowitz, J.R.; Galati, A.; Stoner, G.D.; Nesnow, S.; Mass, M.J. Adenomas induced by polycyclic aromatic hydrocarbons in strain A/J mouse lung correlate with time-integrated DNA adduct levels. *Cancer Res.* **1995**, *55*, 1039–1044.
88. Smith, B.A.; Fullerton, N.F.; Heflich, R.H.; Beland, F.A. DNA adduct formation and T-lymphocyte mutation induction in F344 rats implanted with tumorigenic doses of 1,6-dinitropyrene. *Cancer Res.* **1995**, *55*, 2316–2324.
89. Yamazaki, H.; Gillam, E.M.; Dong, M.S.; Johnson, W.W.; Guengerich, F.P.; Shimada, T. Reconstitution of recombinant cytochrome P450 2C10(2C9) and comparison with cytochrome P450 3A4 and other forms: Effects of cytochrome P450–P450 and cytochrome P450–$b_5$ interactions. *Arch. Biochem. Biophys.* **1997**, *342*, 329–337.
90. Yamazaki, H.; Shimada, T.; Martin, M.V.; Guengerich, F.P. Stimulation of cytochrome P450 reactions by apo-cytochrome $b_5$: Evidence against transfer of heme from cytochrome P450 3A4 to apo-cytochrome $b_5$ or heme oxygenase. *J. Biol. Chem.* **2001**, *276*, 30885–30891.
91. Schenkman, J.B.; Jansson, I. The many roles of cytochrome $b_5$. *Pharmacol. Ther.* **2003**, *97*, 139–152.
92. Zhang, H.; Myshkin, E.; Waskell, L. Role of cytochrome $b_5$ in catalysis by cytochrome P450 2B4. *Biochem. Biophys. Res. Commun.* **2005**, *338*, 499–506.
93. Zhang, H.; Im, S.C.; Waskell, L. Cytochrome $b_5$ increases the rate of product formation by cytochrome P450 2B4 and competes with cytochrome P450 reductase for a binding site on cytochrome P450 2B4. *J. Biol. Chem.* **2007**, *282*, 29766–29776.
94. Kotrbová, V.; Aimová, D.; Ingr, M.; Borek-Dohalská, L.; Martínek, V.; Stiborová, M. Preparation of a biologically active apo-cytochrome $b_5$ via heterologous expression in *Escherichia coli*. *Protein Expr. Purif.* **2009**, *66*, 203–209.
95. Rendic, S.; Guengerich, F.P. Contributions of human enzymes in carcinogen metabolism. *Chem. Res. Toxicol.* **2012**, *25*, 1316–1383.

96. Aimová, D.; Svobodová, L.; Kotrbová, V.; Mrázová, B.; Hodek, P.; Hudeček, J.; Václavíková, R.; Frei, E.; Stiborová, M. The anticancer drug ellipticine is a potent inducer of rat cytochromes P450 1A1 and 1A2, thereby modulating its own metabolism. *Drug Metab. Dispos.* **2007**, *35*, 1926–1934.
97. Finn, R.D.; McLaughlin, L.A.; Ronseaux, S.; Rosewell, I.; Houston, J.B.; Henderson, C.J.; Wolf, C.R. Defining the *in vivo* role for cytochrome $b_5$ in cytochrome P450 function through the conditional hepatic deletion of microsomal cytochrome $b_5$. *J. Biol. Chem.* **2008**, *283*, 31385–31393.
98. Henderson, C.J.; McLaughlin, L.A.; Wolf, C.R. Evidence that cytochrome $b_5$ and cytochrome $b_5$ reductase can act as sole electron donors to the hepatic cytochrome P450 system. *Mol. Pharmacol.* **2013**, *83*, 1209–1217.
99. Ma, J.; Waxman, D.J. Collaboration between hepatic and intratumoral prodrug activation in a P450 prodrug-activation gene therapy model for cancer treatment. *Mol. Cancer Ther.* **2007**, *6*, 2879–2890.
100. Lu, H.; Chen, C.S.; Waxman, D.J. Potentiation of methoxymorpholinyl doxorubicin antitumor activity by *P*450 3A4 gene transfer. *Cancer Gene Ther.* **2009**, *16*, 393–404.

# *Příloha 4*

Volker M. Arlt, Annette M. Krais, Roger W. Godschalk, Yanira Riffo-Vasquez, **Iveta Mrízová,** Candice A. Roufosse, Charmaine Corbin, Shi Quan, Eva Frei, Marie Stiborová, Frederik-Jan van Schooten, David H. Phillips, Domenico Spina

**PULMONARY INFLAMMATION IMPACTS ON CYP1A1-MEDIATED RESPIRATORY TRACT DNA DAMAGE INDUCED BY THE CARCINOGENIC AIR POLLUTANT BENZO[A]PYRENE**

*Tox. Sci.* 146, 213-225, 2015

$IF_{2014}$ = 3.854

OXFORD
SOT | Society of Toxicology
www.toxsci.oxfordjournals.org

TOXICOLOGICAL SCIENCES, 2015, 1–13

doi: 10.1093/toxsci/kfv086
Advance Access Publication Date: April 23, 2015

# Pulmonary Inflammation Impacts on CYP1A1-Mediated Respiratory Tract DNA Damage Induced by the Carcinogenic Air Pollutant Benzo[*a*]pyrene

Volker M. Arlt*,[1], Annette M. Krais*, Roger W. Godschalk†, Yanira Riffo-Vasquez‡, Iveta Mrizova§, Candice A. Roufosse¶, Charmaine Corbin*, Quan Shi†, Eva Frei||, Marie Stiborova§, Frederik-Jan van Schooten†, David H. Phillips*, and Domenico Spina‡

*Analytical and Environmental Sciences Division, MRC-PHE Centre for Environment & Health, King's College London, London SE1 9NH, United Kingdom, †Department of Toxicology, School for Nutrition, Toxicology and Metabolism (NUTRIM), Maastricht University Medical Centre, 6200 MD Maastricht, The Netherlands, ‡Sackler Institute of Pulmonary Pharmacology, Institute of Pharmaceutical Science, King's College London, London SE1 9NH, United Kingdom, §Department of Biochemistry, Faculty of Science, Charles University, 12840 Prague 2, Czech Republic; ¶Department of Histopathology, Imperial College Healthcare NHS Trust, Hammersmith Hospital, London W12 0HS, United Kingdom, and ||Division of Preventive Oncology, National Center for Tumor Diseases, German Cancer Research Center (DKFZ), Im Neuenheimer Feld 280, 69120 Heidelberg, Germany

[1]To whom correspondence should be addressed atAnalytical and Environmental Sciences Division, MRC-PHE Centre for Environment & Health, King's College London, Franklin-Wilkins Building, 150 Stamford Street, London SE1 9NH, United Kingdom. Fax: +44-207-848-4086; E-mail: volker.arlt@kcl.ac.uk.



## ABSTRACT

Pulmonary inflammation can contribute to the development of lung cancer in humans. We investigated whether pulmonary inflammation alters the genotoxicity of polycyclic aromatic hydrocarbons (PAHs) in the lungs of mice and what mechanisms are involved. To model nonallergic acute inflammation, mice were exposed intranasally to lipopolysaccharide (LPS; 20 μg/mouse) and then instilled intratracheally with benzo[*a*]pyrene (BaP; 0.5 mg/mouse). BaP-DNA adduct levels, measured by $^{32}$P-postlabeling analysis, were approximately 3-fold higher in the lungs of LPS/BaP-treated mice than in mice treated with BaP alone. Pulmonary Cyp1a1 enzyme activity was decreased in LPS/BaP-treated mice relative to BaP-treated mice suggesting that pulmonary inflammation impacted on BaP-induced Cyp1a1 activity in the lung. Our results showed that Cyp1a1 appears to be important for BaP detoxification *in vivo* and that the decrease of pulmonary Cyp1a1 activity in LPS/BaP-treated mice results in a decrease of pulmonary BaP detoxification, thereby enhancing BaP genotoxicity (ie, DNA adduct formation) in the lung. Because less BaP was detoxified by Cyp1a1 in the lungs of LPS/BaP-treated mice, more BaP circulated via the blood to extrapulmonary tissues relative to mice treated with BaP only. Indeed, we observed higher BaP-DNA adduct levels in livers of LPS/BaP-treated mice compared with BaP-treated mice. Our results indicate that pulmonary inflammation could be a critical determinant in the induction of genotoxicity in the

lung by PAHs like BaP. Cyp1a1 appears to be involved in both BaP bioactivation and detoxification although the contribution of other enzymes to BaP-DNA adduct formation in lung and liver under inflammatory conditions remains to be explored.

**Key words**: benzo[*a*]pyrene; pulmonary inflammation; cytochrome P450; carcinogen metabolism; DNA adducts; bronchoalveolar lavage

Globally, lung cancer is the leading cause of cancer death. Tobacco smoking is the overwhelming cause of lung cancer, although vehicle engine exhaust (eg, diesel exhaust) and ambient air pollution are also implicated (IARC, 2013; Loomis *et al.*, 2013). Inflammatory diseases of the lung, including fibrosis and chronic obstructive pulmonary disease (COPD), are associated with higher lung cancer risk (Brody and Spira, 2006; Schottenfeld and Beebe-Dimmer, 2006). Lung cancer risk in smokers with COPD is increased up to 10-fold in comparison to smokers without COPD (Brody and Spira, 2006). Many inflammatory agents can contribute to the development of diseases like COPD or asthma, including inhaled combustion-derived particles such as cigarette smoke, ambient air particulate matter, and diesel exhaust particles (Kelly and Fussell, 2011). Inhalation of such particles can cause a local pulmonary response which is characterized by the influx of neutrophils into the airways (Knaapen *et al.*, 2006). In contrast to their innate protective role in immunity, neutrophils contribute to the pathogenesis of inflammatory lung diseases like COPD and promote tumor development (Grivennikov *et al.*, 2010; Knaapen *et al.*, 2006).

A number of studies have found that occupational exposure to diesel exhaust leads to increased risk of lung cancer (Attfield *et al.*, 2012; Silverman *et al.*, 2012) and the International Agency for Research on Cancer (IARC) has classified diesel engine exhaust as carcinogenic to humans (Group 1) (IARC, 2013). However, the mechanism of diesel carcinogenesis and precise identity of the carcinogenic components of diesel exhaust are still incompletely understood, as is the magnitude of the carcinogenic risk from environmental exposure. Although exposure to diesel exhaust material induces pulmonary inflammation and exacerbates chronic respiratory inflammatory conditions (Kelly and Fussell, 2011), the contribution of such inflammation to diesel exhaust associated carcinogenic risk potential has not been examined in any great detail. By analogy with the causation of lung cancer by tobacco smoking (Walser *et al.*, 2008), it was therefore the aim of this study to examine how inflammation in the lung alters the genotoxicity of polycyclic aromatic hydrocarbons (PAHs), which occur in the particulate phase of diesel exhaust, and what specific mechanisms are involved.

PAHs such as benzo[*a*]pyrene (BaP), also an IARC Group 1 carcinogen (IARC, 2010), exert their carcinogenic effects only after metabolic activation. As shown in Figure 1 BaP is activated by cytochrome P450 (CYP) enzymes, CYP1A1 and CYP1B1 being the most important isoenzymes (Baird *et al.*, 2005), resulting in highly reactive diol-epoxides capable of forming covalent DNA adducts that can lead to mutations through errors in DNA replication (Phillips, 2005). Inflammatory reactions *in vivo* involve the production and release of a range of signaling molecules including cytokines and chemokines (Grivennikov *et al.*, 2010; Schwarze *et al.*, 2013). *In vitro* experiments have shown that cytokines like tumor necrosis factor-α (TNF-α) formed after environmental exposures can alter the expression of metabolic enzymes such as CYPs (eg, CYP1A1, CYP1B1) involved in BaP bioactivation (Smerdova *et al.*, 2014; Umannova *et al.*, 2008). Other *in vitro* studies have revealed that neutrophil-derived myeloperoxidase can activate the BaP metabolite BaP-7,8-dihydrodiol to reactive species (ie, BaP-7,8-dihydrodiol-9,10-epoxide [BPDE]) that form DNA adducts in lung cells (Borm *et al.*, 1997; Petruska *et al.*, 1992).

In this study, we investigated whether lung inflammation alters the capacity for diesel exhaust carcinogens like BaP to cause DNA damage (eg, DNA adducts) *in vivo* and the mechanisms involved. To model nonallergic acute inflammation, mice were exposed to lipopolysaccharide (LPS) and then instilled with BaP. DNA adduct formation was determined by $^{32}$P-postlabeling analysis.

## MATERIALS AND METHODS

*Carcinogen.* BaP (purity ≥96%) was obtained from Sigma Aldrich.

*Animal treatment.* C57B16 mice (male; approximately 8–10 weeks old, 20-25 g) were obtained from Charles River Laboratories. All animal experiments were carried out at King's College London under license according to protocols approved by the Home Office under "The Animals (Scientific Procedures) Act (1986)" after approval by the institutional ethics committee. Animals were kept under controlled pathogen-free conditions and allowed food and water *ad libitum*. In total, 4 groups of mice ($n = 4$ per experiment; repeated in triplicate; $n = 12$ in total) were used as follows (see Fig. 2): Group I: mice were instilled nasally with saline and 24 h later instilled intratracheally with vehicle, tricaprylin (25 µl/mouse). Group II: to induce acute pulmonary inflammation mice received an intranasal dose of 20 µg LPS (*Escherichia coli*, serotype O55:B5; 1 mg/ml; Sigma), and 24 h later they received tricaprylin (25 µl/mouse) by intratracheal instillation. Group III: mice were instilled nasally with saline and 24 h later instilled intratracheally with BaP (0.5 mg BaP dissolved in 25 µl tricaprylin). Group IV: mice received an intranasal administration of 20 µg LPS followed 24 h later with BaP (0.5 mg BaP/mouse) by intratracheal instillation. In order to have sufficient material available for histopathology and several biological assays, experiments were performed in triplicate on separate occasions ($3 \times n = 4$/group). All instillations were performed under anesthesia with isoflurane (Sigma) following injection with ketamine/zylazine (1 mg/0.166 mg per mouse, respectively; Sigma). Mice were killed 3 days after exposure after anesthesia with 2 g/kg body weight urethane (Sigma) by intraperitoneal administration and a cannula was inserted into the exposed trachea. For the collection of inflammatory cells by bronchoalveolar lavage (BAL) 3 0.5-ml aliquots of sterile saline were injected into the lungs. Lung and liver tissue were also collected, snap-frozen in liquid nitrogen and stored at −80°C until analysis. For histopathology lung sections were fixed for 48 h in PBS containing 4% paraformaldehyde.

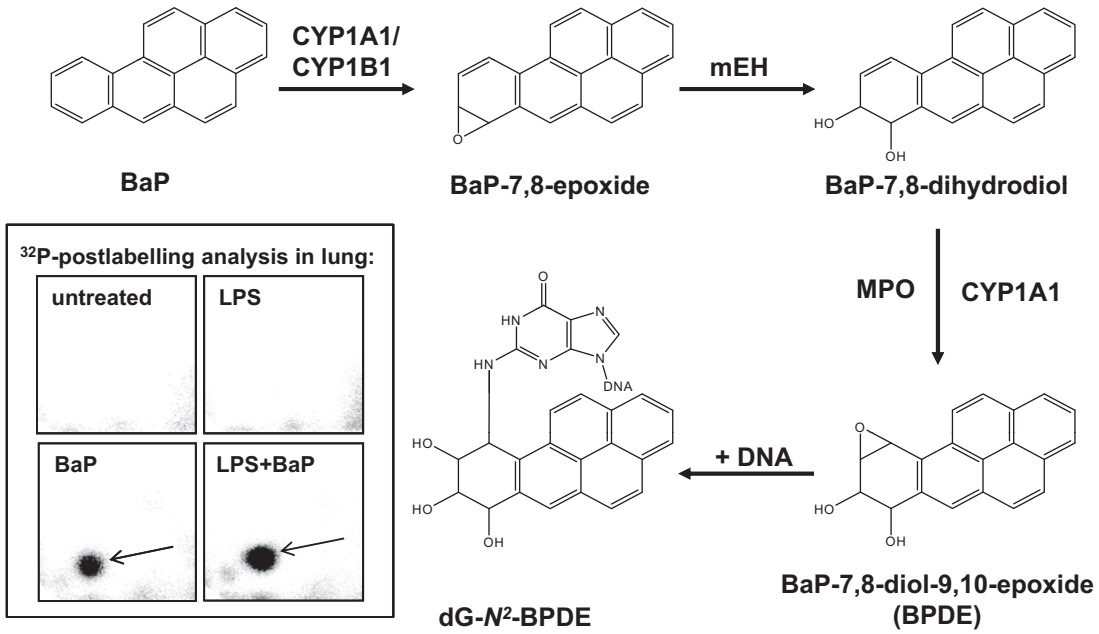


FIG. 1. Main metabolic pathway in the bioactivation and DNA adduct formation of BaP in lung. See text for details. CYP, cytochrome P450; mEH, microsomal epoxide hydrolase; MPO, myeloperoxidase. Inserts: autoradiographic profiles of DNA adducts in lungs formed in mice; the origin, at the bottom left-hand corner, was cut off before exposure. Autoradiographic profiles in the lungs are representative of those observed in the livers. The arrow shows 10-(deoxyguanosin-$N^2$-yl)-7,8,9-trihydroxy-7,8,9,10-tetrahydro-BaP (dG-$N^2$-BPDE).

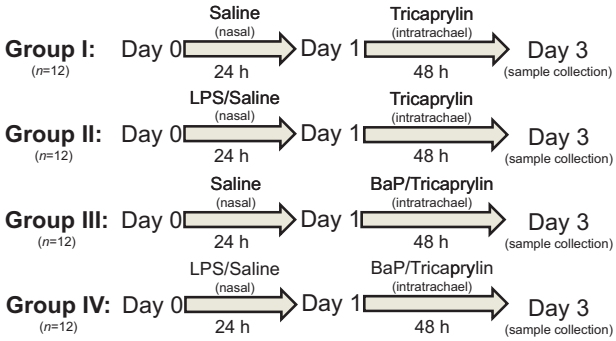


FIG. 2. Study design and animal treatment. See Materials and Methods for additional information.

*Assessment of the pulmonary inflammation by histopathology and BAL analysis*. Fixed lung sections were embedded in paraffin and 7-micron sections were cut and stained with hematoxylin–eosin (H&E) (Arlt *et al.*, 2011). Slides were randomized and analyzed at ×10 magnification for the number of fields with inflammation, expressed as percentage of the total number of fields of lung tissue on the section. At ×40 magnification, inflammation was qualified as either predominantly neutrophilic or predominantly monocytic.

From the collected BAL fluid, a 50-µl aliquot was added to 50 µl of hemolysis (Turk) solution. The total number of cells in the BAL fluid was counted with an improved Neubauer hemocytometer. For differential cell counts, cytospin preparations were prepared from aliquots of BAL fluid (100 µl), centrifuged at 250 × g for 1 min using a Shandon Cytospin 2 (Shandon Southern Instruments, Sewickley, Pennsylvania) at room temperature and stained with Diffquick. Two hundred cells were counted to determine the proportion of neutrophils, eosinophils, and monocytes using standard morphological criteria (Holand *et al.*, 2014).

*Detection of DNA adducts*. DNA from tissue was isolated by a standard phenol–chloroform extraction method. DNA adduct analysis was performed by the nuclease P1 enrichment version of the $^{32}$P-postlabeling method as described previously (Phillips and Arlt, 2007, 2014) with minor modifications. DNA samples (4 µg) were digested with micrococcal nuclease (288 mU; Sigma) and calf spleen phosphodiesterase (1.2 mU; MP Biomedical), and then enriched and labeled as reported. Resolution of $^{32}$P-labeled adducts was performed by polyethyleneimine-cellulose thin-layer chromatography (TLC) (Arlt *et al.*, 2008). After chromatography TLC plates were scanned using a Packard Instant Imager (Dowers Grove, Illinois). DNA adduct levels (RAL, relative adduct labeling) were calculated from adduct counts per minute, the specific activity of [$\gamma$-$^{32}$P]ATP and the amount of DNA (pmol) used. Results were expressed as DNA adducts/$10^8$ normal nucleotides (nt). An external BPDE-modified DNA standard was used to identify BaP-DNA adducts.

*Preparation of pulmonary and hepatic microsomal and cytosolic samples*. Pooled pulmonary and hepatic microsomal and cytosolic fractions ($n = 4$) were isolated as described (Arlt *et al.*, 2008; Martin *et al.*, 2010). Briefly, tissue samples were pulverized by grinding snap-frozen pooled lung or liver specimens in a Teflon container frozen in liquid nitrogen with a steel ball using a dismembrator (2600 UPM for 30 s; Braun Melsungen AG, Germany). The frozen tissue powder was then homogenized by hand in.067 M potassium phosphate buffer (pH 7.4) with 0.5% potassium chloride in a Potter-Elvehjem glass-Teflon homogenizer. The buffer volume (in µl) used was 3 times the weight (in mg) of the organ. Nuclei and debris were removed by centrifugation at 18 × g for 30 min at 4°C. From the supernatant, microsomal pellets were obtained at 100 000 *g* after 1 h. Supernatant (cytosolic fraction) was gently levered off the sediment into 200-µl aliquots and stored at −80°C until further analysis. The sediment (microsomal fraction) was resuspended in phosphate buffer (lung in approximately the same volume (in µl) as their weight

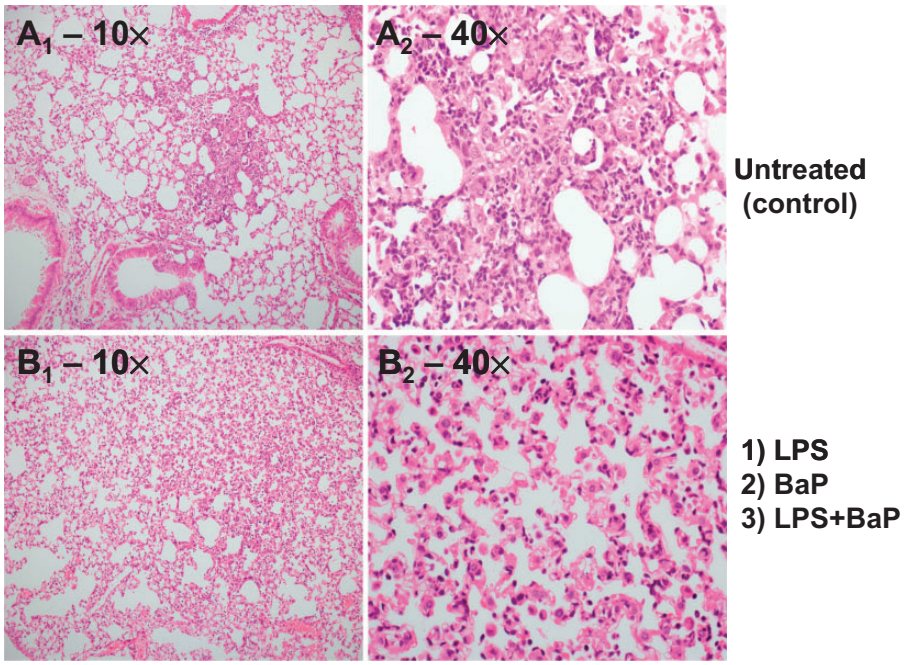


**FIG. 3.** Histological analysis of pulmonary inflammation. Representative photomicrographs of lung tissue section stained with H&E. A, Control mice: small sense foci of predominantly neutrophils; B, LPS-, BaP-, or LPS + BaP-treated lung: large loose foci of predominantly monocytes. Original magnification ×10, left panel; ×40, right panel. Semiquantitative assessment of pulmonary inflammation is summarized in Table 1.

**TABLE 1.** Semiquantitative Assessment of Pulmonary Inflammation From H&E Staining of Lung Sections

| Treatment Group ($n = 4$ per group) | Percentage of Fields with Inflammation (median) | Size of Inflammatory Foci | Predominant Cell Type |
|---|---|---|---|
| Controls (Group I) | 5-14 (6.5) | Small dense | Neutrophils |
| LPS (Group II) | 26-92 (79) | Large loose | Monocytes |
| BaP (Group III) | 4-32 (12.5) | Large loose | Monocytes |
| LPS + BaP (Group IV) | 4-41 (18.5) | Large loose | Monocytes |

(in mg), liver in twice their weight) and small aliquots (100 μl) were stored at −80°C until further analysis. Protein concentrations in cytosolic and microsomal fractions were measured using the bicinchoninic acid protein assay with bovine serum albumin as a standard.

*Expression of pulmonary and hepatic Cyp1 protein.* Immunoquantitation of Cyp1a1 and Cyp1b1 in microsomal fractions was carried out by sodium dodecyl sulfate-10% polyacrylamide gel electrophoresis of samples containing 30 μg microsomal proteins. After migration, proteins were transferred onto polyvinylidenedifluoride membranes. Mouse Cyp1a1 protein was probed with goat-anti rat CYP1A1 polyclonal antibodies (1:2500, Antibodies-online GmbH, Aachen, Germany) as reported elsewhere (Stiborova *et al.*, 2014). The goat-anti rat CYP1A1 antibodies recognize this enzyme in mouse pulmonary and hepatic microsomes as 1 protein band. Rat recombinant CYP1A1 (in Supersomes, Gentest Corp., Woburn, Massachusetts) was used as positive controls to identify the band of Cyp1a1 in murine microsomes. Mouse Cyp1b1 protein was probed with rabbit-anti human CYP1B1 polyclonal antibodies (G-25) (1:200, Santa Cruz Biotechnology, Dallas, Texas). The goat-anti rabbit CYP1B1 antibodies recognize this enzyme as 1 protein band. Human recombinant CYP1B1 (in Supersomes) was used as positive control. The antigen–antibody complex was visualized with an alkaline phosphatase-conjugated rabbit anti-chicken IgG antibody and 5-bromo-4-chloro-3-indolylphosphate/nitrobluetetrazolium as chromogenic substrate (Stiborova *et al.*, 2006). Glyceraldehyde phosphate dehydrogenase was used as loading control and detected by its antibody (1:750, Millipore, Massachusetts). Band intensity was quantified using the GeneTools software.

*Measurement of pulmonary and hepatic Cyp1a enzyme activity.* Microsomal Cyp1a enzyme activity (measured as relative fluorescence unit [RFU]/minute) was determined by following the conversion of 7-ethoxyresorufin into resorufin (EROD assay) using fluorescent measurement on a Synergy HT Plate Reader (Bio-TEK Instruments; 530 nm excitation, 580 nm emission) (Mizerovska *et al.*, 2011). Cyp1a enzyme activity (measured as RFU/minute) was also measured with 3-cyano-7-ethoxycoumarin (CEC) as substrate (Martin *et al.*, 2010). Briefly, in a 96-well plate the incubation mixture (200 μl) contained 67 mM potassium phosphate buffer (pH 7.4), 9 mM glucose-6-phosphate, 0.9 U glucose-6-phosphate dehydrogenase, 4.5 mM magnesium chloride, 0.9 mM NADP, 5 μM CEC (dissolved in DMSO (dimethylsulfoxide)), and 50 μg of microsomal fraction. The reaction was initiated by the addition of CEC and the formation of 3-cyano-7-hydroxycoumarin was measured every 2 min for 30 min (409 nm excitation, 460 nm emission).

*Measurement of pulmonary and hepatic Nqo1 enzyme activity*. Nqo1 enzyme activity in cytosolic samples was measured with menadione (2-methyl-1,4-naphthoquinone) as substrate essentially as described previously (Mizerovska *et al.*, 2011). The standard assay system in a 24-well plate contained in 1 ml (final concentration) 25 mM Tris-HCl (pH 7.5), 0.12 % bovine serum albumin, 200 μM NADH, 10 μM menadione (dissolved in methanol), 77 μM cytochrome c, and 50 μg of cytosolic fraction. The reaction was initiated by the addition of the cytosolic fraction. Enzyme activity (measured as RFU/min) was determined by following the conversion of cytochrome c at 550 nm on a Synergy HT Plate Reader.

*Expression of Cyp1b1 gene expression in the lung*. Gene expression analysis was essentially performed as described (Krais *et al.*, 2015). Briefly, RNA was isolated from lung samples using the GenElute Mammalian Total RNA Mini Prep Kit (Sigma, UK) according to the manufacturer's instruction. Reserve transcription was performed using random primers and SuperScript III Reserve Transcriptase (Life Technologies, UK) RNA expression was analyzed by quantitative real-time polymerase chain reaction (qRT-PCR) using TaqMan Universal PCR Master Mix (Life Technologies) and TaqMan gene expression primers according to the manufacturer's protocol with a 7500HT Fast Real Time PCR System (Applied Biosystems, UK). Probe (Life Technologies) *Cyp1b1*-Mm00487229_m1 was used and expression levels were normalized to housekeeping gene *Gapdh* (4352341E). Relative gene expression was calculated using the comparative threshold cycle ($C_T$) method (Kucab *et al.*, 2012).

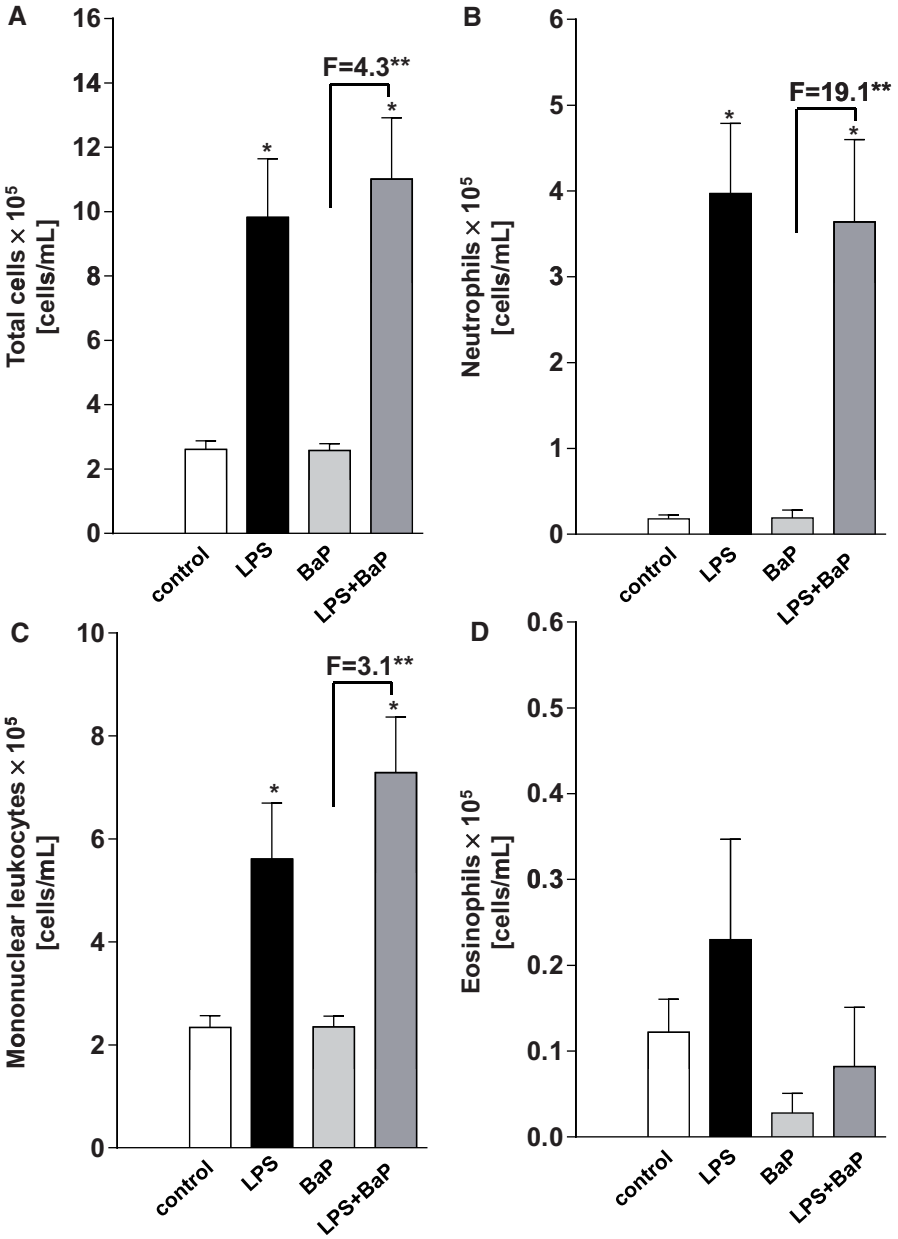


FIG. 4. Effect of BaP treatment on pulmonary inflammation assessing bronchoalveolar lavage fluid. Total (A), neutrophil (B), mononuclear leukocytes (C), and eosinophil (D) cells were quantified by hemocytometry from mice treated with LPS, BaP, LPS + BaP, or vehicle only (control). All values are given as the means ± SEM ($n = 12$ per group). In the figure F = fold difference in cell number in LPS/BaP group compared with cell number in BaP group. Statistical analysis was performed by 2-way ANOVA followed by Tukey's multiple comparisons test (*$P < .05$, vs control [untreated] mice; **$P < .05$, different BaP only treated mice).

*Measurement of nucleotide excision repair capacity*. The ability of nucleotide excision repair (NER)-related enzymes present in isolated tissue extracts to detect and incise substrate DNA containing BPDE-DNA adducts was measured using a modified comet assay (Langie *et al.*, 2006). Tissue protein extracts were prepared as described previously (Gungor *et al.*, 2010a), and protein concentrations were optimized for analysis of lung and liver samples (0.2 mg/ml). The *ex vivo* repair incubation and electrophoresis were performed according to the published protocol (Langie *et al.*, 2006). Dried slides stained with ethidium bromide (10 μg/ml) were viewed with a Zeiss Axioskop fluorescence microscope. Comets were scored using the Comet III system (Perceptive Instruments, UK). Fifty nucleoids were assessed per slide and each sample was analyzed in duplicate. All samples were measured blindly. Tail intensity (% tail DNA) was used to calculate repair capacity of the tissue extracts (Langie *et al.*, 2006).

*Statistical analysis*. Statistical analyses were performed with Prism GraphPad Software and $P < .05$ was considered significant.

## RESULTS

*Pulmonary histopathology*. Pulmonary inflammation 3 days after exposure to LPS was assessed by H&E staining (Fig. 3). The semi-quantitative assessment is summarized in Table 1. The bronchi and vessels in all groups appeared unaffected. In all 4 groups, there were foci of alveolar inflammation (pneumonia), but the size of the foci and the composition of inflammatory cells were different. Controls (Group I) showed few inflammatory foci (5%–14% of fields), which were small in size and composed predominantly of neutrophils. LPS-treated animals (Group II) showed an increase in inflammatory foci (26%–92% of fields) as loose collections mainly of macrophages extending over a larger area. BaP and LPS + BaP treated animals (Groups III and IV) showed an intermediate number of inflammatory foci (4%–32% and 4%–41% respectively), roughly of the same composition and size as seen in the LPS-treated animals (Group II).

*Inflammatory response in BAL*. Using morphological criteria the number of monocytes, eosinophils, and neutrophils were counted in BAL fluid (Fig. 4). LPS treatment (Group II) caused significant increases in neutrophils (Fig. 4B) and mononuclear leucocytes (Fig. 4C) recruitment to the lung relative to control mice (Group I). No such effect was seen for eosinophils (Fig. 4D). The recruitment of neutrophils, used as a measure of pulmonary inflammation, in mice treated with LPS and LPS/BaPwas high (Fig. 4B). In LPS-treated mice (Group II) the number of neutrophils was approximately 22-fold higher than in control mice (Group I) and BaP-treated mice (Group III), however, additional treatment with BaP (Group IV) had no additional effect on

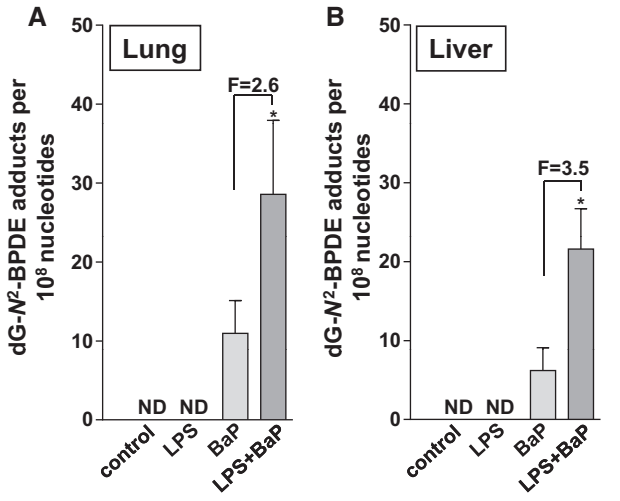


FIG. 5. BaP-DNA adduct formation. DNA adduct levels (RAL, relative adduct labeling) were measured by $^{32}$P-postlabeling in lung (A) and liver (B) of mice treated with LPS, BaP, LPS + BaP, or vehicle only (control). All values are given as the means ± SD ($n = 4$ per group). ND, not detected. In the figure F = fold difference in DNA binding in LPS/BaP group compared with DNA binding in BaP group. Statistical analysis was performed by unpaired 2-tailed *t* test (*$P < .05$, vs BaP only treated mice).

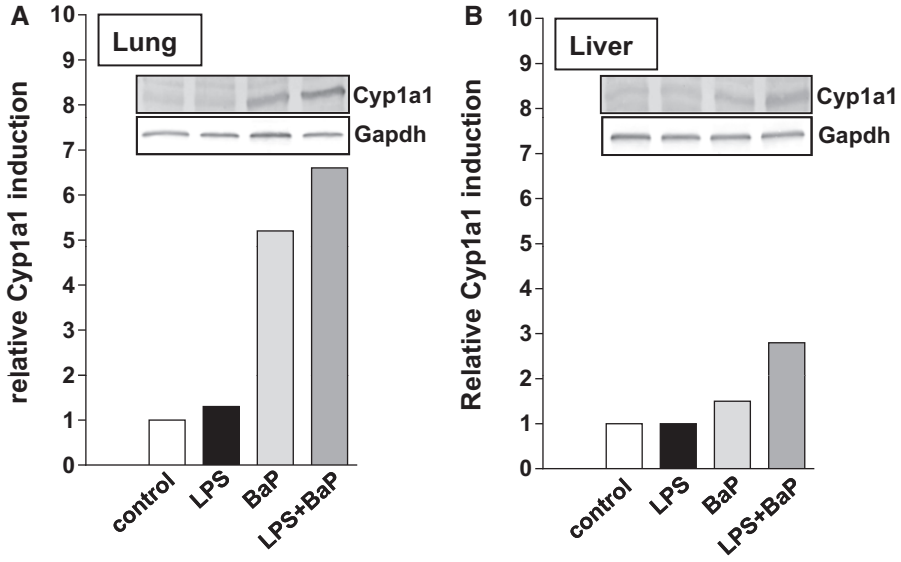


FIG. 6. Western blot analysis of Cyp1a1 protein expression in lung (A) and liver (B) of mice treated with LPS, BaP, LPS + BaP, or vehicle only (control). Representative images of the Western blotting are shown; duplicate analysis was performed on separate occasions. Gapdh protein expression was used as loading control.

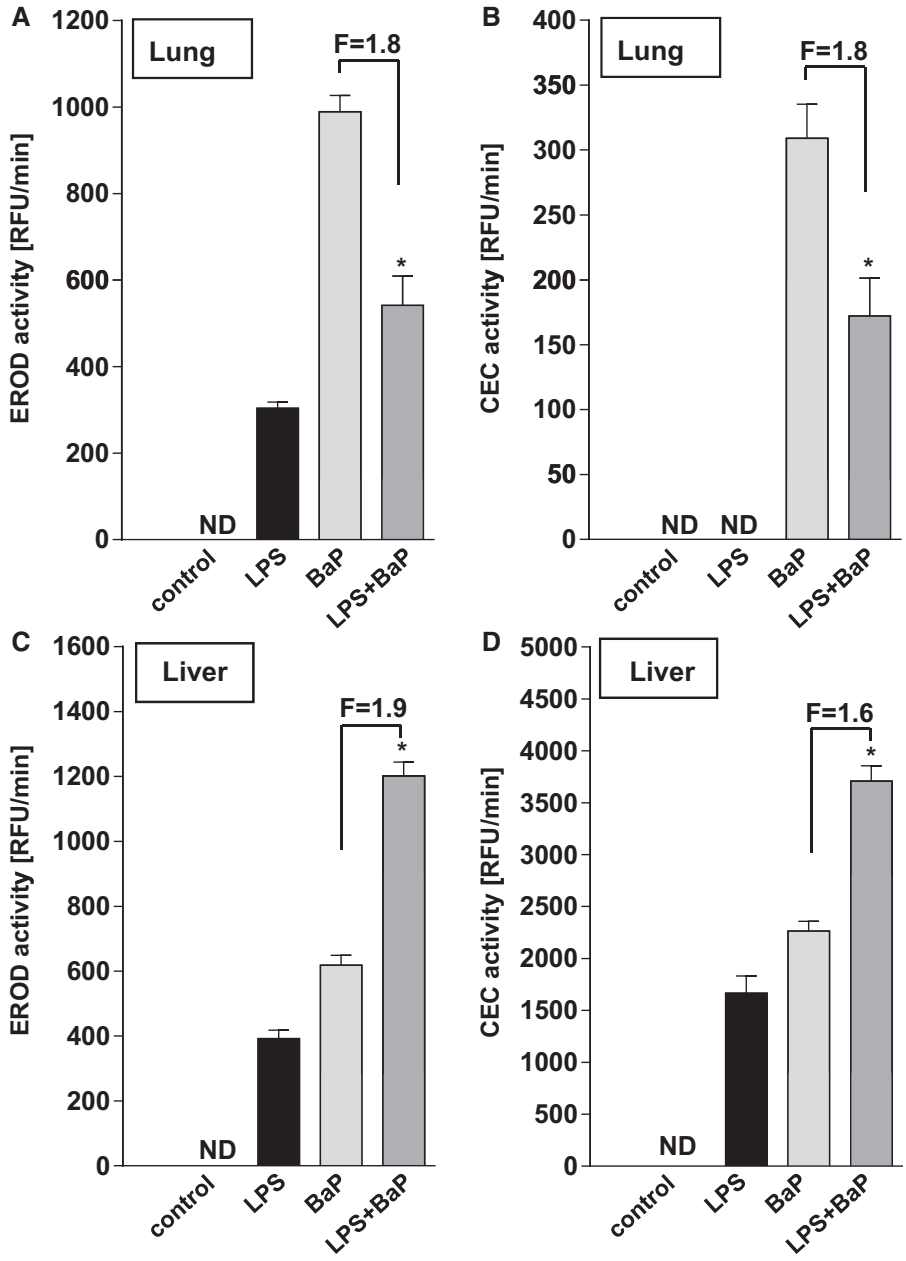


FIG. 7. Effect of BaP treatment on Cyp1a enzyme activity. Cyp1a1 enzyme activity as measured by EROD (A + C) or CEC activity (B + D) in microsomal fractions isolated from lung (A + B) or liver (C + D) tissues of mice treated with LPS, BaP, LPS + BaP, or vehicle only (control). All values are given as the means ± SD of 3 separate determinations. RFU, relative fluorescence unit. ND, not detected. In the figure F = fold difference in enzyme activity in LPS/BaP group compared with enzyme activity in BaP group. Statistical analysis was performed by unpaired 2-tailed t test (*$P < .05$, vs BaP only treated mice).

neutrophil recruitment. More specifically, 2-way ANOVA showed a statistically significant effect of LPS-induced inflammation on neutrophil recruitment [$F(1,41) = 31.11$, $P < .0001$] but was not affected by BaP treatment. There was no significant interaction effect.

*DNA adduct formation in lung and liver*. The DNA adduct pattern observed by TLC $^{32}$P-postlabeling in BaP-treated mice (Groups III and IV) consisted of a single adduct spot, in both lung and liver. Although the $^{32}$P-postlabeling method does not provide any structural information of the BaP-derived DNA adduct formed, using mass spectrometry the adduct formed *in vivo* was previously identified (Arlt *et al.*, 2008) as 10-(deoxyguanosin-$N^2$-yl)-7,8,9-trihydroxy-7,8,9,10-tetrahydro-BaP (dG-$N^2$-BPDE) (Fig. 1; inserts). DNA adducts were not detected either in control (Group I) or in LPS-treated animals (Group II). BaP-DNA adduct levels ranged from 10 to 30 adducts per $10^8$ nt (Fig. 5). Adduct levels were significantly higher in both lung (approximately 2.5-fold) and liver (approximately 3.5-fold) of LPS/BaP-treated mice (Group IV) than in mice treated with BaP alone (Group III).

*Expression of BaP-metabolizing enzymes in lung and liver*. Cyp1a1 protein levels measured by Western blotting showed a approximately 5-fold induction in the lungs after BaP treatment (Group III) (Fig. 6A). Similarly pulmonary Cyp1a1 protein levels increased approximately 5-fold in LPS/BaP-treated mice (Group IV) relative to mice treated with LPS alone (Group II). Even

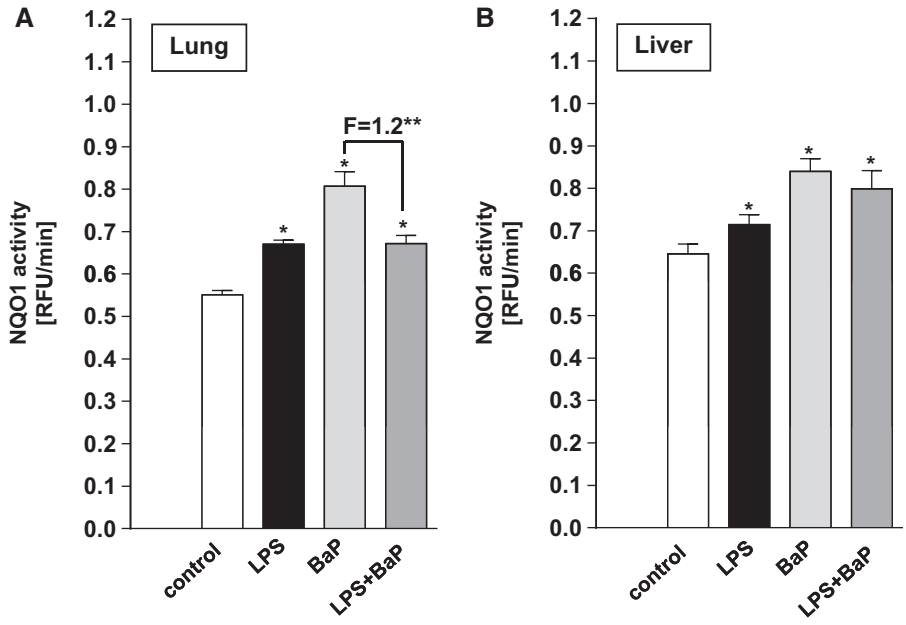


**FIG. 8.** Effect of BaP treatment on Nqo1 enzyme activity. Nqo1 enzyme activity was measured in cytosolic fractions isolated from lung (A) or liver (B) tissues of mice treated with LPS, BaP, LPS + BaP, or vehicle only (control). All values are given as the means ± SD of 3 separate determinations. RFU, relative fluorescence unit. In the figure F = fold difference in enzyme activity in LPS/BaP group compared with enzyme activity in BaP group. Statistical analysis was performed by 2-way ANOVA followed by Tukey's multiple comparisons test (*$P < .05$ vs control [untreated] mice; **$P < .05$, vs BaP only treated mice).

though intensities of the Cyp1a1 protein bands in control (untreated) and LPS-treated mice were weak, a clear increase in Cyp1a1 protein levels was detectable in BaP- and LPS/BaP-treated mice. In accordance with these findings treatment of mice with BaP led to a strong increase in EROD (Fig. 7A) and CEC activity (Fig. 7B) in pulmonary microsomes. Interestingly, pulmonary Cyp1a enzyme activity was significantly lower (approximately 2-fold) in LPS/BaP-treated mice (Group IV) than in mice treated with BaP alone (Group III).

Using Western blotting, we found only a slight increase (approximately 1.5-fold) in Cyp1a1 protein levels in the liver after BaP treatment (Group III) (Fig. 6B). Hepatic Cyp1a1 protein levels increased further in the LPS/BaP-treated mice (Group IV) relative to mice treated with BaP only (Group III). Similarly, hepatic EROD (Fig. 7C) and CEC activity (Fig. 7D) was up to approximately 2-fold higher in LPS/BaP-treated mice (Group IV) compared with mice treated with BaP only (Group III). In addition, LPS exposure alone let to a detectable Cyp1a1 activity in the liver with both substrates (Group II).

As BaP derivates can also be partly metabolized by NQO1, we also determined the activity of Nqo1 in mice exposed to BaP. Nqo1 activity was detected in both lung and liver cytosolic samples of all groups (Fig. 8). Nqo1 enzyme activity was higher after LPS (Group II), BaP (Group III) and LPS/BaP exposure (Group IV) relative to controls (Group I), in both lung (Fig. 8A) and liver (Fig. 8B). Interestingly, pulmonary Nqo1 enzyme activity was significantly lower in LPS/BaP-treated mice (Group IV) than mice treated with BaP alone (Group III), although the magnitude of the effect was modest (1.2-fold) (Fig. 8A). No difference in Nqo1 enzyme activity between the BaP (Group III) and LPS/BaP group (Group IV) was observed in the liver (Fig. 8B).

As previous studies have indicated that CYP1B1 may play a role in the metabolic activation of BaP within inflamed tissue (Smerdova *et al.*, 2013, 2014; Umannova *et al.*, 2008), expression of *Cyp1b1* mRNA in the lung was determined by qRT-PCR. However, as shown in Figure 9A no difference in *Cyp1b1* expression was observed between treatment groups. These results were in line with Cyp1b1 protein expression determined in pulmonary microsomes (Fig. 9B). Only very faint Cyp1b1 protein bands were detectable by Western blotting in all treatment groups (Groups I–IV) which could not be accurately quantified.

*DNA repair capacity in lung and liver*. We assessed whether pulmonary inflammation had an influence on NER activity. We found that in the lung the repair capacity was higher (approximately 4-fold) in LPS-treated mice (Group II) than in controls (Group I) (Fig. 10A). More specifically, 2-way ANOVA of the log-transformed data indicated that pulmonary repair capacity was significantly increased following LPS-induced inflammation [$F(1,8) = 10.9$, $P = .0131$] (Group II) but was not further affected by BaP treatment (Groups III and IV). There was no significant interaction effect.

BaP treatment alone (Group III) had no effect on NER activity. Pulmonary repair capacities in the LPS (Group II) and LPS/BaP (Group IV) groups were similar to each other but not significantly different in the LPS/BaP group (Group IV) relative to controls (Group I) due to large interindividual variability (Fig. 10A). In the liver no significant changes in NER capacity were observed between groups (Fig. 10B).

## DISCUSSION

In this study, we have shown that pulmonary inflammation modulates the bioactivation of BaP and the concomitant respiratory tract DNA damage induced by it. To induce pulmonary inflammation we treated mice with LPS which is an established model to study non-allergic inflammation (Gungor *et al.*, 2010a; Medan *et al.*, 2002; Moriya *et al.*, 2012). The BaP dose used in this study (0.5 mg/mouse) has been shown to induce mutagenicity in the lung of *gpt* delta mice after a single intratracheal instillation (Hashimoto *et al.*, 2005). We found that BaP-induced DNA adduct formation in the lung was approximately 3-fold higher

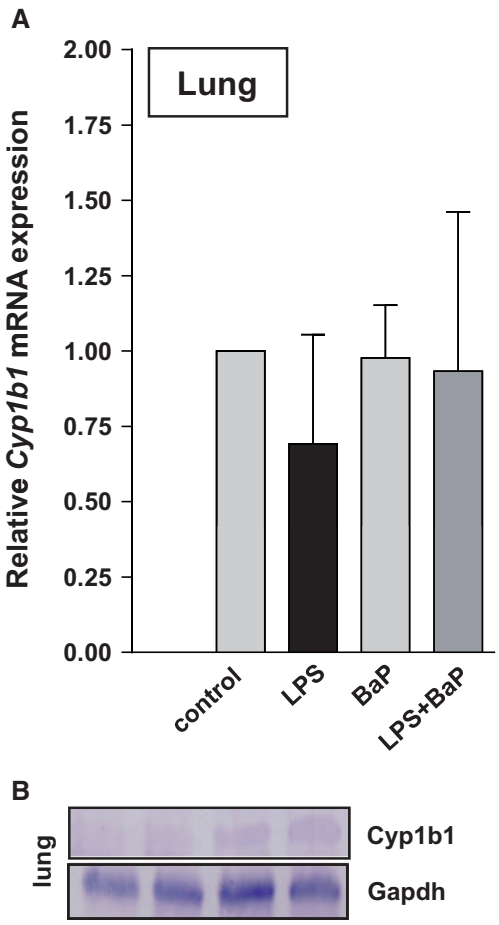


FIG. 9. Expression of Cyp1b1 in the lung of mice treated with LPS, BaP, LPS + BaP, or vehicle only (control). A, Gene expression of *Cyp1b1* assessed by RT-PCR. All values are given as the means ± SD ($n = 4$ per group). For statistical analysis, the relative mRNA expression data were log2 transformed and analyzed using a single sample *t* test with Bonferroni correction against the population control mean of 0; no significant differences were observed. B, Cyp1b1 protein expression determined by Western blot analysis. Representative images are shown; duplicate analysis was performed on separate occasions. Gapdh protein expression was used as loading control.

in LPS/BaP-treated mice compared with mice treated with BaP alone. Considering that inhaled combustion-derived particles such as cigarette smoke, ambient air particulate matter, and diesel exhaust particles contribute to pulmonary inflammation in humans (Kelly and Fussell, 2011) our results demonstrate that pulmonary inflammation could be a critical determinant in the induction of genotoxicity in the lung by particle-bound PAHs like BaP.

Pulmonary inflammation induced by LPS initiates the synthesis of proinflammatory cytokines (Gungor *et al.*, 2010b; Holand *et al.*, 2014). It has been shown that LPS-induced expression of cytokines like TNF-α and interleukin-1β in the liver is associated with altered *CYP* gene expression and CYP enzymes activities during inflammation (Warren *et al.*, 1999). In particular, it has been observed that *Cyp1a1* gene expression is suppressed by LPS and TNF-α in mouse liver and that activation of the nuclear factor-κB (NF-κB) plays an important role in *Cyp1a1* suppression (Ke *et al.*, 2001; Zordoky and El-Kadi, 2009). LPS-mediated decrease of hepatic Cyp1a1 was enhanced and accelerated in mice that lack the aryl hydrocarbon receptor (AhR) (ie, *AhR(−/−)* mice) compared with *AhR(+/+)* mice (Wu *et al.*, 2011). Others have shown that enhanced expression of AhR in the thymus of LPS-treated mice was accompanied by increased Cyp1a1 expression which could be repressed by inhibition of NF-κB (Vogel *et al.*, 2014). Further, induction of Cyp1a1 by LPS in the thymus depended on functional AhR as shown in *AhR(−/−)* mice (Vogel *et al.*, 2014). Together these data show that there is a cross-talk between AhR and inflammatory response that can be critical for the expression of CYP1A1 (Vondracek *et al.*, 2011). However, the observed responses are complex and tissue-specific, but it is noteworthy that PAHs like BaP can induce *Cyp1a1* transcription through binding to AhR (Shimizu *et al.*, 2000; Wang *et al.*, 2011).

In this study, we found a clear induction of Cyp1a1 protein in the lungs after BaP treatment both alone and in combination with LPS. In contrast no change of pulmonary Cyp1a1 protein was observed after LPS treatment alone. Interestingly, pulmonary Cyp1a1 enzyme activity was lower in LPS/BaP-treated mice than in mice treated with BaP alone suggesting that pulmonary inflammation impacted on BaP-induced Cyp1a1 enzyme activity in the lung. Because BaP-DNA adduct levels in the lung were increased in LPS/BaP-treated mice compared with BaP-treated mice this observation may appear puzzling at first. However, previous studies (Arlt *et al.*, 2008, 2012; Nebert *et al.*, 2013) have revealed a paradox, whereby CYP enzymes (particularly CYP1A1) appear to be more important for detoxification of BaP *in vivo*, despite being involved in its metabolic activation *in vitro*. Therefore, the decrease in pulmonary Cyp1a1 enzyme activity in LPS/BaP-treated mice relative to BaP-treated mice, as measured in pulmonary microsomes, led to a decrease in BaP detoxification, thereby enhancing BaP genotoxicity (ie, DNA adduct formation) in the lung. It remains to be investigated how pulmonary inflammation really impacts on Cyp1a1 enzyme activity but not Cyp1a1 protein expression (see below). Some other studies have suggested that CYP1B1 could play a role in the bioactivation of BaP within inflamed tissue as CYP1B1 can be up-regulated by proinflammatory cytokines (ie, TNF-α) in BaP-treated cells *in vitro* and thus may redirect BaP metabolism to form higher amounts of BPDE and to potentiate DNA adduct formation (Smerdova *et al.*, 2013, 2014; Umannova *et al.*, 2008). However, *Cyp1b1* gene expression and Cyp1b1 protein analysis in the lung provided no evidence for an impact of pulmonary inflammation on Cyp1b1-mediated BaP bioactivation *in vivo*.

One mediator that may be involved in the suppression of pulmonary Cyp1a1 enzyme activity after LPS challenge could be the formation of reactive oxygen species (ROS; Morel and Barouki, 1999). In this context it is noteworthy that CYP1A1 can produce ROS during its catalytic cycle (Morel and Barouki, 1999). It has been shown not only that LPS results in increased ROS production but also that ROS suppresses CYP1A1 expression in cultured human cells *in vitro* (Morel and Barouki, 1998). Therefore, it has been proposed that ROS such as hydrogen peroxide are involved in hemoprotein inactivation followed by heme loss (Karuzina and Archakov, 1994a,b). Similarly, BaP *o*-quinones formed during BaP metabolism have been shown to generate ROS (Park *et al.*, 2009). Other potential mechanisms might involve the modification of certain amino acids at or near the active centre of the CYP1A1 enzyme by hydrogen peroxide (Karuzina and Archakov, 1994b). Importantly, inactivated Cyp1a1 protein will retain the epitope for its recognition when assayed by Western blot analysis (El-Kadi *et al.*, 2000) but Cyp1a1 enzyme activity will be lost. Therefore, despite the induction of pulmonary Cyp1a1 protein, as measured by Western blotting in the LPS/BaP-treated mice, we propose that

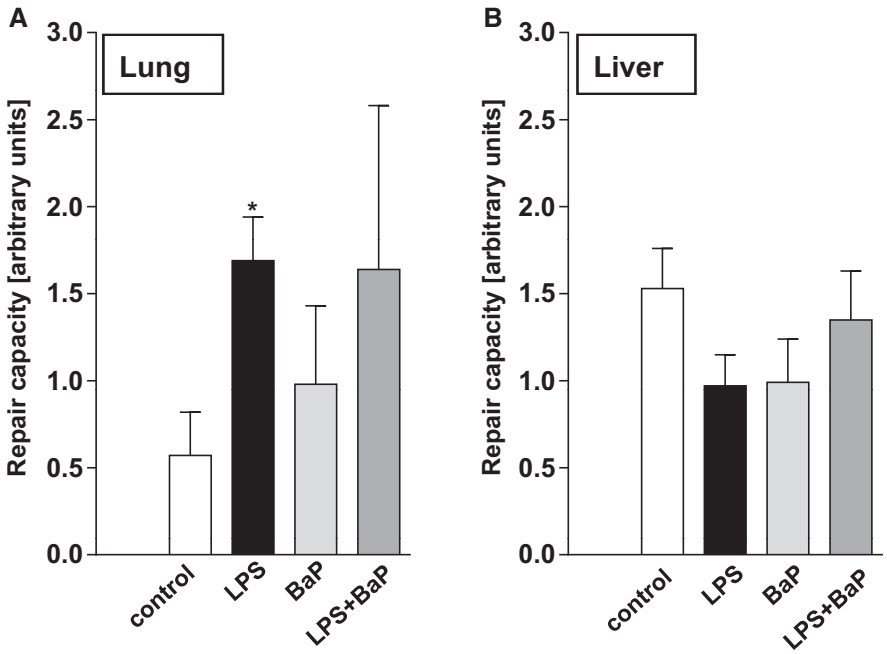


**FIG. 10.** NER repair capacity was measured in tissue extracts isolated from lung (A) or liver (B) tissues of mice treated with LPS, BaP, LPS + BaP, or vehicle only (control). All values are given as the means ± SD ($n = 3$ per group). For statistical analysis, the relative repair capacity data were log-transformed and analyzed by 2-way ANOVA followed by Sidak's multiple comparisons test (*$P < .05$, vs control [untreated] mice).

ROS formation leads to an inhibition of Cyp1a1 enzyme activity under the present experimental conditions.

If BaP is detoxified more slowly by Cyp1a1 in the lungs of LPS/BaP-treated mice, it would be predicted that more BaP circulates via the blood to extra-pulmonary tissues in these mice relative to mice treated with BaP alone. Indeed, we observed higher BaP-DNA adduct levels in the livers of LPS/BaP-treated mice compared with BaP-treated mice. Further, it would be predicted that if in LPS/BaP-treated mice more BaP is transported from the lung via the blood to the liver than in BaP-treated mice, induction of Cyp1a1 protein and Cyp1a1 enzyme activity should be higher in the livers of LPS/BaP-treated mice relative to mice treated with BaP alone. Indeed, we found Cyp1a1 protein induction as well as an increase in Cyp1a1 enzyme activity in the livers of LPS/BaP-treated mice compared with BaP-treated mice, as measured in hepatic microsomes. Thus it would appear that a higher circulation of BaP to the liver results in higher DNA adduct levels, overriding the tendency of increased Cyp1a1 enzyme activity to result in a greater capacity to detoxify BaP. Our results suggest a dual role of Cyp1a1 in both bioactivation and detoxification of BaP *in vivo*. Similarly, a dual role of CYP1A1 has been shown in the metabolism of the plant carcinogen aristolochic acid I (AAI) where CYP1A1 is able to catalyze the reductive activation of AAI to *N*-hydroxyaristolactam I and the oxidative detoxification to 8-hydroxyaristolochic acid (Stiborova *et al.*, 2012, 2014). These results in the liver also indicate that the presence of acute inflammation in 1 organ (ie, lung) can influence the bioavailability of PAHs like BaP in other organs (ie, liver) suggesting a systemic effect.

LPS-induced pulmonary inflammation also impacted on the expression of other xenobiotic-metabolizing enzymes such as Nqo1 which may be important as BaP derivatives can be metabolized by NQO1 (Joseph and Jaiswal, 1994, 1998; Shen *et al.*, 2010). We found that Nqo1 enzyme activity was increased in the lung, after LPS and BaP treatment both alone and in combination. This may be critical for the bioactivation of diesel exhaust particle-bound nitro-PAHs as NQO1 has been shown to be a key enzyme in the metabolic activation of nitro-PAHs (Purohit and Basu, 2000; Stiborova *et al.*, 2010). Interestingly, pulmonary Nqo1 enzyme activity was decreased in LPS/BaP-treated mice relative to BaP-treated mice suggesting that the bioactivation of nitro-PAHs would be suppressed in these animals.

NER is considered to be the main DNA repair pathway for bulky DNA adducts (Friedberg, 2001). Using a modified comet assay, we showed that tissue-specific NER capacity did not contribute to the higher BaP-DNA adduct levels observed in LPS/BaP-treated mice than in BaP-treated mice in either lung or liver. LPS treatment led to a significant increase (approximately 4-fold) in NER capacity in the lung. In contrast, Gungor *et al.* (2010a) found that LPS exposure reduced NER capacity in lung tissue homogenate by approximately 50%. Although the LPS dose used was the same in both studies the discrepancy between the 2 studies might be attributable to the different LPS administration regimes (intratracheal instillation vs intranasal administration) but otherwise it remains unexplained at present.

In summary we found that pulmonary inflammation can impact on enzymes (eg, CYPs) involved the activation and detoxification of PAHs. Our findings suggest that inflammatory signals and carcinogenic PAHs like BaP may interact and that LPS-induced pulmonary inflammation inhibits Cyp1a1 enzyme activity, which leads to increased DNA damage through the enhanced formation of covalent BaP-DNA adducts in the lungs *in vivo*. Thus pulmonary inflammation could be a critical contributor to the induction of genotoxicity by particle-bound PAHs in the lung.

## FUNDING

Work at King's College London is supported by Cancer Research UK (Grant C313/A14329) and the Wellcome Trust

(Grants 101 126/Z/12/Z and 101 126/B/13/Z). A.M.K. was supported by a fellowship from the German Research Foundation (DFG). Work at Charles University was supported by the Czech Science Foundation (Grant 15-02328S). C.C. was supported by the MSc Program in Biomedical and Molecular Sciences Research at King's College London. Q.S. is supported by a personal grant from the Chinese Scholarship Council (CSC).

## REFERENCES

Arlt, V. M., Poirier, M. C., Sykes, S. E., John, K., Moserova, M., Stiborova, M., Wolf, C. R., Henderson, C. J., and Phillips, D. H. (2012). Exposure to benzo[a]pyrene of hepatic cytochrome P450 reductase null (HRN) and P450 reductase conditional null (RCN) mice: detection of benzo[a]pyrene diol epoxide-DNA adducts by immunohistochemistry and 32P-postlabelling. *Toxicol. Lett.* **213**, 160–166.

Arlt, V. M., Stiborova, M., Henderson, C. J., Thiemann, M., Frei, E., Aimova, D., Singh, R., Gamboa da Costa, G., Schmitz, O. J., Farmer, P. B., *et al.* (2008). Metabolic activation of benzo[a]pyrene in vitro by hepatic cytochrome P450 contrasts with detoxification in vivo: experiments with hepatic cytochrome P450 reductase null mice. *Carcinogenesis* **29**, 656–665.

Arlt, V. M., Zuo, J., Trenz, K., Roufosse, C. A., Lord, G. M., Nortier, J. L., Schmeiser, H. H., Hollstein, M., and Phillips, D. H. (2011). Gene expression changes induced by the human carcinogen aristolochic acid I in renal and hepatic tissue of mice. *Int. J. Cancer* **128**, 21–32.

Attfield, M. D., Schleiff, P. L., Lubin, J. H., Blair, A., Stewart, P. A., Vermeulen, R., Coble, J. B., and Silverman, D. T. (2012). The Diesel Exhaust in Miners Study: a cohort mortality study with emphasis on lung cancer. *J. Natl. Cancer Inst.* **104**, 869–883.

Baird, W. M., Hooven, L. A., and Mahadevan, B. (2005). Carcinogenic polycyclic aromatic hydrocarbon-DNA adducts and mechanism of action. *Environ. Mol. Mutagen.* **45**, 106–114.

Borm, P. J., Knaapen, A. M., Schins, R. P., Godschalk, R. W., and Schooten, F. J. (1997). Neutrophils amplify the formation of DNA adducts by benzo[a]pyrene in lung target cells. *Environ. Health Perspect.* **105**(Suppl. 5), 1089–1093.

Brody, J. S., and Spira, A. (2006). State of the art. Chronic obstructive pulmonary disease, inflammation, and lung cancer. *Proc. Am. Thorac. Soc.* **3**, 535–537.

El-Kadi, A. O., Bleau, A. M., Dumont, I., Maurice, H., and du Souich, P. (2000). Role of reactive oxygen intermediates in the decrease of hepatic cytochrome P450 activity by serum of humans and rabbits with an acute inflammatory reaction. *Drug Metab Dispos.* **28**, 1112–1120.

Friedberg, E. C. (2001). How nucleotide excision repair protects against cancer. *Nat. Rev.* **1**, 22–33.

Grivennikov, S. I., Greten, F. R., and Karin, M. (2010). Immunity, inflammation, and cancer. *Cell* **140**, 883–899.

Gungor, N., Haegens, A., Knaapen, A. M., Godschalk, R. W., Chiu, R. K., Wouters, E. F., and van Schooten, F. J. (2010a). Lung inflammation is associated with reduced pulmonary nucleotide excision repair in vivo. *Mutagenesis* **25**, 77–82.

Gungor, N., Pennings, J. L., Knaapen, A. M., Chiu, R. K., Peluso, M., Godschalk, R. W., and Van Schooten, F. J. (2010b). Transcriptional profiling of the acute pulmonary inflammatory response induced by LPS: role of neutrophils. *Respir. Res.* **11**, 24.

Hashimoto, A. H., Amanuma, K., Hiyoshi, K., Takano, H., Masumura, K., Nohmi, T., and Aoki, Y. (2005). In vivo mutagenesis induced by benzo[a]pyrene instilled into the lung of gpt delta transgenic mice. *Environ. Mol. Mutagen.* **45**, 365–373.

Holand, T., Riffo-Vasquez, Y., Spina, D., O'Connor, B., Woisin, F., Sand, C., Marber, M., Bacon, K. B., Rohlff, C., and Page, C. P. (2014). A role for mitogen kinase kinase 3 in pulmonary inflammation validated from a proteomic approach. *Pulm. Pharmacol. Ther.* **27**, 156–163.

IARC (2010). Some non-heterocyclic polycyclic aromatic hydrocarbons and some related exposures. *IARC Monogr. Eval. Carcinog. Risks Hum.* **92**, 1–853.

IARC (2013). Diesel and gasoline engine exhaust and some nitroarenes. *IARC Monogr. Eval. Carcinog. Risks Hum.* **105**, 1–703.

Joseph, P., and Jaiswal, A. K. (1994). NAD(P)H:quinone oxidoreductase$_1$ (DT diaphorase) specifically prevents the formation of benzo[a]pyrene quinone-DNA adducts generated by cytochrome P4501A1 and P450 reductase. *Proc. Natl. Acad. Sci. USA* **91**, 8413–8417.

Joseph, P., and Jaiswal, A. K. (1998). NAD(P)H:quinone oxidoreductase 1 reduces the mutagenicity of DNA caused by NADPH:P450 reductase-activated metabolites of benzo(a)-pyrene quinones. *Br. J. Cancer* **77**, 709–719.

Karuzina, I. I., and Archakov, A. I. (1994a). Hydrogen peroxide-mediated inactivation of microsomal cytochrome P450 during monooxygenase reactions. *Free Radic. Biol. Med.* **17**, 557–567.

Karuzina, I. I., and Archakov, A. I. (1994b). The oxidative inactivation of cytochrome P450 in monooxygenase reactions. *Free Radic. Biol. Med.* **16**, 73–97.

Ke, S., Rabson, A. B., Germino, J. F., Gallo, M. A., and Tian, Y. (2001). Mechanism of suppression of cytochrome P-450 1A1 expression by tumor necrosis factor-alpha and lipopolysaccharide. *J. Biol. Chem.* **276**, 39638–39644.

Kelly, F. J., and Fussell, J. C. (2011). Air pollution and airway disease. *Clin. Exp. Allergy* **41**, 1059–1071.

Knaapen, A. M., Gungor, N., Schins, R. P., Borm, P. J., and Van Schooten, F. J. (2006). Neutrophils and respiratory tract DNA damage and mutagenesis: a review. *Mutagenesis* **21**, 225–236.

Krais, A. M., Mühlbauer, K.-R., Kucab, J. E., Chinbuah, H., Cornelius, M. G., Wei, Q.-X., Hollstein, M., Phillips, D. H., Arlt, V. M., and Schmeiser, H. H. (2015). Comparison of the metabolic activation of environmental carcinogens in mouse embryonic stem cells and mouse embryonic fibroblasts. *Toxicol. in vitro* **29**, 34–43.

Kucab, J. E., Phillips, D. H., and Arlt, V. M. (2012). Metabolic activation of diesel exhaust carcinogens in primary and immortalized human TP53 knock-in (Hupki) mouse embryo fibroblasts. *Environ. Mol. Mutagen.* **53**, 207–217.

Langie, S. A., Knaapen, A. M., Brauers, K. J., van Berlo, D., van Schooten, F. J., and Godschalk, R. W. (2006). Development and validation of a modified comet assay to phenotypically assess nucleotide excision repair. *Mutagenesis* **21**, 153–158.

Loomis, D., Grosse, Y., Lauby-Secretan, B., El Ghissassi, F., Bouvard, V., Benbrahim-Tallaa, L., Guha, N., Baan, R., Mattock, H., Straif, K., *et al.* (2013). The carcinogenicity of outdoor air pollution. *Lancet Oncol.* **14**, 1262–1263.

Martin, F. L., Patel, I. I., Sozeri, O., Singh, P. B., Ragavan, N., Nicholson, C. M., Frei, E., Meinl, W., Glatt, H., Phillips, D. H., *et al.* (2010). Constitutive expression of bioactivating enzymes in normal human prostate suggests a capability to activate pro-carcinogens to DNA-damaging metabolites. *Prostate* **70**, 1586–1599.

Medan, D., Wang, L., Yang, X., Dokka, S., Castranova, V., and Rojanasakul, Y. (2002). Induction of neutrophil apoptosis and secondary necrosis during endotoxin-induced pulmonary inflammation in mice. *J. Cell Physiol.* **191**, 320–326.

Mizerovska, J., Dracinska, H., Frei, E., Schmeiser, H. H., Arlt, V. M., and Stiborova, M. (2011). Induction of biotransformation enzymes by the carcinogenic air-pollutant 3-nitrobenzanthrone in liver, kidney and lung, after intra-tracheal instillation in rats. *Mutat. Res.* **720**, 34–41.

Morel, Y., and Barouki, R. (1998). Down-regulation of cytochrome P450 1A1 gene promoter by oxidative stress. Critical contribution of nuclear factor 1. *J. Biol. Chem.* **273**, 26969–26976.

Morel, Y., and Barouki, R. (1999). Repression of gene expression by oxidative stress. *Biochem. J.* **342**(Pt 3), 481–496.

Moriya, N., Kataoka, H., Fujino, H., Nishikawa, J., and Kugawa, F. (2012). Effect of lipopolysaccharide on the xenobiotic-induced expression and activity of hepatic cytochrome P450 in mice. *Biol. Pharm. Bull.* **35**, 473–480.

Nebert, D. W., Shi, Z., Galvez-Peralta, M., Uno, S., and Dragin, N. (2013). Oral benzo[a]pyrene: understanding pharmacokinetics, detoxication, and consequences—Cyp1 knockout mouse lines as a paradigm. *Mol. Pharmacol.* **84**, 304–313.

Park, J. H., Mangal, D., Frey, A. J., Harvey, R. G., Blair, I. A., and Penning, T. M. (2009) Aryl hydrocarbon receptor facilitates DNA strand breaks and 8-oxo-2'-deoxyguanosine formation by the aldo-keto reductase product benzo[a]pyrene-7,8-dione. *J. Biol. Chem.* **284**, 29725–29734.

Petruska, J. M., Mosebrook, D. R., Jakab, G. J., and Trush, M. A. (1992). Myeloperoxidase-enhanced formation of (+-)-trans-7,8-dihydroxy-7,8-dihydrobenzo[a]pyrene-DNA adducts in lung tissue in vitro: a role of pulmonary inflammation in the bioactivation of a procarcinogen. *Carcinogenesis* **13**, 1075–1081.

Phillips, D. H. (2005). Macromolecular adducts as biomarkers of human exposure to polycyclic aromatic hydrocarbons. In *The Carcinogenic Effects of Polycyclic Aromatic Hydrocarbons* (A. Luch, Ed.), pp. 137–169. Imperial College Press, London.

Phillips, D. H., and Arlt, V. M. (2007). The 32P-postlabeling assay for DNA adducts. *Nat. Protoc.* **2**, 2772–2781.

Phillips, D. H., and Arlt, V. M. (2014). 32P-postlabeling analysis of DNA adducts. *Methods Mol Biol.* **1105**, 127–138.

Purohit, V., and Basu, A. K. (2000). Mutagenicity of nitroaromatic compounds. *Chem. Res. Toxicol.* **13**, 673–692.

Schottenfeld, D., and Beebe-Dimmer, J. (2006). Chronic inflammation: a common and important factor in the pathogenesis of neoplasia. *CA Cancer J. Clin.* **56**, 69–83.

Schwarze, P. E., Totlandsdal, A. I., Lag, M., Refsnes, M., Holme, J. A., and Ovrevik, J. (2013). Inflammation-related effects of diesel engine exhaust particles: studies on lung cells in vitro. *BioMed Res. Int.* **2013**, 685142.

Shen, J., Barrios, R. J., and Jaiswal, A. K. (2010). Inactivation of the quinone oxidoreductases NQO1 and NQO2 strongly elevates the incidence and multiplicity of chemically induced skin tumors. *Cancer Res.* **70**, 1006–1014.

Shimizu, Y., Nakatsuru, Y., Ichinose, M., Takahashi, Y., Kume, H., Mimura, J., Fujii-Kuriyama, Y., and Ishikawa, T. (2000). Benzo[a]pyrene carcinogenicity is lost in mice lacking the aryl hydrocarbon receptor. *Proc. Natl. Acad. Sci. USA* **97**, 779–782.

Silverman, D. T., Samanic, C. M., Lubin, J. H., Blair, A. E., Stewart, P. A., Vermeulen, R., Coble, J. B., Rothman, N., Schleiff, P. L., Travis, W. D., *et al.* (2012). The Diesel Exhaust in Miners Study: a nested case-control study of lung cancer and diesel exhaust. *J. Natl. Cancer Inst.* **104**, 855–868.

Smerdova, L., Neca, J., Svobodova, J., Topinka, J., Schmuczerova, J., Kozubik, A., Machala, M., and Vondracek, J. (2013) Inflammatory mediators accelerate metabolism of benzo[a]pyrene in rat alveolar type II cells: the role of enhanced cytochrome P450 1B1 expression. *Toxicology* **314**, 30–38.

Smerdova, L., Svobodova, J., Kabatkova, M., Kohoutek, J., Blazek, D., Machala, M., and Vondracek, J. (2014). Upregulation of CYP1B1 expression by inflammatory cytokines is mediated by the p38 MAP kinase signal transduction pathway. *Carcinogenesis* **35,** 2534–2543.

Stiborova, M., Barta, F., Levova, K., Hodek, P., Frei, E., Arlt, V. M., and Schmeiser, H. H. (2014). The influence of ochratoxin A on DNA adduct formation by the carcinogen aristolochic acid in rats. *Arch Toxicol.* Sep 11 [Epub ahead of print].

Stiborova, M., Dracinska, H., Hajkova, J., Kaderabkova, P., Frei, E., Schmeiser, H. H., Soucek, P., Phillips, D. H., and Arlt, V. M. (2006). The environmental pollutant and carcinogen 3-nitrobenzanthrone and its human metabolite 3-aminobenzanthrone are potent inducers of rat hepatic cytochromes P450 1A1 and -1A2 and NAD(P)H:quinone oxidoreductase. *Drug Metab. Dispos.* **34**, 1398–1405.

Stiborova, M., Frei, E., Arlt, V. M., and Schmeiser, H. H. (2014) Knockout and humanized mice as suitable tools to identify enzymes metabolizing the human carcinogen aristolochic acid. *Xenobiotica* **44**, 135–145.

Stiborova, M., Levova, K., Barta, F., Shi, Z., Frei, E., Schmeiser, H. H., Nebert, D. W., Phillips, D. H., and Arlt, V. M. (2012) Bioactivation versus detoxication of the urothelial carcinogen aristolochic acid I by human cytochrome P450 1A1 and 1A2. *Toxicol. Sci.* **125**, 345–358.

Stiborova, M., Martinek, V., Svobodova, M., Sistkova, J., Dvorak, Z., Ulrichova, J., Simanek, V., Frei, E., Schmeiser, H. H., Phillips, D. H., *et al.* (2010). Mechanisms of the different DNA adduct forming potentials of the urban air pollutants 2-nitrobenzanthrone and carcinogenic 3-nitrobenzanthrone. *Chem. Res. Toxicol.* **23**, 1192–1201.

Umannova, L., Machala, M., Topinka, J., Novakova, Z., Milcova, A., Kozubik, A., and Vondracek, J. (2008). Tumor necrosis factor-alpha potentiates genotoxic effects of benzo[a]pyrene in rat liver epithelial cells through upregulation of cytochrome P450 1B1 expression. *Mutat. Res.* **640**, 162–169.

Vogel, C. F., Khan, E. M., Leung, P. S., Gershwin, M. E., Chang, W. L., Wu, D., Haarmann-Stemmann, T., Hoffmann, A., and Denison, M. S. (2014). Cross-talk between aryl hydrocarbon receptor and the inflammatory response: a role for nuclear factor-kappaB. *J. Biol. Chem.* **289**, 1866–1875.

Vondracek, J., Umannova, L., and Machala, M. (2011). Interactions of the aryl hydrocarbon receptor with inflammatory mediators: beyond CYP1A regulation. *Curr. Drug Metab.* **12**, 89–103.

Walser, T., Cui, X., Yanagawa, J., Lee, J. M., Heinrich, E., Lee, G., Sharma, S., and Dubinett, S. M. (2008). Smoking and lung cancer: the role of inflammation. *Proc. Am. Thorac. Soc.* **5**, 811–815.

Wang, T., Gavin, H. M., Arlt, V. M., Lawrence, B. P., Fenton, S. E., Medina, D., and Vorderstrasse, B. A. (2011). Aryl hydrocarbon receptor activation during pregnancy, and in adult nulliparous mice, delays the subsequent

development of DMBA-induced mammary tumors. *Int. J. Cancer* **128**, 1509–1523.

Warren, G. W., Poloyac, S. M., Gary, D. S., Mattson, M. P., and Blouin, R. A. (1999). Hepatic cytochrome P-450 expression in tumor necrosis factor-alpha receptor (p55/p75) knockout mice after endotoxin administration. *J. Pharmacol. Exp. Ther.* **288**, 945–950.

Wu, D., Li, W., Lok, P., Matsumura, F., and Vogel, C. F. (2011). AhR deficiency impairs expression of LPS-induced inflammatory genes in mice. *Biochem. Biophys. Res. Commun.* **410**, 358–363.

Zordoky, B. N., and El-Kadi, A. O. (2009). Role of NF-kappaB in the regulation of cytochrome P450 enzymes. *Curr. Drug Metab.* **10**, 164–178.

# *Příloha 5*

Petr Hodek, Johana Hrdinová, Iva Mácová, Pavel Souček, **Iveta Mrízová**, Kamila Burdová, René Kizek, Jiří Hudeček, Marie Stiborová

**PREPARATION AND APPLICATION OF ANTI-PEPTIDE ANTIBODIES FOR DETECTION OR ORPHAN CYTOCHROMES P450**

*Neuro Endocrinol. Lett.* 36 (Suppl. 1), 101-108, 2015

$IF_{2014} = 0.799$

**Neuroendocrinology Letters** Volume 36 Suppl. 1 2015
ISSN: 0172-780X; ISSN-L: 0172-780X; Electronic/Online ISSN: 2354-4716
*Web of Knowledge / Web of Science:* Neuroendocrinol Lett
*Pub Med / Medline:* Neuro Endocrinol Lett

# Preparation and application of anti-peptide antibodies for detection of orphan cytochromes P450

**Petr Hodek [1], Johana Hrdinova [1], Iva Macova [1], Pavel Soucek [2], Iveta Mrizova [1], Kamila Burdova [3], Rene Kizek [4], Jiri Hudecek [1], Marie Stiborova [1]**

1 Department of Biochemistry, Faculty of Science, Charles University in Prague, Czech Republic
2 Centre of Toxicology and Health Safety, National Institute of Public Health, Prague, Czech Republic
3 Institute of Molecular Genetics of the ASCR, v. v. i., Prague, Czech Republic
4 Department of Chemistry and Biochemistry, Faculty of Agronomy, Mendel University of Agriculture and Forestry, Brno, Czech Republic

*Correspondence to:* Prof. RNDr. Petr Hodek CSc.
Department of Biochemistry, Faculty of Science, Charles University, Prague
Albertov 2030, 128 40 Prague 2, Czech Republic.
TEL: +420-221951285, FAX: +420-221951283, E-MAIL: hodek@natur.cuni.cz

*Submitted: 2015-07-18* *Accepted: 2015-09-09* *Published online: 2015-10-15*

*Key words:* **peptide; yolk antibody; immunodetection; cancer; cytochrome P450; cell lines**

Neuroendocrinol Lett 2014; **35**(Suppl. 1):101–108 **PMID:** ----- NEL360915AXX 

## Abstract

**OBJECTIVES:** Cytochromes P450 (CYP) are monooxygenases, which metabolize mostly hydrophobic endogenous and exogenous compounds. CYPs without any clear connection to metabolism are called "orphans". Interestingly, these "orphan" CYPs are over-expressed in tumor tissues. Thus, the main aim of the paper is the development of antibodies for immunodetection of these CYPs as potential malignancy markers.
**METHODS:** Unique sequences of CYP2S1 and 2W1 were selected and peptides synthesized. Chickens were immunized with peptides bound to hemocyanin (KLH). The antibodies were isolated from egg yolks and their reactivity was tested by ELISA. Antibodies were further affinity purified on immobilized peptides. Western blots containing CYP2S1 and 2W1 standards were developed with purified antibodies.
**RESULTS:** Using unique peptide immunogens of CYP2S1 and 2W1 the antibody were developed. As judged from ELISA all chickens produced specific antibodies against the respective peptides. Both affinity purified antibodies against CYP2S1 peptide recognized the CYP2S1 standard on Western blots, but only one of four anti-peptide antibodies against CYP2W1 reacted with CYP2W1 standard. The antibodies were used for the detection of CYPs in cancer cell lines and human tissues samples. Although both CYPs were frequently co-expressed in cancer cells, CYP2S1 was solely induced in the cell line BxPC3, while CYP2W1 was predominantly present in cell lines MCF7 and HeLa. Our data show that anti-peptide antibodies are an indispensable tool for detection of homologous CYPs.
**CONCLUSIONS:** The anti-peptide antibodies successfully recognized CYP2S1 and 2W1 in the cancer cell lines and tissue samples.

ORIGINAL ARTICLE

**Abbreviations**

| | |
|---|---|
| BCIP | - 5-bromo-4-chloro-3′-indolyphosphate |
| CNBr | - cyanogen bromide |
| CYP | - cytochrome P450 |
| ELISA | - enzyme immunosorbent assay |
| IgY | - chicken yolk antibody |
| KLH | - keyhole limpet hemocyanin |
| NBT | - nitro-blue tetrazolium |
| PAGE | - polyacrylamide gel electrophoresis |
| PBS | - sodium phosphate buffered isotonic saline pH 7.4 |
| PBS-Tw | - PBS containing 0.05% Tween 20 |
| SD | - standard deviation |
| SDS | - sodium dodecyl sulfate |
| 3D | - 3-dimensional |

## INTRODUCTION

Cytochromes P450 (CYP) are monooxygenases, which catalyze oxidative metabolism of endogenous (e.g. steroid hormones, prostaglandins, vitamin D, fatty acids) and exogenous compounds (e.g. drugs, carcinogens, pollutants). Of the 57 human CYP genes in 18 families, the members of the CYP1 to CYP4 families oxygenate mainly xenobiotics (and some endogenous compounds), whereas other CYP families are usually involved in highly specific metabolism of endogenous substrates (Nebert & Dalton 2006). There is a battery of CYPs without any clear connection to metabolism. Because of that these CYPs were originally called "orphans", CYPs lacking their specific substrates and functions. They are members of CYP2 and CYP4 families (Guengerich & Cheng 2011). Recently, great efforts have been made to "deorphanization" of these CYPs in respect of reactions they catalyze (Edson *et al.* 2013).

Interestingly, orphan CYPs belong among those which are also over-expressed in cancer cells. Immunochemical analyses indicated that orphan CYP2S1 is highly expressed in many human tumors of epithelial origin (Saarikoski *et al.* 2005). There is growing evidence that CYP2S1 participates in metabolism of retinoids during embryogenesis. Similarly to CYP1 family, the CYP2S1 is inducible by dioxin. In addition to involvement in metabolism of important endogenous substrates CYP2S1 was recently shown that metabolizes naphthalene (Karlgren *et al.* 2005). It is unclear why CYP2S1 is mostly expressed in tissues exposed to the environment, e.g., the gastrointestinal, respiratory, and urinary tracts. Likewise, another orphan CYP2W1 is expressed in several tumors, e.g. of colon and liver, but much less in corresponding normal cells. Moreover, the embryonic expression of CYP2W1 at protein and mRNA levels was confirmed in human fetal colon (Choong *et al.* 2015). The CYP2W1 expression in both colon and liver tumors negatively correlates with the prognosis of cancer patient survival. CYP2W1 can be induced by e.g. the antitumor agent imatinib and thus increased CYP2W1-mediated activation of prodrug (duocarmycin) and efficacy of therapy. However, the role of CYP2W1 in metabolism of endogenic compounds remains unknown. As tumorigenesis and embryogenesis are sharing common pathways the overexpression of CYP2S1 and CYP2W1 in tumors indicates the causal relation between their presence and a cancer progression. Hence, CYP2S1 and CYP2W1 have been suggested as markers of specific cancer development and their prognosis. In addition, these orphan CYPs are promising targets for an immunotherapy and the activation of prodrugs to cytotoxic metabolites in tumor tissues.

To develop an antibody diagnostic tool for detection of CYP2S1 and CYP2W1 expression in clinical tissue samples there are basically two approaches: the first is based on the CYP protein isolated from a biological sample or on the CYP protein recombinantly expressed and purified from cell lysate, the second makes the use of a synthetic peptide derived from the primary structure of the parent CYP protein. However, both ways of antibody preparation suffer from some drawbacks. The limitations of the "protein approach" arise from the difficulties with CYP expression as well as the protein purification. Moreover, because of CYP2S1 and CYP2W1 homology and more than 40% identity in their sequences, the antibody cross-reactivity is likely to occur between these CYPs and potentially among others of the CYP2 family. The "peptide approach" relies on the unique peptide sequence (at least 8 amino acid residues), the hapten, which is characteristic for the particular CYP only. To produce antibodies this peptidic hapten needs to be coupled to macromolecular carrier, usually protein, to prepare an immunogen. Nevertheless, the successful development of anti-peptide antibodies does not guarantee that they will recognize the peptide epitopes in the whole protein, which is on Western blots possibly denatured. Based on the literature data, the probability of generating a successful anti-protein antibody is up to 50%, depending on the peptide length immunogenicity and position in the protein structure (Hancock & O'Reilly 2005). Despite these limitations, anti-peptide antibodies can be extremely useful for protein detection when probing the expression of proteins e.g. on Western blots.

In the present study, we report the preparation of anti-peptide antibodies and their application as a diagnostic tool for detection of CYP2S1 and CYP2W1 expression in cancer cell line and tissue samples. Moreover, rabbit antibodies against CYP2S1 and CYP2W1 proteins were also tested for comparison.

## MATERIAL AND METHODS

### *Chemicals*

Bicinchoninic acid, anti-chicken IgG alkaline phosphatase conjugate, 5-bromo-4-chloro-3'-indolyphosphate/nitro-blue tetrazolium (BCIP/NBT) tablets CNBr-activated Sepharose, and Freund's adjuvant were purchased from Sigma Chemical Co. (St. Louis, MO); p-nitrophenyl phosphate and Tween 20 were from Serva (Heidelberg, Germany); Immobilon-P membrane from

Millipore (Bedford, MA); Pierce mcKLH and SulfoLink Coupling Resin from Thermo Scientific (Rockford, IL). All chemicals used in the experiments were of analytical grade purity or better. Antisera were prepared in rabbits immunized with recombinant CYP2S1 and CYP2W1 (Soucek 1999). Plasmid producing CYP2S1 and 2W1 were kindly provided by Prof. Guengerich (Vanderbilt Universtiy, Nashville, TN). Samples of cell lines and tumor tissues were kindly provided by Dr. Burdova (Institute of Molecular Genetics of the ASCR, CR) and Dr. Soucek (National Institute of Public Health, CR), respectively.

*Peptide selection and immunogen preparation*

Primary structures of human CYP2S1 (Entry #Q96SQ9) and CYP2W1 (Entry #Q8TAV3) were obtained from The UniProt Knowledgebase (http://www.uniprot.org). Their regular structures were calculated by Consensus Secondary Structure Prediction server of PBIL at Lyon-Gerland (https://npsa-prabi.ibcp.fr). Candidate peptide sequences were analyzed by Protein Analysis Tools on the ExPASy server (Gasteiger *et al.* 2005) and evaluated by on-line Invitrogen PeptideSelect service (http://rnaidesigner.lifetechnologies.com/peptide/design.do) and an AbDesigner tool (http://helixweb.nih.gov/AbDesigner/index.jsp). Three-dimensional structures of CYP2S1 and CYP2W1 were modeled by fully automated protein structure homology-modeling server at ExPASy (http://swissmodel.expasy.org) (Biasini *et al.* 2014). Peptide uniqueness was searched against the protein database by BLAST service at The National Center for Biotechnology Information (http://www.ncbi.nlm.nih.gov). Selected peptides were synthesized by biotechnology company VIDIA (Jesenice, CR). To prepare immunogens, peptides were coupled to maleimide-activated keyhole limpet hemocyanin (KLH) *via* their Cys HS-groups according to manufacturer's manual (Thermo Scientific, Rockford, IL). In the case of peptide ending with Lys residue KLH was first modified with maleic anhydride to introduce HOOC-groups and then coupled *via* EDC with the peptide Lys $H_2N$-group (Butler *et al.* 1969).

*Immunization and antibody preparation*

Leghorn hens were immunized weekly by three subcutaneous injections with peptide-KLH conjugates (0.1 mg/dose/animal). The study was conducted in accordance with the Regulations for the Care and Use of Laboratory Animals (311/1997, Ministry of Agriculture, Czech Republic). Pre-immune IgY sample was purified from 6 eggs laid a week prior to immunization and the antigen-specific IgY sample from 6 eggs collected between 5–6 weeks after the immunization. IgY fractions were prepared from egg yolks by technique based on freezing-thawing of the water diluted yolks followed by a specific sodium chloride precipitation of IgY at low pH as described by Hodek *et al.* (2013). For purified IgY, the concentration ($mg.mL^{-1}$) was calculated from the absorbance at 280 nm using the experimentally determined factor of 1.094.

*ELISA*

The antibody immunoreactivity was tested by ELISA. An ELISA plate (Nunc-Maxisorp, Denmark) was coated with 100 µL per well of antigen solution (4 µg peptide. $mL^{-1}$ in 50 $mmol.L^{-1}$ sodium carbonate buffer, pH 9.6) and incubated at 4 °C overnight. After washing 3 times with PBS containing 0.05% Tween 20 (PBS-Tw), each well was loaded with 150 µL of 2% solution of ovalbumin in PBS-Tw and incubated for 1 h at 37 °C. Wells were washed (3 times) with PBS-Tw and then in doublets loaded with 100 µL of antibody solution in PBS (pre-immune and immune IgY preparations, concentration series 3, 10 and 30 $\mu g.mL^{-1}$; affinity purified IgY fractions concentration series 0.3, 1.0, 3.0 and 10 $\mu g.mL^{-1}$). After washing (3 times) with PBS-Tw, 100 µL of alkaline phosphatase-conjugated rabbit anti-chicken IgG in PBS was added to each well (2000 times diluted commercial preparation, Sigma) and incubated at 37 °C for 1 hr. After washing with PBS-Tw, 100 µL of substrate solution (1 $mg.mL^{-1}$ p-nitrophenyl phosphate in carbonate buffer) was added and the plate kept for 10 min at room temperature. Reaction was stopped by 50 µL of 3 $mol.L^{-1}$ NaOH to each well and the color developed was measured at 405 nm with an ELISA reader ELX 800 (Bio-Tek Instruments, Winooski, VT).

*Affinity purification of IgY fractions*

To prepare affinity sorbent sulfhydryl-containing peptides were immobilize to SulfoLink coupling resin (1 mg of peptide per 1 mL of the gel) according to a reference manual. Solutions of anti-peptide CYP2S1 or CYP2W1 antibodies were end-over-end incubated with respective affinity sorbent at 4 °C overnight. The unbound IgY fraction was washed out with 1 $mol.L^{-1}$ NaCl in PBS. The specific anti-peptide antibodies were eluted with 50 $mmol.L^{-1}$ diethylamine (pH 11.5) and collected fractions (1 mL) were neutralized with 1 $mol.L^{-1}$ potassium phosphate pH 6.7). Pooled fractions were dialyzed against PBS with 0.1% sodium azide and stabilized by the addition of bovine serum albumin (1 $mg.mL^{-1}$).

*Western blot analysis*

Western blotting was carried out as described earlier (Krizkova *et al.* 2008, 2009; Hodek *et al.* 2014; Kubickova *et al.* 2014). Protein concentrations in samples of recombinant CYP2S1 and CYP2W1, tissue lysates and sera were determined using the bicinchoninic acid protein assay with bovine serum albumin as the standard (Weichelman *et al.* 1988). The concentration of CYP was estimated according to Omura & Sato (1964) based on the absorption of the complex of reduced CYP with carbon monoxide. For sodium dodecyl sulfate (SDS)-electrophoresis (8% polyacrylamide gel), 15 µg protein/well of cell or tissue lysates were applied. The CYP2S1

and 2W1 proteins were detected by Western blotting on the Immobilon-P membrane (Millipore, Bedford, MA) using specific chicken anti-peptide CYP2S1 and 2W1 antibodies (15–30 μg.mL$^{-1}$ or 1–5 μg.mL$^{-1}$ for affinity purified IgYs). The visualization of protein bands on the membrane was performed using an anti-chicken IgG alkaline phosphatase-conjugated antibody (diluted 1:2,000) and BCIP/NBT substrate tablets (10 mg) for alkaline phosphatase.

## RESULTS AND DISCUSSION

Orphan CYP2S1 and 2W1 are highly homologous and sharing more than 40% sequence identity. Thus to develop specific diagnostic antibodies for the detection of CYP2S1 and 2W1 in cancer cells the approach based on anti-peptide antibodies was chosen.

### *Peptide antigen design and immunogen construction*

CYP2S1 and 2W1 primary structures were analyzed by free bioinformatics web services to design peptide antigens ensuring the production of the CYP specific antibodies. Unique peptides of and 2W1 from sequence regions without any ordered structures having high scores of antigenicity, hydrophilicity and surface probability were selected from N- and C-terminus. The CYP2S1 and 2W1 peptide sequences for immunogen production are shown in Figure 1. In the case that there were no Cys or Lys residues present at any sequence terminus (peptides 2W1-B, 2W1-C or CYP2S1-B) Cys or Lys amino acid was added to provide the HS- or $H_2N$-group for an oriented coupling to carrier protein KLH. To prevent a random coupling of peptide CYP2S1-B to carrier protein KLH was first modified with maleic anhydride to introduce HOOC-groups for EDC-mediated condensation with the peptide Lys or N terminal $H_2N$-groups.

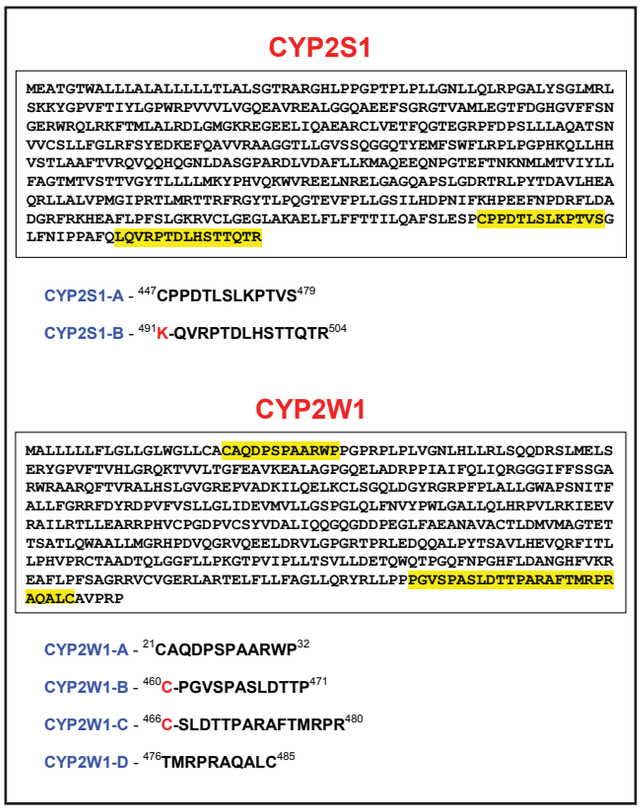


**Fig. 1.** Candidate sequences of CYP2S1 and 2W1 for the specific antibody production. In frames, there are the primary structures of both CYPs. The regions of the peptide selection are in yellow. An additional amino acid residue introduced is marked in red.

### *ELISA and affinity purification of anti-peptide IgYs*

The antibodies were isolated from egg yolks using a water dilution & freezing/thawing technique followed by IgY specific precipitation with 1.5 mol.L$^{-1}$ NaCl at pH 4. Of each chicken immunized with peptide immunogen two fractions, pre-immune IgY (control) and peptide-specific IgY, were prepared. When comparing total amounts of IgY protein per ml of yolks of these two fractions, the IgY production was almost doublet after chicken immunization (ranging 1.58–1.97 folds depending on the chicken). This elevation of IgY contents is in line with the hypersensitization of chickens with complete Freud's adjuvant as well as the formation of antibodies against the carrier protein KLH and also peptide. Then, the peptide specific immune responses of chickens were examined by ELISA. All IgY fractions prepared from egg yolks of immunized chickens were probed for the presence of anti-peptide IgYs using free peptides as coating antigens. The results of ELISA are present in Figure 2. Data indicate that the immunization of chickens with peptide immunogens proceeded successfully as all specific IgY fractions proved to react with corresponding peptide antigens.

Antibody fractions reacting with peptide antigens were further purified on affinity columns prepared by immobilization of peptides on a Sepharose gel. This purification step was carried out in order to prevent cross-reactivity of polyspecific IgYs present in a specific fraction with proteins of mammalian origin in cell or tissue lysates. Severe cross-reactivity of IgY fractions, which interfered with the CYP protein band detection on Western blots, has been described for e.g. human keratin (Macova *et al.* 2013). The progress of the purification of individual anti-peptide IgYs was monitored by IgY protein determination (based on absorbance at 280 nm) and by ELISA with the peptide antigen. Figure 3 shows a representative picture of the affinity chromatography used to prepare highly purified antibodies against two CYP2W1 peptides. To obtain anti-peptide IgY with high avidity towards the antigens loosely bound IgYs were eluted with 1 mol.L$^{-1}$ NaCl prior to the elution of the main specific fraction. When comparing ELISA data for equally diluted IgY fractions before and after the affinity purification the anti-peptide IgY fractions were enriched 15–35 times (data not shown). The yields of affinity purified antibodies were 0.08–0.28% of total IgY amounts applied on the column.

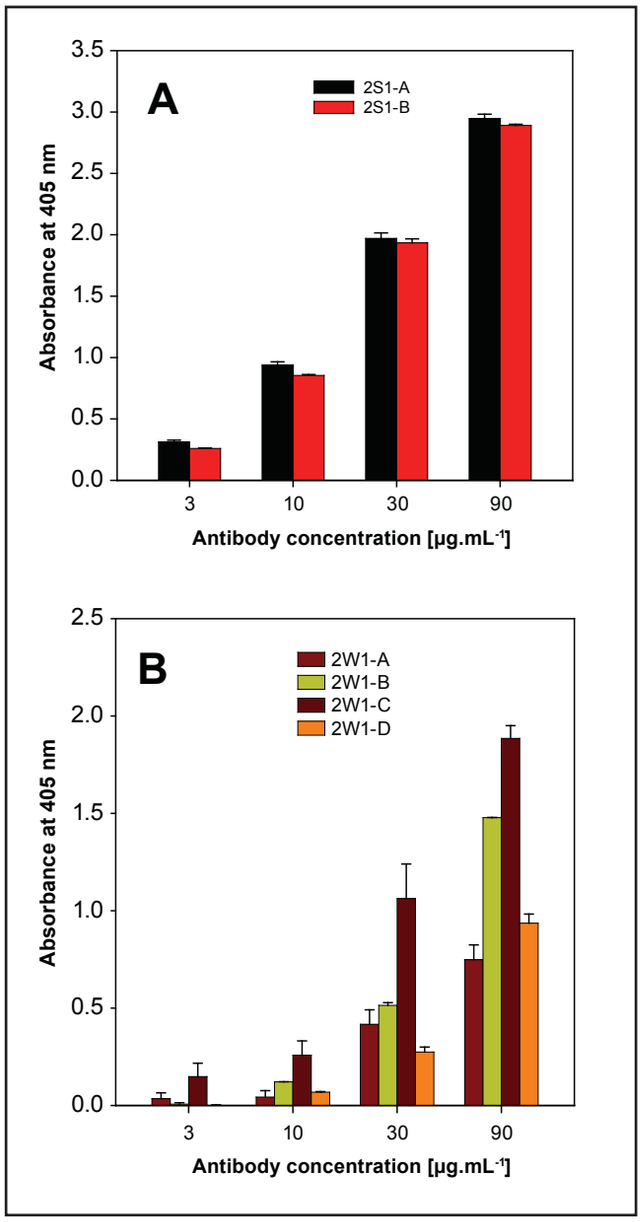


**Fig. 2.** ELISA of anti-peptide antibodies. As antigens peptides CYP2S1-A and CYP2S1-B or CYP2W1-A, CYP2W1-B, CYP2W1-C and CYP2W1-D were used for plates in panels **A** or **B**, respectively. Graph shows absorbance values at 405 nm of specific IgY fractions after subtraction of control values (pre-immune IgYs). The plotted data are means of triplicates ± SD.

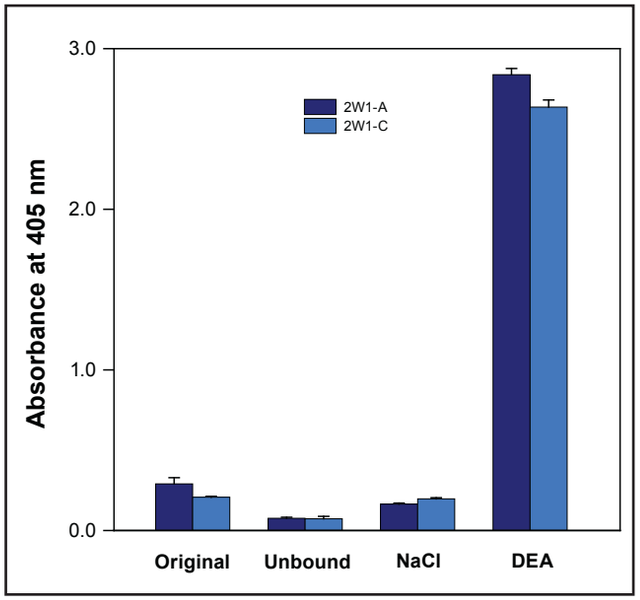


**Fig. 3.** Representative ELISA of IgY affinity chromatography. Anti-peptide antibodies were purified on immobilized peptides CYP2W1-A (dark blue bars) and CYP2W1-C (light blue bars). During the chromatography individual IgY fractions were collected: non-retained (UNBOUND), eluted with 1 mol.L$^{-1}$ NaCl in PBS (NaCl), and eluted with 50 mmol.L$^{-1}$ diethylamine, pH 11.5 (DEA). For comparison a non-purified IgY (ORIGINAL) was included. All IgY fractions were diluted to 10 µg.mL$^{-1}$ of PBS. The plotted data are means of triplicates ± SD.

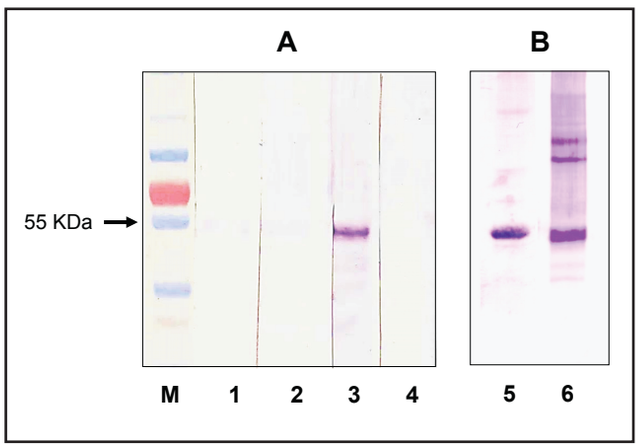


**Fig. 4.** Western blots of CYP2S1 and 2W1. Standards of CYP2W1 (panel **A**) and 2S1 (panel **B**) were electro-transferred on membranes and probed with affinity purified antibodies. Strips **1**, **2**, **3** and **4** containing CYP2W1 standard (2 pmol) were developed with antibodies (1 µg.mL$^{-1}$) against peptides CYP2W1-A, CYP2W1-B, CYP2W1-C and CYP2W1-D, respectively, while trips **5** and **6** containing CYP2S1 standard (1 pmol) were developed with antibodies (2 µg.mL$^{-1}$) against peptides CYP2W1-C and CYP2W1-D, respectively. In strip **M** the position of a protein standard with molecular weight 55 KDa is marked.

### *Western blots of CYP2S1 and 2W1*

All six affinity purified anti-peptide IgYs were tested for their ability to react with the peptide epitope in CYP2S1 and 2W1 standards. Using Western blots, recombinantly expressed CYP standards were probed with anti-peptide IgYs. Both CYP2S1 anti-peptide antibodies reacted with a corresponding CYP standard, while only one of four CYP2W1 anti-peptide antibodies recognized a protein band of a CYP2W1 standard (see Figure 4). By their nature, anti-peptide antibodies are strictly site-directed probes for proteins. Both the sequence and position of the antibody epitope is quite important. Indeed, these antibodies are specific for a given linear peptide epitope occurring in the parent protein. Figure 5 shows the 3-dimensional (3D) homology model of CYP2W1 with highlighted peptides selected for the antibody production. Surprisingly, in the 3D CYP2W1 model the successful peptide epitope

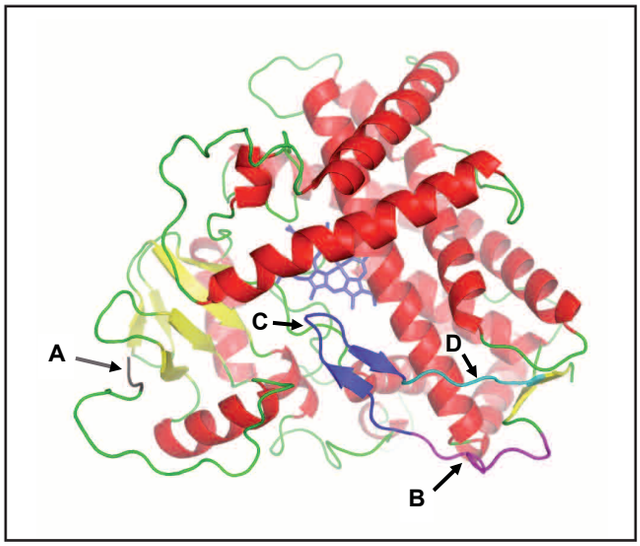


**Fig. 5.** Homology model of CYP2W1. Selected peptides CYP2W1-A (**A**), CYP2W1-B (**B**), CYP2W1-C (**C**) and CYP2W1-D (**D**) for the antibody production are highlighted in grey, magenta, blue and cyan, respectively.

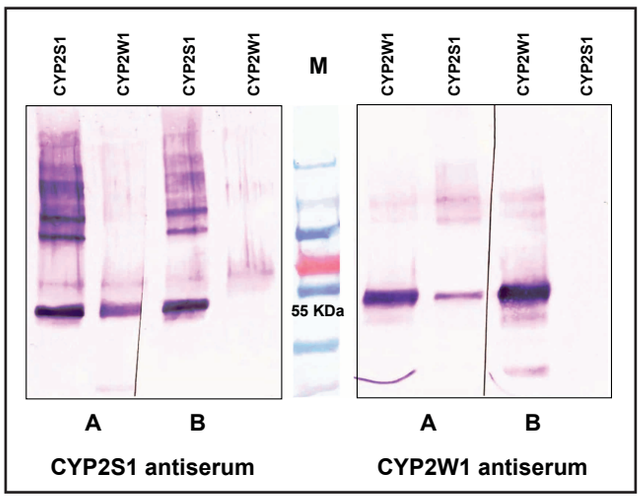


**Fig. 6.** Western blotting of CYP2W1 and CYP2S1 standards with rabbit antisera. Standards of CYP2S1 and 2W1 (1 pmol) were electro-transferred from PAGE to membranes and probed with corresponding rabbit antisera (5 μg.mL$^{-1}$) prior (**A**) and after (**B**) their purification on cross-reacting proteins. In strip **M** the position of a protein standard with molecular weight 55 KDa is marked in blue (bellow the red band).

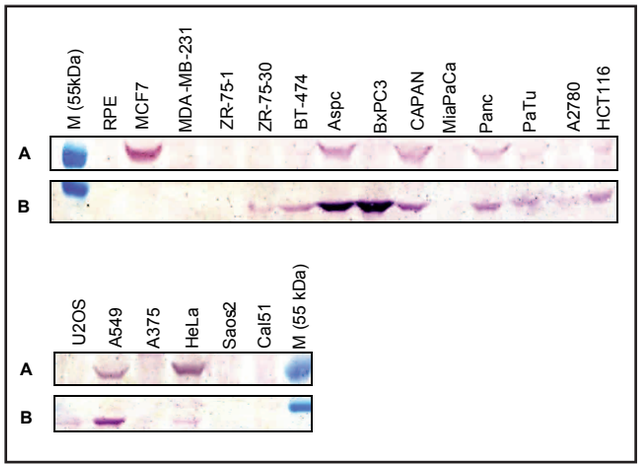


**Fig. 7.** Detection of CYP2W1 and CYP2S1 in biological samples. Western blotting was carried out with cell lysates (30 μg protein per well), which were electro-transferred from PAGE to membranes and probed with affinity purified anti-peptide IgYs against human CYP2W1 and CYP2S1. The abbreviations of the cell samples are explained in Table 1. The line **A** and **B** were developed with anti-peptide antibodies (5 μg.mL$^{-1}$) against human CYP2W1 and CYP2S1, respectively. The position of a protein standard with molecular weight 55 KDa (**M**) is shown in blue.

CYP2W1-C is forming a hairpin loop containing two short antiparallel β-sheets. Likewise, all peptide scores for proceeding CYP2W1-B or following CYP2W1-D peptides were better than those for CYP2W1-C. This precise evaluation of the CYP2W1 sequence part (460–485) clearly documents that *in silico* predictions are of a limited use only. Taking together the results of our antigen predictions have met the 50% probability of successful matches (three functional peptide antigens of six selected) that is in accordance with published data (Hancock & O'Reilly 2005). Finally, it should be noted that CYP2S1 and 2W1 anti-peptide antibodies did not show any cross-reactivity with CYP2W1 and 2S1 standards.

To confirm our results obtained with anti-peptide IgYs identical blots were also developed with rabbit antisera raised against CYP2S1 and 2W1 proteins expressed in *E. coli*. The results shown in Figure 6, however, depict a high cross-reactivity of both antisera with CYP2S1 and 2W1 standards. Furthermore, an antiserum against e.g. CYP2W1 reacted also with a human CYP2B6 standard (data not shown). This cross-reactivity problem of CYP2S1 antiserum was circumvented by trapping of the IgG fraction recognizing CYP2W1 with immobilized CYP2W1 on gel beads and *vise versa* with CYP2W1 antiserum. Although rather high amounts of IgG (47% and 63% for CYP2S1 and 2W1 antisera, respectively) were removed from the original samples, this procedure was necessary to improve the antisera specifity. Blots presented in Figure 6 confirm that the cross-reactivity of rabbit antisera was entirely eliminated by their treatment with crossing antigens. The developed protein bands with higher molecular weights than that of a parent protein are most probable bands of di- and trimers of CYP2S1.

### *Immunodetection of CYP2S1 and 2W1 in biological samples*

Immunoaffinity enriched anti-peptide antibodies were employed for the detection of CYP2S1 and 2W1 expression in cancer cell lines and tissue samples. The results of a Western blot analysis of tumour whole cell lysates are collectively shown in Figure 7. The presence of CYP2W1 was detected in MCF7, Aspc, CAPAN,

Panc, A549 and HeLa cell lysates and in a small amouns in BT-474, PaTu and HCT116 cell lysates (for cell line description see Table 1). A band of unknown identity was observed at approximately 62 kDa at the BxPC3 cell line (not shown). This band may belong to the glycosylated form of the CYP2W1 (Gomez *et al.* 2010). The expression of CYP2S1 protein was determined in Aspc, BxPC3, CAPAN and A549 whole cell lysates. In addition low levels of CYP2S1 expression was observed in ZR-75-30, BT-474, Panc, PaTu, A2780, HCT116, U2OS and HeLa cell lysates, too. It is interesting to note, that the presence of both studied proteins, CYP2W1 and CYP2S1, was determined in the majority of pancreatic tumour (except of MiaPaCa), cervical cancer (HeLa), colorectal cancer (HCT116) and a lung adenocarcinoma (A549) cell lines. On the other hand, the presence of CYP2W1 was determined just in one out of six studied breast cancer cell lines (MCF7) and in the case of CYP2S1 in only two out of six studied breast cancer cell lines (ZR-75-30, BT-474). These findings are consistent with our previous findings, showing CYP2W1 not to be a proper independent biomarker for breast carcinoma, because its expression in breast tumors is not high enough (Hlavac *et al.* 2014). The CYP2W1 may rather be used as diagnostics tool for patients with stages II and III of colorectal cancer (Edler *et al.* 2009), while CYP2S1 may serve as a prognostic marker in both, colorectal and breast cancers (Kumarakulasingham *et al.* 2005; Murray *et al.* 2010). Since the elevated expression of CYP2W1 in pancreatic tumor cells was determined by our anti-peptide antibody as well as by immunohistochemical staining (Uhlen *et al.* 2010) this CYP should be also considered as a specific for pancreatic cancer. Likewise, we found increased levels of CYP2S1 in pancreatic tumor cells (in five out of six cell lines). However this result is inconsistent with immunohistochemical staining of eleven studied pancreas tumor tissue (Uhlen *et al.* 2010).

The present data indicate that the anti-peptide antibodies were successfully employed for the screening of the individual expression of CYP2S1 and 2W1, highly homologous CYPs, in a battery of cell lines and tissue samples. These chicken yolk antibodies may serve as markers of various malignancies.

**Tab. 1.** Human cells used for CYP2S1 and CYP2W1 detection.

| Biological material | Specification |
|---|---|
| RPE | transformed retinal pigment epithelial cell line |
| U2OS | bone osteosarcoma epithelial cell line |
| A549 | lung adenocarcinoma epithelial cell line |
| A375 | malignant melanoma cell line |
| HeLa | cervical cancer cell line |
| Saos-2 | osteosarcoma cell line |
| Cal51 | breast cancer cell lines |
| MCF7 | |
| MDA-MB-231 | |
| ZR-75-1 | |
| ZR-75-30 | |
| BT-474 | |
| Aspc | pancreatic cancer cell lines |
| BxPC3 | |
| CAPAN | |
| MiaPaCa | |
| Panc | |
| PaTu | |
| A2780 | ovarian carcinoma cell line |
| HCT116 | colorectal carcinoma cell lines |

## ACKNOWLEDGMENTS

Supported by MH CZ - DRO (NIPH, 75010330) and by grant P303/12/G163 from the Grant Agency of the Czech Republic.

REFERENCES

1 Biasini M, Bienert S, Waterhouse A, Arnold K, Studer G, Schmidt T, *et al.* (2014). SWISS-MODEL: modelling protein tertiary and quaternary structure using evolutionary information. Nucleic Acids Res. **42**: W252–258.

2 Butler PJ, Harris JI, Hartley BS, Lebeman R (1969). The use of maleic anhydride for the reversible blocking of amino groups in polypeptide chains. Biochem J. **112**: 679–689.

3 Choong E, Guo J, Persson A, Virding S, Johansson I, Mkrtchian S, *et al.* (2015). Developmental regulation and induction of cytochrome P450 2W1, an enzyme expressed in colon tumors. PLoS One. **10**: e0122820.

4 Edler D, Stenstedt K, Ohrling K, Hallström M, Karlgren M, Ingelman-Sundberg M, *et al.* (2009). The expression of the novel CYP2W1 enzyme is an independent prognostic factor in colorectal cancer - a pilot study. Eur J Cancer. **45**: 705–712.

5 Edson KZ, Prasad B, Unadkat JD, Suhara Y, Okano T, Guengerich FP, *et al.* (2013). Cytochrome P450-dependent catabolism of vitamin K: ω-hydroxylation catalyzed by human CYP4F2 and CYP4F11. Biochemistry. **52**: 8276–8285.

6 Gasteiger E, Hoogland C, Gattiker A, Duvaud S, Wilkins MR, Appel RD, *et al.* (2005). Protein identification and analysis tools on the ExPASy Server *in* The proteomics protocols handbook, (Walker JM, ed), Humana Press, pp. 571–607.

7 Gomez A, Nekvindova J, Travica S, Lee MY, Johansson I, Edler D, *et al.* (2010). Colorectal cancer-specific cytochrome P450 2W1: intracellular localization, glycosylation, and catalytic activity. Mol Pharmacol. **78**: 1004–1011.

8 Guengerich FP, Cheng Q (2011). Orphans in the human cytochrome P450 superfamily: approaches to discovering functions and relevance in pharmacology. Pharmacol Rev. **63**: 684–699.

9 Hancock DC, O'Reilly NJ (2005). Synthetic peptides as antigens for antibody production *in* Meth Mol Biol. **295**: Immunochemical Protocols (Burns R, ed) Humana Press, pp. 13–25.

10 Hlavac V, Brynychova V, Vaclavikova R, Ehrlichova M, Vrana D, Pecha V, *et al.* (2014). The role of cytochromes P450 and aldo-keto reductases in prognosis of breast carcinoma patients. Medicine (Baltimore). **93**: e255.

11 Hodek P, Trefil P, Simunek J, Hudecek J, Stiborova M (2013). Optimized protocol of chicken antibody (IgY) purification providing electrophoretically homogenous preparations. Int J Electrochem Sci. **5**: 113–124.
12 Hodek P, Fousova P, Brabencova E, Moserova M, Pavek P, Anzenbacherova E, *et al.* (2014). Effect of dihydromyricetin on benzo[a] pyrene activation in rats. Neuroendocrinol Lett. **35**(Suppl. 2): 158–168.
13 Karlgren M, Miura S, Ingelman-Sundberg M (2005). Novel extrahepatic cytochrome P450s. Toxicol Appl Pharmacol. **207**: 57–61.
14 Krizkova J, Burdova K, Hudecek J, Stiborova M, Hodek P (2008). Induction of cytochromes P450 in small intestine by chemopreventive compounds. Neuroendocrinol Lett. **29**: 717–721.
15 Krizkova J, Burdova K, Stiborova M, Kren V, Hodek P (2009). The effects of selected flavonoids on cytochromes P450 in rat liver and small intestine. Interdiscip Toxicol. **2**: 201–204.
16 Kubickova B, Majerova B, Hadrabova J, Noskova L, Stiborova M, Hodek P (2014) Effect of chicken antibodies on inflammation in human lung epithelial cell lines. Neuroendocrinol Lett. **35**(Suppl. 2): 99–104.
17 Kumarakulasingham M, Rooney PH, Dundas SR, Telfer C, Melvin WT, Curran S, *et al.* (2005). Cytochrome p450 profile of colorectal cancer: identification of markers of prognosis. Clin Cancer Res. **11**: 3758–3765.
18 Macova I, Krizkova J, Frankova J, Stiborova M, Hodek P (2013). Keratin cross-reactivity in electro-transfer (Western blot): How to suppress it. Int J Electrochem Sci. **8**: 1551–1558.
19 Murray GI, Patimalla S, Stewart KN, Miller ID, Heys SD (2010). Profiling the expression of cytochrome P450 in breast cancer. Histopathology. **57**: 202–211.
20 Nebert DW, Dalton TP (2006). The role of cytochrome P450 enzymes in endogenous signalling pathways and environmental carcinogenesis. Nat Rev Cancer. **6**: 947–960.
21 Omura T, Sato R (1964). The carbon monoxide-binding pigment of liver microsomes. I. Evidence for its hemoprotein nature. J Biol Chem. **239**: 2370–2378.
22 Saarikoski ST, Rivera SP, Hankinson O, Husgafvel-Pursiainen K (2005). CYP2S1: a short review. Toxicol Appl Pharmacol. **207**: 62–69.
23 Soucek P (1999). Expression of cytochrome P450 2A6 in *Escherichia coli*, purification, spectral, and catalytic characterization, and preparation of polyclonal antibodies. Arch Biochem Biophys. **370**: 190–200.
24 Uhlen M, Oksvold P, Fagerberg L, Lundberg E, Jonasson K, Forsberg M, *et al.* (2010). Towards a knowledge-based Human Protein Atlas. Nat Biotechnol. 28: 1248–1250.
25 Weichelman KJ, Braun RD, Fitzpatrick JD (1988). Investigation of the bicinchoninic acid protein assay: identification of the groups responsible for color formation. Anal Biochem. **175**: 231–237.

# *Příloha 6*

Marie Stiborová, Michaela Moserová, **Iveta Mrízová**, Helena Dračínská, Václav Martínek, Radek Indra, Eva Frei, Vojtěch Adam, René Kizek, Heinz H. Schmeiser, Kateřina Kubáčková, Volker M. Arlt

**INDUCED EXPRESSION OF MICROSOMAL CYTOCHROME $B_5$ DETERMINED AT mRNA AND PROTEIN LEVELS IN RATS EXPOSED TO ELLIPTICINE, BENZO[A]PYRENE, AND 1-PHENYLAZO-2-NAPHTOL (SUDAN I)**

*Monatsh. Chem.* 147, 897-904, 2016

$IF_{2014}$ = 1.222

Monatsh Chem (2016) 147:897–904
DOI 10.1007/s00706-015-1636-z

ORIGINAL PAPER

# Induced expression of microsomal cytochrome $b_5$ determined at mRNA and protein levels in rats exposed to ellipticine, benzo[*a*]pyrene, and 1-phenylazo-2-naphthol (Sudan I)

**Marie Stiborová[1] · Michaela Moserová[1] · Iveta Mrízová[1] · Helena Dračínská[1] · Václav Martínek[1] · Radek Indra[1] · Eva Frei[1] · Vojtěch Adam[2] · René Kizek[2] · Heinz H. Schmeiser[3] · Kateřina Kubáčková[4] · Volker M. Arlt[5]**

Received: 24 October 2015 / Accepted: 13 December 2015 / Published online: 12 January 2016


**Abstract** The microsomal protein cytochrome $b_5$, which is located in the membrane of the endoplasmic reticulum, has been shown to modulate many reactions catalyzed by cytochrome P450 (CYP) enzymes. We investigated the influence of exposure to the anticancer drug ellipticine and to two environmental carcinogens, benzo[*a*]pyrene (BaP) and 1-phenylazo-2-naphthol (Sudan I), on the expression of cytochrome $b_5$ in livers of rats, both at the mRNA and protein levels. We also studied the effects of these compounds on their own metabolism and the formation of DNA adducts generated by their activation metabolite(s) in vitro. The relative amounts of cytochrome $b_5$ mRNA, measured by real-time polymerase chain reaction analysis, were induced by the test compounds up to 11.7-fold in rat livers. Western blotting using antibodies raised against cytochrome $b_5$ showed that protein expression was induced by up to sevenfold in livers of treated rats. Microsomes isolated from livers of exposed rats catalyzed the oxidation of ellipticine, BaP, and Sudan I and the formation of DNA adducts generated by their reactive metabolite(s) more effectively than hepatic microsomes isolated from control rats. All test compounds are known to induce CYP1A1. This induction is one of the reasons responsible for increased oxidation of these xenobiotics by microsomes. However, induction of cytochrome $b_5$ can also contribute to their enhanced metabolism.

*Graphical abstract*

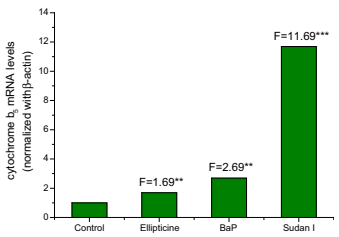


**Keywords** DNA · Drug research · Enzymes · High pressure liquid chromatography

✉ Marie Stiborová
stiborov@natur.cuni.cz

[1] Department of Biochemistry, Faculty of Science, Charles University, Albertov 2030, 128 40 Prague 2, Czech Republic

[2] Department of Chemistry and Biochemistry, Faculty of Agronomy, Mendel University in Brno, 613 00 Brno, Czech Republic

[3] Division of Radiopharmaceutical Chemistry, German Cancer Research Center (DKFZ), Im Neuenheimer Feld 280, 69120 Heidelberg, Germany

[4] Department of Oncology, 2nd Faculty of Medicine, Charles University and University Hospital Motol, V Uvalu 84, 150 06 Prague 5, Czech Republic

[5] Analytical and Environmental Sciences Division, MRC-PHE Centre for Environment and Health, King's College London, London SE1 9NH, UK

## Introduction

Cytochromes $b_5$ are heme proteins which are capable of accepting and transferring a single electron [1]. One cytochrome $b_5$ protein, which is located in the membrane of endoplasmic reticulum (microsomal cytochrome $b_5$), is involved in fatty acid desaturation, cholesterol and plasmalogen biosynthesis, as well as in various hydroxylation reactions catalyzed by cytochrome P450 (CYP) enzymes [1–7]. The endoplasmic reticulum (microsomal) cytochrome $b_5$ is an integral membrane protein located on the

outer surface of this cell compartment [3–5, 8] and consists of two domains, the larger soluble N-terminal heme-binding core and the smaller hydrophobic C-terminal tail, which anchors the protein to the membrane. A 15-amino acid flexible linker connects these two domains providing the heme domain with sufficient mobility to bind different redox partners, whereas the protein remains in the membrane. It has been postulated that the linker, consisting of at least sevenamino acids, is necessary for a productive interaction with CYP enzymes [9].

Cytochrome $b_5$ can accept an electron from either NADH:cytochrome $b_5$ reductase or NADPH:cytochrome P450 (CYP) oxidoreductase (POR) [4, 7, 10] and then reduced cytochrome $b_5$ transfers this electron to CYPs or other enzymes (Fig. 1). The role of microsomal cytochrome $b_5$ in the catalytic function of CYPs has not yet been fully understood. Cytochrome $b_5$ has been shown to be able to stimulate, inhibit or to have no effect on CYP-mediated reactions (reviewed in [2, 6, 7, 10]. One hypothesis trying to explain the influence of cytochrome $b_5$ on CYP reactions suggests a role of cytochrome $b_5$ in the direct transfer of the second electron to the CYP enzyme, which is considered to be the rate-limiting step in the catalytic cycle of the CYP monooxygenase reaction [10]. The electron transfer from reduced cytochrome $b_5$ to CYP is faster than the input of electrons from POR [7, 11]. Another possible mechanism of the cytochrome $b_5$ action is the formation of a complex between cytochrome $b_5$ and CYP, which can receive two electrons from POR in a single step, one for the reduction of CYP and the other for the reduction of cytochrome $b_5$ [7]. While CYP without cytochrome $b_5$ has to undergo two separate interactions with POR to complete one catalytic cycle, in the presence of cytochrome $b_5$ only one single interaction complex of CYP and cytochrome $b_5$ with POR is sufficient; cytochrome $b_5$ provides the second electron to CYP promptly after oxygen binding. Interaction of cytochrome $b_5$ with CYP may also induce conformational changes in CYP proteins leading to the breakdown of the oxygenated hemoprotein complex with substrates to products. This hypothesis is based on findings showing that not only the holoprotein of cytochrome $b_5$, but also its apo-form (devoid of heme) which is not capable of electron transfer, can contribute to stimulation effects [6, 7, 10, 12].

It has become clear from these investigations that the expression levels of cytochrome $b_5$ are crucial for the efficiency of several CYPs to oxidize some xenobiotics. This is also true for the oxidation of the anticancer drug ellipticine and the two environmental carcinogens benzo[*a*]pyrene (BaP) and 1-phenylazo-2-naphthol (Sudan I). The oxidation of these xenobiotics by CYP1A1 and/or 3A4 which dictates their biological effects can be strongly influenced by cytochrome $b_5$ [12–19]. However, the expression levels of cytochrome $b_5$ as well as the regulation of its expression after xenobiotic exposure remains largely unknown. Therefore, in this study we investigated the effect of ellipticine, BaP, and Sudan I on expression of cytochrome $b_5$ in vivo, both at the transcriptional and translational levels. Rats, shown to mimic the metabolism of these compounds in humans [14–25], were used as the animal model.

## Results and discussion

### Expression of cytochrome $b_5$ mRNA and protein levels in rat liver after treatment with ellipticine, BaP, and Sudan I

We examined the effect of exposure of rats to three xenobiotics, the anticancer drug ellipticine and the two environmental carcinogens BaP and Sudan I, on the expression of cytochrome $b_5$ at the mRNA and protein levels in the liver, the major organ responsible for xenobiotic metabolism. We used the real-time polymerase chain reaction (RT-PCR) and Western blotting utilizing antibodies raised against rat cytochrome $b_5$, to measure the mRNA and protein expression levels,

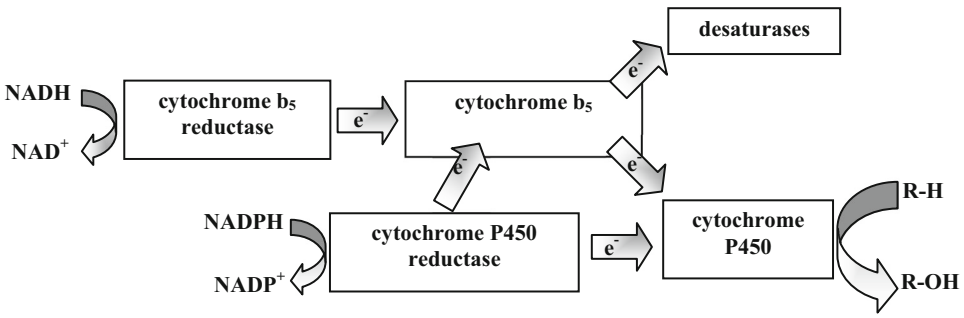


**Fig. 1** Electron transfer between components of the mixed-function oxidase system (adopted from [4])

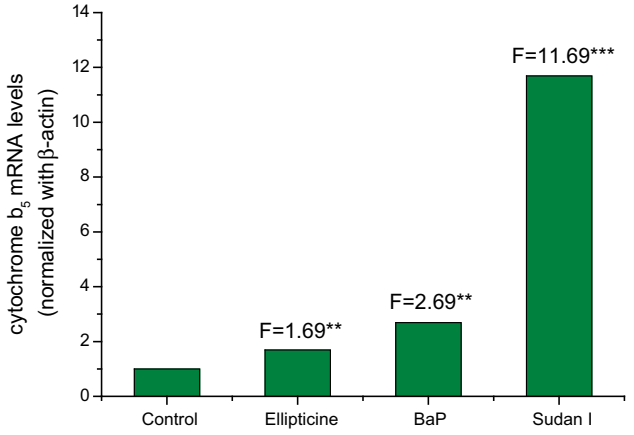


**Fig. 2** Ellipticine-, BaP-, and Sudan I increased expression of cytochrome $b_5$ mRNA in rat livers. Values represent mean ($n = 3$); SDs were less than 10 %. Numbers (F) represent the fold increase over the control in the amounts of mRNA caused by the treatment of rats with ellipticine, BaP, and Sudan I. $^{**}P < 0.01$; $^{***}P < 0.001$ (Student's $t$ test), significantly different from controls

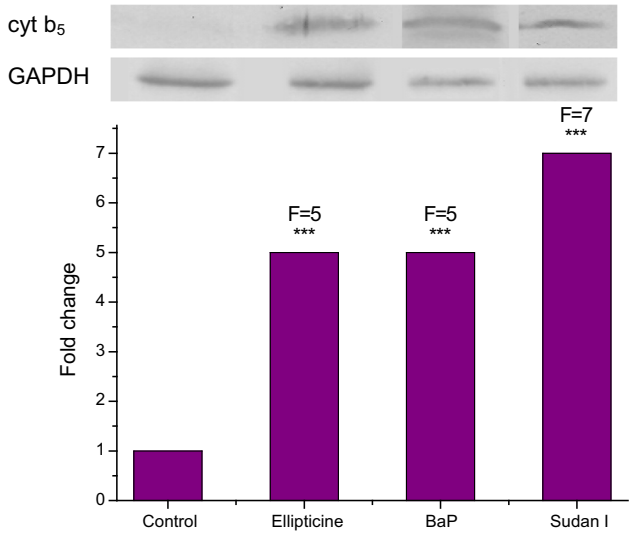


**Fig. 3** Induction of cytochrome $b_5$ protein in livers of untreated (control) rats or rats treated with 40 mg/kg b.w. ellipticine, 125 mg/kg b.w. BaP, and 60 mg/kg b.w. Sudan I determined by Western blotting. *Insert*: Representative immunoblots of hepatic microsomal cytochrome $b_5$ (cyt $b_5$) stained with antibody against rat cytochrome $b_5$; imunoblots of glyceraldehyde phosphate dehydrogenase (GAPDH) that was used as loading control. Control, microsomal fractions of control (untreated) rats. Values represent mean ($n = 3$); SDs were less than 10 %. Numbers (F) represent the fold increase over the control in the amounts of protein caused by the treatment of rats with ellipticine, BaP and Sudan I. $^{***}P < 0.001$ (Student's $t$ test), significantly different from control

respectively. As shown in Fig. 2, treatment of rats with ellipticine, BaP, and Sudan I induced expression of hepatic cytochrome $b_5$ mRNA. The highest induction was seen in the livers of Sudan I-exposed rats, where cytochrome $b_5$ mRNA expression increased more than 11-fold; mRNA expression was up to 1.7- and 2.7-fold higher in rats after treatment with ellipticine and BaP, respectively (Fig. 2).

In addition to the induction of cytochrome $b_5$ mRNA, treatment of rats to the test compounds resulted in an up to sevenfold increase in cytochrome $b_5$ protein levels. This increase in cytochrome $b_5$ protein levels was similar for all compounds tested; ellipticine and BaP both caused a five-fold increase, while Sudan I elevated the level of this protein by sevenfold (Fig. 3).

The differences in cytochrome $b_5$ mRNA and protein induction by individual test xenobiotics might be caused by several phenomena, i.e. a route of administration of test compounds, a dosage scheme and/or different induction potency of these xenobiotics. Since ellipticine, BaP, and Sudan I are strong inducers of CYP1A1, we here used the route of administration and the dosage schemes that were analogous to those utilized in studies evaluating the induction of CYP1A1 mRNA and protein of this enzyme. Under these conditions, the ~34- and ~40-fold increases in expression levels of CYP1A1 protein were due to ellipticine and BaP, respectively [13, 26], whereas higher potency to induce this enzyme was caused by Sudan I; an ~80-fold increase in CYP1A1 protein expression levels was found [27]. These results indicate that the tendency for induction of CYP1A1 by the compounds examined was similar to that of cytochrome $b_5$ found in the present work (see Figs. 2 and 3).

## The effect of the treatment of rats with ellipticine, BaP, and Sudan I on hepatic microsomal oxidation of these compounds and formation of DNA adducts by their reactive metabolite(s)

Using microsomes isolated from the livers of untreated and treated rats, we analyzed the oxidation of the test compounds to their metabolites by HPLC. As shown in Fig. 4, conversion of each of the test compounds to their metabolites by hepatic microsomes was changed by treatment of rats with the examined xenobiotic, thereby indicating that the test compound can influence their own metabolism. The main metabolites formed after the microsomal oxidation of ellipticine are 9-hydroxy-, 12-hydroxy-, 13-hydroxy-, 7-hydroxyellipticine, and ellipticine $N^2$-oxide (Fig. 4A) which is in line with previous studies [28]. Microsomal incubation with Sudan I resulted in the formation of 1-(4-hydroxyphenylazo)-2-naphthol (4′-OH-Sudan I), 1-(phenylazo)-naphthalene-2,6-diol (6-OH-Sudan I), and 1-(4-hydroxyphenylazo)-naphthalene-2,6-diol (4′,6-diOH-Sudan I) (Fig. 4C) which is in accordance with studies published previously [20]. Whereas pretreatment of the rats with ellipticine and Sudan I both resulted in an increase of the metabolites formed by these test compounds in microsomal incubations, the changes in the

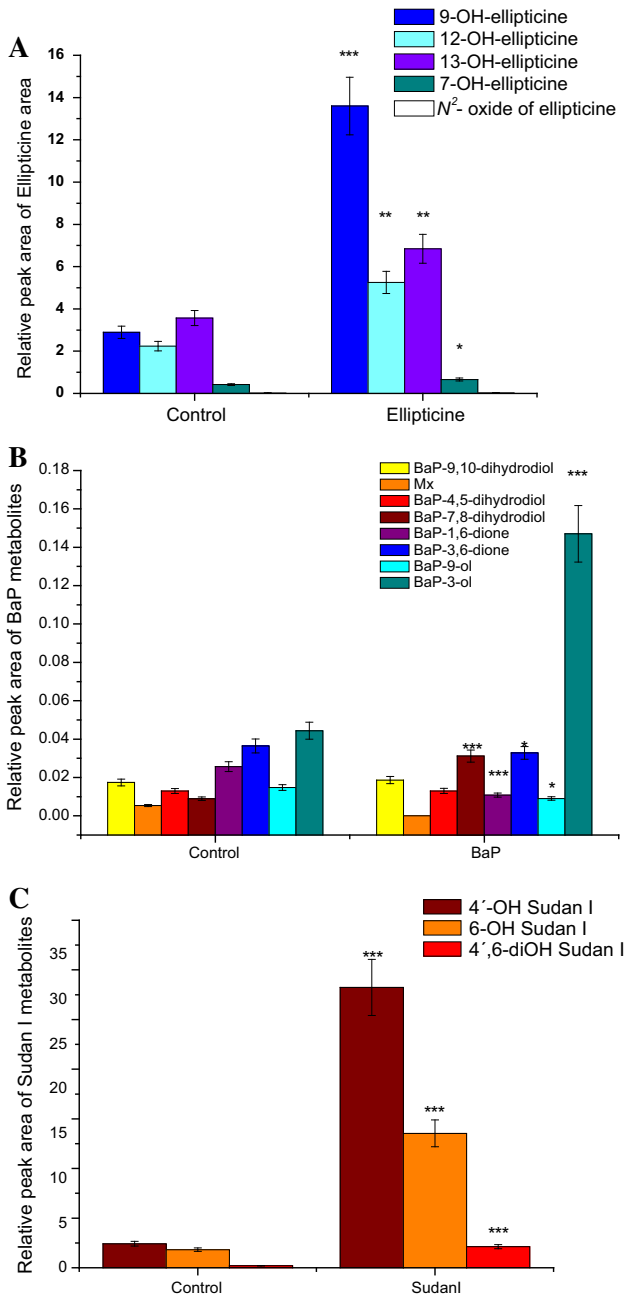


**Fig. 4** Oxidation of ellipticine (**a**), BaP (**b**), and Sudan I (**c**) in microsomes isolated from livers of untreated (control) rats or rats pretreated with 40 mg/kg b.w. ellipticine, 125 mg/kg b.w. BaP, and 60 mg/kg b.w. Sudan I. Values represent mean ± SD from three parallel measurements. $*P < 0.05$, $**P < 0.01$, $***P < 0.001$ (Student's *t* test), significantly different from control

metabolic profile of BaP were more complex (Fig. 4b). The main BaP metabolites structurally identified previously in hepatic microsomal incubation [18] are: BaP-4,5-dihydrodiol, BaP-7,8-dihydrodiol, BaP-9,10-dihydrodiol, BaP-1,6-dione, BaP-3,6-dione, BaP-3-ol, and BaP-9-ol. In addition one metabolite (assigned metabolite Mx) has been found which structure has not yet been identified. The pattern of individual BaP metabolites formed by control microsomes was different from that generated by microsomes isolated from BaP-pretreated rats. While the formation of BaP-7,8-dihydrodiol and BaP-3-ol significantly increased in hepatic microsomal fraction isolated from BaP-pretreated rats, a significant decrease was found for the metabolites BaP-1,6-dione, BaP-3,6-dione, BaP-9-ol, and Mx (Fig. 4b). In this context it is noteworthy that a previous study showed that the formation of BaP-7,8-dihydrodiol and BaP-3-ol in an enzyme system containing rat CYP1A1 was increased by cytochrome $b_5$ [25]. Therefore, the elevated amounts of these BaP metabolites formed by liver microsomes of BaP-pretreated rats (compare Fig. 4b) might therefore be attributable to the BaP-mediated induction of cytochrome $b_5$.

In further experiments, DNA adduct formation by ellipticine, BaP, and Sudan I incubated with microsomes isolated from the livers of untreated and pretreated rats was compared in vitro. Results with ellipticine and Sudan I have been previously published [13, 27, 29]. Ellipticine was activated by these microsomes to form four DNA adducts (data not shown), two of them were identical to those formed by 13-hydroxyellipticine and 12-hydroxyellipticine. Additionally, two minor ellipticine-derived DNA adducts were observed which have been also formed in vivo [22, 24, 30–32] and in vitro in several enzymatic systems including CYP enzymes and peroxidases [21, 23, 31–33], but the low adduct levels have prevented their structural characterization. As shown in Fig. 5 ellipticine-DNA adduct levels generated by hepatic microsomes isolated from ellipticine-pretreated rats were twofold higher than those formed by microsomes isolated from untreated rats [13].

BaP was activated by rat hepatic microsomes to form two DNA adducts (Fig. 5b). The DNA adduct pattern obtained by thin-layer chromatography is shown in the insert of Fig. 5; BaP-derived DNA adducts 1 and 2 were generated by incubation of BaP with DNA and microsomes isolated from livers of both untreated and BaP-pretreated rats. As discussed previously [18, 34], adduct 1 is probably derived from 9-hydroxy-BaP-4,5-epoxide with guanine and adduct 2 formed from BaP-7,8-dihydrodiol-9,10-epoxide with guanine (i.e. 10-(deoxyguanosin-$N^2$-yl)-7,8,9-trihydroxy-7,8,9,10-tetrahydro-BaP; dG-$N^2$-BPDE). Pretreatment of rats with BaP resulted in more than 40- and 15-fold higher levels of DNA adducts 1 and 2 in microsomal incubations, respectively (Fig. 5b).

As shown previously [20, 27, 35], hepatic microsomes isolated from both untreated and Sudan I-pretreated rats incubated with Sudan I and DNA in vitro generated one major DNA adduct and two minor adducts (partly overlapping with the major adduct). The major adduct was previously identified by $^{32}$P-postlabeling to be the 3′,5′-

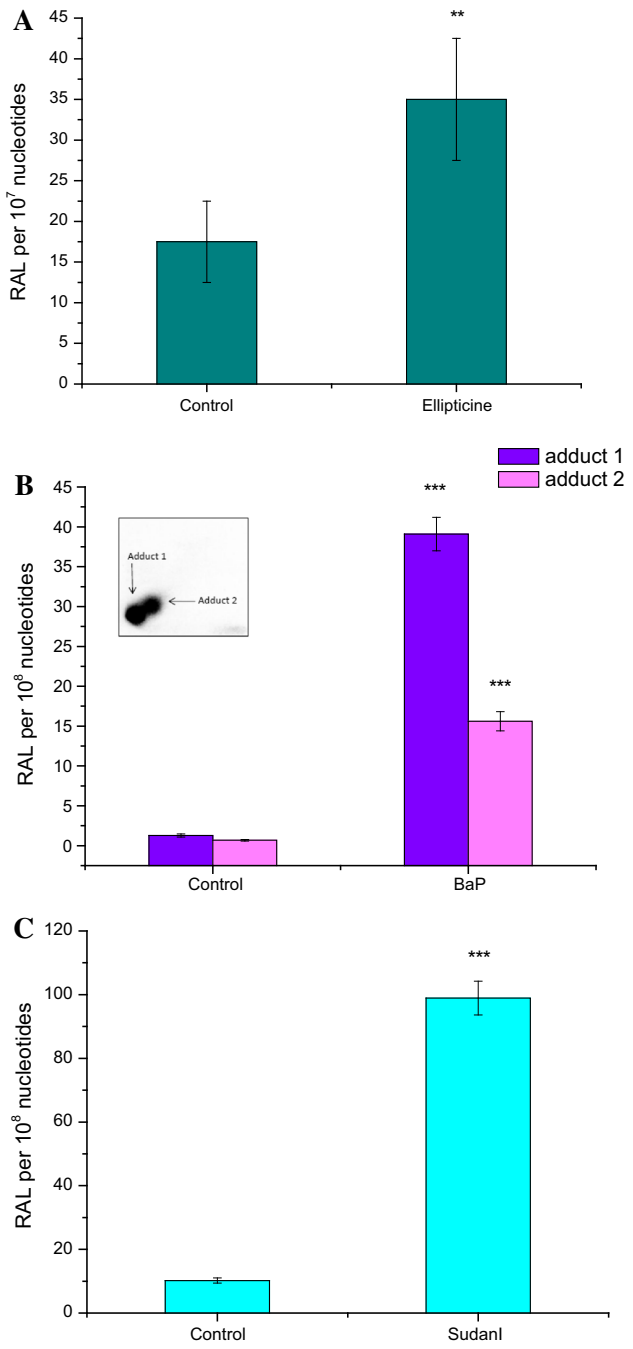


**Fig. 5** DNA adduct formation by ellipticine (**a**), BaP (**b**), and Sudan I (**c**) activated with microsomes isolated from livers of untreated (control) rats or rats pretreated with 40 mg/kg b.w. ellipticine, 125 mg/kg b.w. BaP, and 60 mg/kg b.w. Sudan I. **a** Adduct data has been published previously [13]. **b** *Insert* Autoradiographic profile of BaP-DNA adducts formed by hepatic microsomes of BaP-pretreated rats incubated with BaP and NADPH. The *arrows* show adduct 1 formed from 9-hydroxy-BaP-4,5-epoxide with deoxyguanosine in DNA [18] and dG-$N^2$-BPDE adduct (adduct 2). **c** Adduct data has been published previously [26]. For all panels, values represent mean total RAL (relative adduct labeling) ± SD ($n = 4$; duplicate analyses of two independent in vitro incubations). $^{**}P < 0.01$, $^{***}P < 0.001$ (Student's $t$ test), significantly different from control

bisphospho-derivative of the 8-(phenylazo)deoxyguanosine adduct [20, 29]. Microsomes isolated from livers of Sudan I-pretreated rats were tenfold more efficient to form Sudan I-derived DNA adducts than those from untreated rats (compare Fig. 5c).

The increases in oxidation of ellipticine, BaP, and Sudan I and enhanced DNA adduct formation derived from these compounds by hepatic microsomes isolated from pre-treated rats might be caused by several phenomena. As shown previously, ellipticine, BaP, and Sudan I act as strong inducers of CYP1A1 in livers of several species including rats [13, 14, 27, 35] and all test compounds are substrates of CYP1A1 [13–15, 18, 23–25, 27, 29, 36, 37]. Therefore, induction of CYP1A1 should be one of the reasons responsible for the elevated oxidation of these compounds and higher DNA adduct levels. This was also postulated by us and others in several former studies [13, 14, 27, 35].

However, for ellipticine and BaP, induction of cytochrome $b_5$ also seems to modulate their CYP-mediated metabolism. The results showing an increase in the oxidation of ellipticine to 7-hydroxyellipticine and 9-hydroxyellipticine by pretreatment of rats with this drug (Fig. 4a) are consistent with the fact that their formation is mainly catalyzed by CYP1A1 which is induced by ellipticine treatment [15, 23, 24, 32]. In addition, a twofold increase in the generation of 12-hydroxy- and 13-hydroxyellipticine was observed which, in the absence of cytochrome $b_5$, are mainly formed by CYP3A (Fig. 4a). However, under the increased levels of this protein, caused by its induction in rat liver microsomes, the increase in formation of these ellipticine metabolites seems to be mediated mainly by CYP1A1. Namely, a previous study has shown that cytochrome $b_5$ alters the ellipticine metabolite profile formed by rat CYP1A1, demonstrating that the formation of 12-hydroxyellipticine and 13-hydroxyellipticine by rat CYP1A1 increased significantly by cytochrome $b_5$ [15]. The increase in ellipticine oxidation by hepatic microsomes from the ellipticine-pretreated rats to 12-hydroxy- and 13-hydroxyellipticine also explains the increase in the levels of ellipticine-derived DNA adducts 1 and 2, because these DNA adducts are generated by 12-hydroxy- (adduct 2) and 13-hydroxyellipticine (adduct 1) [23, 31].

## Conclusion

Our study demonstrates that ellipticine, BaP, and Sudan I are capable of inducing cytochrome $b_5$ in the livers of rats exposed to these xenobiotics. Cytochrome $b_5$ mRNA expression was 1.7-, 2.7-, and 11-fold higher by treatment

rats with ellipticine, BaP, and Sudan I, respectively, while 5-, 5- and 7-times higher levels of cytochrome $b_5$ protein were caused by the test xenobiotics. Since cytochrome $b_5$ is important for the oxidation of these xenobiotics by CYP1A1, the induction of both this enzyme and cytochrome $b_5$ by the test compounds exerts a concerted regulatory control on the CYP1A1-mediated oxidation of these xenobiotics, thereby modulating their own pharmacological and genotoxic potency. However, the mechanism of cytochrome $b_5$ induction is not yet known. As shown in several previous studies, all test compounds are ligands of the aryl hydrocarbon receptor (AhR) [13, 14, 18, 27, 32, 35, 38–42], the receptor whose activation is essential for the induction of several xenobiotic-metabolizing enzymes. Consequently, ellipticine, BaP, and Sudan I induce enzymes that are regulated by the activation of AhR such as CYP1A1 and NADPH:quinone oxidoreductase (NQO1) [13, 14, 18, 19, 27, 32, 35]. These findings suggest that the mechanism of induction of cytochrome $b_5$ might be analogous to the induction of these enzymes, namely a mechanism which depends on the activation of AhR. However, this hypothesis needs to be explored in future investigations.

## Experimental

Ellipticine, BaP, and Sudan I (1-(phenylazo)-2-hydroxynaphthalene) were from Sigma Chemical Co (St Louis, MO, USA).

### Animal experiments and isolation of microsomes

All animal experiments were conducted in accordance with the Regulations for the Care and Use of Laboratory Animals (311/1997, Ministry of Agriculture, Czech Republic), which is in compliance with the Declaration of Helsinki. Male Wistar rats (~125–150 g, AnLab, Czech Republic) placed in cages in temperature- and humidity-controlled rooms were acclimatized for 5 days and maintained at 22 °C with a 12 h light/dark period. Standardized diet (ST-1 diet from Velaz, Czech Republic) and water were provided ad libitum. Rats were treated with ellipticine, BaP, and Sudan I as follows: (1) Three 5-week-old male Wistar rats (~125–150 g) were treated i.p. with one dose of 40 mg of ellipticine per kg body weight (b.w.) by intraperitoneal injection as reported previously [13]. Ellipticine was dissolved in sunflower oil/dimethyl sulfoxide (1:1 (v/v), 1 $cm^3$). Three control animals received an equal volume of solvent only [13]. This route of ellipticine administration was used here, because we utilized it in our former study that investigated ellipticine potency to induce CYP1A1 [13]. Rats were killed 48 h after the treatment by cervical dislocation. (2) Three 5-week-old male Wistar rats (~125–150 g) were treated p.o. by gastric gavages with a single dose of 150 mg/kg b.w. BaP dissolved in 1 $cm^3$ sunflower oil as described previously [42]. Animals in the control group were treated with 1 $cm^3$ of sunflower oil only. This route of BaP administration was used, because we utilized it in our former study that investigated potency of BaP to induce CYP1A1 [26]. Rats were killed 24 h after the last treatment by cervical dislocation. (3) Three 5-week-old male Wistar rats (~125–150 g) were injected i.p. with 20 mg/kg b.w. Sudan I dissolved in 1 $cm^3$ maize oil once a day for 3 consecutive days as reported previously [27]. Animals in the control group received the same volume of maize oil on 3 days. This route of Sudan I administration and a dosage scheme were used, because we utilized them in our former study that investigated potency of Sudan I to induce CYP1A1 [27]. Rats were killed 24 h after the last treatment by cervical dislocation. For all treatment groups, livers of the animals were removed immediately after killing, frozen in liquid nitrogen, and stored at −80 °C until isolation of microsomal fractions. Pooled microsomes were prepared from 3 rat livers/group as reported [22, 26, 27]. Microsomal fractions were stored at −80 °C until analysis. Protein concentrations in the microsomal fractions were assessed using the bicinchoninic acid protein assay with bovine serum albumin as a standard [43].

### Content of cytochrome $b_5$ mRNA in rat livers

Total RNA was isolated from another aliquot of frozen organs using Trizol Reagent (Invitrogen, Carlsbad, CA, USA) according to the procedure supplied by the manufacturer. The quality of isolated RNA was verified by horizontal agarose gel electrophoresis, RNA quantity was assessed by UV–Vis spectrophotometry on a Carry 300 spectrophotometer (Varian, Palo Alto, CA, USA). RNA samples (1 μg) were reversely transcribed into cDNA using 200 U of reverse transcriptase per sample with random hexamer primers utilizing RevertAid™ First Strand cDNA Synthesis Kit (MBI Fermentas, Vilnius, Lithuania) according to the manufacturer's instructions. RT-PCR was performed in RotorGene 2000 (Corbett Research, Sydney, Australia) under the following cycling conditions: incubation at 50 °C for 2 min and initial denaturation at 95 °C for 10 min, then 50 cycles of denaturation at 95 °C for 15 s and annealing at 60 °C for 1 min, and elongation for 30 s at 72 °C. Gain was set to 7 and fluorescence was acquired after elongation step. The PCR reaction mixtures (0.02 $cm^3$) contained 0.009 $cm^3$ cDNA diluted 10-times in Milli-Q ultrapure water (Biocel A10, Millipore, Billerica, MA, USA), 0.01 $cm^3$ TaqMan Universal PCR Master Mix (Applied Biosystems, Foster City, CA, USA), and

0.001 $cm^3$ TaqMan Gene Expression Assay Mix (commercially available unlabeled PCR primers and FAM™ dye-labeled probe for rat *cytochrome* $b_5$ as the target gene and *β-actin* as internal reference standard gene). Each sample was analyzed in two parallel aliquots. Negative controls had the same compositions as samples but cDNA was omitted from the mixture. Data were analyzed by the program RotorGene v6 (Corbett Research, Sydney, Australia) and evaluated by comparative cycle threshold ($c_T$) method for relative quantitation of gene expression as described [13].

### Cytochrome $b_5$ protein content in microsomes isolated from rat livers

Microsomes containing 30 µg microsomal proteins were subjected to electrophoresis on the 15 % polyacrylamide gel and applied onto a polyvinylidene fluoride (PVDF) membrane as reported [44]. The membranes were then exposed to specific rabbit polyclonal anti-cytochrome $b_5$ (1:750, AbCam, MA, USA) antibodies overnight at 4 °C and the antigen–antibody complex was visualized with an alkaline phosphatase-conjugated goat anti-rabbit IgG antibody (1:1428, Sigma-Aldrich, USA) and 5-bromo-4-chloro-3-indolylphosphate/nitrobluetetrazolium as chromogenic substrate. Protein bands were expressed as arbitrary units (AU)/mg protein as described previously [14, 19, 20]. Antibody against glyceraldehyde phosphate dehydrogenase (GAPDH) (1:750, Millipore, MA, USA) was used as loading control as recommended by the antibody producer.

### Microsomal incubations to study metabolism of ellipticine, BaP, and Sudan I

Incubation mixtures used to study ellipticine oxidation were performed as described previously [21, 24]. Besides the NADPH-generation system the incubation mixtures contained 0.5 mg protein of pooled hepatic microsomal fraction and 0.01 mmol $dm^{-3}$ ellipticine (dissolved in 0.005 $cm^3$ methanol) in a final volume of 0.5 $cm^3$. The reaction was initiated by adding ellipticine. In the control incubation, ellipticine or NADPH-generating system was omitted from the incubation mixture. After 20 min (37 °C) the reaction was stopped by adding 0.1 $cm^3$ of 2 mol $dm^{-3}$ NaOH. The oxidation of ellipticine has been shown to be linear up to 30 min of incubation [23, 28]. After incubation, 0.005 $cm^3$ of 1 mol $dm^{-3}$ phenacetin in methanol was added as an internal standard and the ellipticine metabolites were extracted twice with ethyl acetate (2 × 1 $cm^3$). Subsequently the solvent was evaporated to dryness, the residues dissolved in 0.025 $cm^3$ methanol and ellipticine metabolites separated by HPLC as described [15, 17, 23, 28].

Incubation mixtures used for studying BaP metabolism by hepatic microsomes contained 100 mmol $dm^{-3}$ potassium phosphate buffer (pH 7.4), NADPH–generating system (1 mmol $dm^{-3}$ $NADP^+$, 10 mmol $dm^{-3}$ D–glucose-6-phosphate, 1 U/$cm^3$ D-glucose-6-phosphate dehydrogenase), 0.5 mg protein of pooled hepatic microsomal fraction and 0.05 mmol $dm^{-3}$ BaP (dissolved in 0.005 $cm^3$ DMSO) in a final volume of 0.5 $cm^3$. The reaction was initiated by adding 0.05 $cm^3$ of the NADPH-generating system. Control incubations were carried out either without microsomes, or without NADPH-generating system, or without BaP. After incubation (37 °C, 20 min), 0.005 $cm^3$ 1 mmol $dm^{-3}$ phenacetin in methanol was added as an internal standard. BaP metabolism by microsomes has been shown to be linear up to 30 min of incubation [18]. BaP metabolites were extracted twice with ethyl acetate (2 × 1 $cm^3$), solvent evaporated to dryness, residues dissolved in 0.025 $cm^3$ methanol and BaP metabolites separated by HPLC as reported [45]. BaP metabolite peaks were collected and analyzed by NMR and/or mass spectrometry as described recently [18].

Incubation mixtures used to study Sudan I oxidation had a final volume of 0.75 $cm^3$, and consisted of 50 mmol $dm^{-3}$ potassium phosphate buffer (pH 7.4), 1 mmol $dm^{-3}$ NADPH, 10 mmol $dm^{-3}$ D-glucose 6-phosphate, 1 unit $cm^{-3}$ D-glucose 6-phosphate dehydrogenase, 10 mmol $dm^{-3}$ $MgCl_2$, 0.5 mg protein of pooled hepatic microsomal fraction, and 0.1 mmol $dm^{-3}$ Sudan I (dissolved in 0.0075 $cm^3$ methanol). After incubation (37 °C, 20 min), Sudan I metabolites were extracted with ethyl acetate (2 × 1 $cm^3$), the extracts evaporated, the residues dissolved 0.025 $cm^3$ in methanol. Sudan I oxidation by microsomes has been shown to be linear up to 30 min [20]. HPLC analysis was performed as described previously [20].

### Determination of DNA adduct formation by ellipticine, BaP, and Sudan I in vitro by $^{32}$P-postlabeling

Incubation mixtures used to assess DNA adduct formation by ellipticine [32], BaP [14], and Sudan I [20, 29] activated with microsomes isolated from rat liver consisted of 50 mmol $dm^{-3}$ potassium phosphate buffer (pH 7.4), 1 mmol $dm^{-3}$ NADPH, 0.5 mg of microsomal proteins, 0.1 mmol $dm^{-3}$ ellipticine, BaP, or Sudan I (all dissolved in 0.0075 $cm^3$ dimethyl sulfoxide), and 0.5 mg of calf thymus DNA in a final volume of 0.75 $cm^3$. The reaction was initiated by adding 0.1 mmol $dm^{-3}$ ellipticine, BaP, or Sudan I. Incubations at 37 °C containing ellipticine, BaP, or Sudan I were carried out for 60, 90, and 60 min, respectively. Ellipticine-, BaP-, and Sudan I-DNA adduct formation has been shown to be linear up to 90 min [14,

16, 20, 29]. Control incubations were carried out either without microsomes, without NADPH, without DNA, or without ellipticine, BaP, or Sudan I. After the incubation, DNA was isolated from the residual water phase by the phenol/chloroform extraction method. DNA adducts were analyzed with the nuclease P1 version of the $^{32}$P-postlabeling technique [32]. Resolution of the adducts by thin-layer chromatography using polyethylenimine-cellulose plates (Macherey and Nagel, Düren, Germany) was carried out as follows: (1) Ellipticine-DNA adducts as reported [13, 32]; (2) BaP-DNA adducts as described [14, 26]; and (3) Sudan I-DNA adducts as reported [27, 29]. DNA adduct levels (RAL, relative adduct labeling) were calculated as described [46].

### Statistical analyses

For statistical data analysis we used Student's *t* test. All *P* values are two-tailed and considered significant at the 0.05 level.

**Acknowledgments** Supported by GACR (Grant 14-8344S) and Charles University (Grant UNCE 204025/2012). Work at King's College London is also supported by Cancer Research UK (Grant Number C313/A14329).

## References

1. Velick SF, Strittmatter P (1956) J Biol Chem 221:265
2. Vergeres G, Ramsden J, Waskell L (1995) J Biol Chem 270:3414
3. Vergeres G, Waskell L (1995) Biochimie 77:604
4. Porter TD (2002) J Biochem Mol Toxicol 16:311
5. Durr UH, Waskell L, Ramamoorthy A (2007) Biochim Biophys Acta 1768:3235
6. Durr UH, Yamamoto K, Im SC, Waskell L, Ramamoorthy A (2007) J Am Chem Soc 129:6670
7. Schenkman JB, Jansson I (2003) Pharmacol Ther 97:139
8. Sobrado P, Goren MA, James D, Amundson CK, Fox BG (2008) Protein Expr Purif 58:229
9. Clarke TA, Im SC, Bidwai A, Waskell L (2004) J Biol Chem 279:36809
10. Guengerich F (2005) Arch Biochem Biophys 440:204
11. Schenkman JB, Jansson I (1999) Drug Metab Rev 31:351
12. Kotrbova V, Aimova D, Ingr M, Borek-Dohalska L, Martinek V, Stiborova M (2009) Protein Expr Purif 66:203
13. Aimová D, Svobodová L, Kotrbová V, Mrázová B, Hodek P, Hudeček J, Václavíková R, Frei E, Stiborová M (2007) Drug Metab Dispos 35:1926
14. Arlt VM, Stiborova M, Henderson CJ, Thiemann M, Frei E, Aimova D, Singhs R, da Costa GG, Schmitz OJ, Farmer PB, Wolf CR, Philips DH (2008) Carcinogenesis 29:656
15. Kotrbova V, Mrazova B, Moserova M, Martinek V, Hodek P, Hudecek J, Frei E, Stiborova M (2011) Biochem Pharmacol 82:669
16. Stiborova M, Martinek V, Schmeiser HH, Frei E (2006) Neuro Endocrinol Lett 27(Suppl 2):35
17. Stiborova M, Indra R, Moserova M, Cerna V, Rupertova M, Martinek V, Eckschlager T, Kizek R, Frei E (2012) Chem Res Toxicol 25:1075
18. Stiborova M, Moserova M, Cerna V, Indra R, Dracinsky M, Šulc M, Henderson CJ, Wolf CR, Schmeiser HH, Phillips DH, Frei E, Arlt VM (2014) Toxicology 318:1
19. Vranová I, Moserová M, Hodek P, Kizek R, Frei E, Stiborová M (2013) Int J Electrochem Sci 8:1586
20. Stiborova M, Martinek V, Rydlova H, Hodek P, Frei E (2002) Cancer Res 62:5678
21. Stiborová M, Stiborová-Rupertová M, Bořek-Dohalská L, Wiessler M, Frei E (2003) Chem Res Toxicol 16:38
22. Stiborová M, Breuer A, Aimová D, Stiborová-Rupertová M, Wiessler M, Frei E (2003) Int J Cancer 107:885
23. Stiborova M, Sejbal J, Bořek-Dohalská L, Aimová D, Poljaková J, Forsterová K, Rupertová M, Wiesner J, Hudeček J, Wiessler M, Frei E (2004) Cancer Res 64:8374
24. Stiborova M, Frei E (2014) Current Med Chem 21:575
25. Indra R, Moserova M, Sulc M, Frei E, Stiborova M (2013) Neuro Endocrinol Lett 34(Suppl 2):55
26. Hodek P, Koblihova J, Kizek R, Frei E, Arlt VM, Stiborova M (2013) Environ Toxicol Pharmacol 36:989
27. Stiborová M, Dračínská H, Martínek V, Svášková D, Hodek P, Milichovský J, Hejduková Ž, Brotánek J, Schmeiser HH, Frei E (2013) Chem Res Toxicol 26:290
28. Stiborová M, Bořek-Dohalská L, Aimová D, Kotrbová V, Kukačková K, Janouchová K, Rupertová M, Ryšlavá H, Hudeček J, Frei E (2006) Gen Physiol Biophys 25:245
29. Stiborová M, Asfaw B, Frei E, Schmeiser HH, Wiessler M (1995) Chem Res Toxicol 8:489
30. Stiborova M, Rupertová M, Aimová D, Ryšlavá H, Frei E (2007) Toxicology 236:50
31. Stiborova M, Poljaková J, Ryšlavá H, Dračínský M, Eckschlager T, Frei E (2007) Int J Cancer 120:243
32. Stiborová M, Rupertová M, Frei E (2011) Biochim Biophys Acta 1814:175
33. Stiborová M, Bieler CA, Wiessler M, Frei E (2001) Biochem Pharmacol 62:1675
34. Krais AM, Speksnijder EN, Melis JP, Indra R, Moserova M, Godschalk RW, van Schooten FJ, Seidel A, Kopka K, Schmeiser HH, Stiborova M, Phillips DH, Luijten M, Arlt VM (2015) Arch Toxicol. doi:10.1007/s00204-015-1531-8
35. Refat NA, Ibrahim ZS, Moustafa GG, Sakamoto KQ, Ishizuka M, Fujita S (2008) J Biochem Mol Toxicol 22:77
36. Stiborová M, Asfaw B, Anzenbacher P, Hodek P (1988) Cancer Lett 40:327
37. Indra R, Moserova M, Kroftova N, Sulc M, Martinkova M, Adam V, Eckschlager T, Kizek R, Arlt VM, Stiborova M (2014) Neuro Endocrinol Lett 35(Suppl 2):105
38. Lubet RA, Connolly G, Kouri RE, Nebert DW, Bigelow SW (1983) Biochem Pharmacol 32:3053
39. Gasiewicz TA, Kende AS, Rucci G, Whitney B, Willey JJ (1996) Biochem Pharmacol 52:1787
40. Chang CY, Puga A (1998) Mol Cell Biol 18:525
41. Nebert DW, Dalton TP, Okey AB, Gonzalez FJ (2004) J Biol Chem 279:23847
42. Endo K, Uno S, Seki T, Ariga T, Kusumi Y, Mitsumata M, Yamada S, Makishima M (2008) Toxicol Appl Pharmacol 230:135
43. Wiechelman KJ, Braun RD, Fitzpatrick JD (1988) Anal Biochem 75:231
44. Arlt VM, Poirier MC, Sykes SE, Kaarthik J, Moserova M, Stiborova M, Wolf R, Henderson CJ, Phillips DH (2012) Toxicol Lett 213:160
45. Moserova M, Kotrbova V, Aimova D, Sulc M, Frei E, Stiborova M (2009) Interdisc Toxicol 2:239
46. Schmeiser HH, Stiborova M, Arlt VM (2013) Methods Mol Biol 1044:389

# *Příloha 7*

**Iveta Mrízová**, Michaela Moserová, Jan Milichovský, Miroslav Šulc, René Kizek, Kateřina Kubáčková, Volker M. Arlt, Marie Stiborová

**HETEROLOGOUS EXPRESSION OF HUMAN CYTOCHROME P450 2S1 IN *ESCHERICHIA COLI* AND INVESTIGATION OF ITS ROLE IN METABOLISM OF BENZO[A]PYRENE AND ELLIPTICINE**

*Monatsh. Chem.* 147, 881–888, 2016

$IF_{2014}$ = 1.222

Monatsh Chem (2016) 147:881–888
DOI 10.1007/s00706-016-1738-2

ORIGINAL PAPER

# Heterologous expression of human cytochrome P450 2S1 in *Escherichia coli* and investigation of its role in metabolism of benzo[*a*]pyrene and ellipticine

**Iveta Mrízová[1] · Michaela Moserová[1] · Jan Milichovský[1] · Miroslav Šulc[1] · René Kizek[2] · Kateřina Kubáčková[3] · Volker M. Arlt[4] · Marie Stiborová[1]**

Received: 19 November 2015 / Accepted: 21 January 2016 / Published online: 30 March 2016


**Abstract** Cytochrome P450 (CYP) 2S1 is "orphan" CYP that is overexpressed in several epithelial tissues and many human tumors. The pure enzyme is required for better understanding of its biological functions. Therefore, human CYP2S1 was considered to be prepared by the gene manipulations and heterologous expression in *Escherichia coli*. Here, the conditions suitable for efficient expression of human CYP2S1 protein from plasmid pCW containing the human CYP2S1 gene were optimized and the enzyme purified to homogeneity. The identity of CYP2S1 as the product of heterologous expression was confirmed by dodecyl sulfate–polyacrylamide gel electrophoresis, Western blotting, and mass spectrometry. To confirm the presence of the enzymatically active CYP2S1, the CO spectrum of purified CYP2S1 was recorded. Since CYP2S1 was shown to catalyze oxidation of compounds having polycyclic aromatic structures, the prepared enzyme has been tested to metabolize the compounds having this structural character; namely, the human carcinogen benzo[*a*]pyrene (BaP), its 7,8-dihydrodiol derivative, and an anticancer drug ellipticine. Reaction mixtures contained besides the test compounds the CYP2S1 enzyme reconstituted with NADPH:CYP reductase (POR) in liposomes, and/or this CYP in the presence of cumene hydroperoxide or hydrogen peroxide. High performance liquid chromatography was employed for separation of BaP, BaP-7,8-dihydrodiol, and ellipticine metabolites. The results found in this study demonstrate that CYP2S1 in the presence of cumene hydroperoxide or hydrogen peroxide catalyzes oxidation of two of the test xenobiotics, a metabolite of BaP, BaP-7,8-dihydrodiol, and ellipticine. Whereas BaP-7,8,9,10-tetrahydrotetrol was formed as a product of BaP-7,8-dihydrodiol oxidation, ellipticine was oxidized to 12-hydroxyellipticine, 13-hydroxyellipticine, and the ellipticine $N^2$-oxide.

*Graphical abstract*

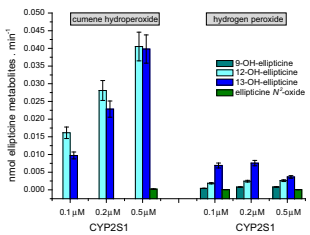


**Keywords** Enzymes · Coenzymes · High pressure liquid chromatography

**Electronic supplementary material** The online version of this article (doi:10.1007/s00706-016-1738-2) contains supplementary material, which is available to authorized users.

✉ Marie Stiborová
stiborov@natur.cuni.cz

[1] Department of Biochemistry, Faculty of Science, Charles University, Albertov 2030, 128 40 Prague 2, Czech Republic

[2] Department of Chemistry and Biochemistry, Faculty of Agronomy, Mendel University in Brno, 613 00 Brno, Czech Republic

[3] Department of Oncology, 2nd Faculty of Medicine, Charles University and University Hospital Motol, V Uvalu 84, 150 06 Prague 5, Czech Republic

[4] Analytical and Environmental Sciences Division, MRC-PHE Centre for Environment and Health, King's College London, London SE1 9NH, UK

## Introduction

Cytochrome P450 (CYP, EC 1.14.14.1) is a superfamily of hemoproteins distributed widely throughout nature, involved in metabolism of a broad variety of substrates and catalyzing a variety of interesting chemical reactions [1–3]. The CYP enzymes are a component of a mixed function oxidase (MFO) system located in the membrane of the endoplasmic reticulum that beside the CYPs also contains other enzymes such as NADPH:CYP oxidoreductase (POR), and cytochrome $b_5$ accompanied by its NADH:-cytochrome $b_5$ reductase [1–5].

A variety of CYP enzymes (e.g., CYP5, 8, 11, 17, 19, 21, 24, 26, and 27) are used by mammals for the synthesis of important endogenous compounds such as steroids and eicosanoids, besides their function in the catabolism of natural products [1, 2]. Of the remainder of the mammalian CYPs, a relatively small set of these enzymes accounts for most of metabolism of drugs (i.e., human CYP1A2, 2C9, 2C19, 2D6, and 3A4). Another group of human CYPs (i.e., human CYP1A1, 1A2, 1B1, 2A6, 2E1, and 3A4) is involved in the metabolism of most pro-toxicants and pro-carcinogens that are CYP substrates [1, 3, 6, 7]. All these data indicate that functions of most CYP enzymes are well known. However, of 57 human CYP enzymes, 13 remain classified as "orphans", because their functions are largely unknown [8–11]. Among them, CYP2S1 was found to be induced by the aryl hydrocarbon receptor (AHR) ligands, by hypoxia via hypoxia-inducible factor 1 and by all-*trans*-retinoic acid [12, 13]. This enzyme is expressed in epithelial cells of tissues exposed to the environment (i.e., skin, respiratory, urinary, and gastrointestinal tracts), and also in many tumors of epithelial origin [10, 12]. Interestingly, CYP2S1 was described that cannot use NADPH for oxidative metabolism of some substrates, because of its inability to accept electrons from the NADPH/POR system [11, 14]. However, the recent results of Guengerich with collaborators show that in the case of CYP2S1-mediated metabolism of 1,4-bis[[2-(dimethylamino-*N*-oxide)ethyl] amino]-5,8-dihydroxyanthra-cene-9,10-dione by CYP2S1, POR is capable of reducing this CYP [15].

Recently, we have found that a human carcinogen benzo[*a*]pyrene (BaP) [16] and an anticancer drug ellipticine [17–19] might be, beside classical CYPs that accept electrons transferred from the NADPH/POR system, oxidized also by other CYP enzymes, whose activities are not dependent on POR [17, 18, 20–24]. We suggested that the CYP2S1 enzyme, which was shown to catalyze the oxidation of compounds having polycyclic aromatic structures (such as BaP) also without participation of POR [8, 10, 11, 14], might be one of the such enzymes. Therefore, to confirm this suggestion, the CYP2S1 efficiency to oxidize BaP and ellipticine should be investigated in detail. However, because purification of CYP2S1 from natural biological materials is experimentally very difficult, heterologous expression was recently employed to obtain the biological active CYP2S1 [9–11]. In this study, we describe an improved method for heterologous expression of human CYP2S1 in a prokaryotic expression system of *Escherichia coli* cells as well as an efficient procedure for its purification to homogeneity. The purified enzyme either reconstituted with POR in liposomes or in the presence of cumene hydroperoxide/hydrogen peroxide in vitro was utilized to investigate its catalytic activity to oxidize carcinogenic BaP, its 7,8-dihydrodiol metabolite, and an anticancer drug ellipticine.

## Results and discussion

### Expression of human CYP2S1 in *E. coli* and its purification

When the procedure for heterologous expression of human CYP2S1 construct in *E. coli* DH5α cells described by [9] was used, the CYP2S1 production was only very low (less than 70 nmol CYP per $dm^3$). Moreover, even though the co-expression of the molecular chaperon GroEL/ES that is a suitable method to elevate the CYP2S1 expression [9] was utilized, no dramatic increase in its expression was found. Therefore, we examined other modifications of the procedure to improve the CYP2S1 expression. First, the effect of volume of the cultured growth media from 50 to 500 $cm^3$ in different size Erlenmeyer flasks was tested. The level of expression CYP2S1 increased up to 200 nmol CYP per $dm^3$ when the 100 $cm^3$ of cultured media in 500 $cm^3$ Erlenmeyer flask was used, compared with 50 or 500 $cm^3$ of growth TB media in 250 $cm^3$ and/or 2 $dm^3$ Erlenmeyer flasks, respectively. Second, in addition to this procedure modification, the cell growth time was found to play a role in the production of CYP2S1, and even in its quality. The maximum levels of expressed CYP occurred after 24-h cultivation, at shaking speed of 190 rpm and 29 °C; higher time of cultivation (up to 40 h) did not result to elevated levels of CYP produced. It, moreover, led to changes in a CYP structure, forming its degraded form, cytochrome P420. Therefore, the 24-h cell cultivation was used in this study and the cells prepared by this procedure were utilized for CYP2S1 purification.

Solubilization of *E. coli* membranes containing CYP2S1 was achieved by 1 % 3-[(3-cholamidopropyl)dimethylammonio]-1-propanesulfonate hydrate (CHAPS) (w/v) present in the solubilization buffer. The resulting supernatant was loaded onto a column of $Ni^{2+}$-nitriloacetic acid agarose

(Ni–NTA agarose) and CYP2S1 was eluted with potassium phosphate buffer containing 300 mmol $dm^{-3}$ imidazole. Using the sodium dodecyl sulfate–polyacrylamide gel electrophoresis (SDS-PAGE), the purified, detergent-free CYP2S1 (see "Experimental"), was shown to be electrophoretically homogeneous, having a molecular mass of ~50 ± 5 kDa (Fig. 1a). The CYP2S1 identity was proved by Western blotting, using the chicken polyclonal antibodies against CYP2S1 [25] (Fig. 1b) and by mass spectrometry (Supplementary Table 1 and Supplementary Scheme 1). The specific content of CYP2S1 was estimated to be 4.5 nmol per mg protein, based on a bicinchoninic acid colorimetric protein estimation method.

### Spectral properties of prepared CYP2S1

The carbon monoxide (CO)-spectrum (see "Experimental") of prepared human CYP2S1 was recorded (Fig. 2). This spectrum was free of cytochrome P420, indicating the correct fold and the high quality of the prepared CYP2S1 enzyme.

### Enzyme activity—oxidation of BaP, BaP-7,8-dihydrodiol, and ellipticine by prepared CYP2S1

To evaluate enzymatic activity of purified CYP2S1, two systems were utilized: (1) CYP2S1 reconstituted with POR in liposomes and (2) CYP2S1 in the presence of cumene hydroperoxide and/or hydrogen peroxide as cofactors. Since BaP and its 7,8-dihydrodiol derivative were found as substrates of CYP2S1 [10, 11], they were used as model

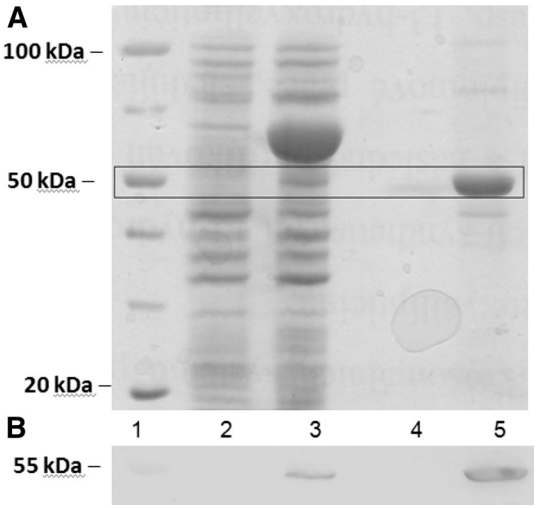


**Fig. 1** SDS-PAGE (**a**) and Western blotting (**b**) of heterologous expression products in *E. coli* and fractions obtained during purification of CYP2S1. *Lane 1* protein $M_r$ marker, *2* sample before induction by IPTG, *3* production of proteins after 24 h, *4* $Ni^{2+}$-nitriloacetic acid agarose purified fraction, *5* a final concentrated protein sample

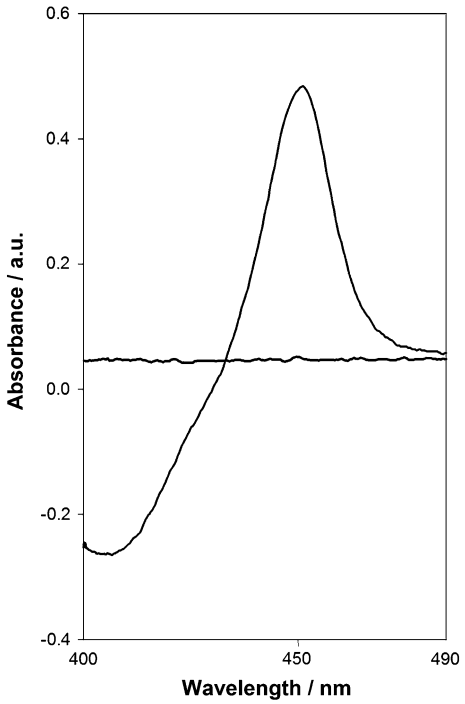


**Fig. 2** The CO-spectrum of purified human CYP2S1. $Fe^{2+}$–CO vs. $Fe^{2+}$ difference spectrum

substrates of these CYP2S1 systems. In addition, because a suggested participation of CYP2S1 in metabolism of an anticancer drug ellipticine [17, 23, 24] has not been examined as yet, its potency to oxidize this drug was investigated, too. The enzyme activity of CYP2S1 to metabolize these compounds in both systems was compared with that of the CYP1A1 and/or 1B1 enzymes, for which the test compounds are excellent substrates [3, 21, 22, 26–28].

Utilizing BaP as a compound that was described by Bui and Hankinson [10] to be a substrate of CYP2S1, no metabolites were detectable in both CYP2S1 systems under the conditions used in our experiments. This finding, namely, the result that BaP is not a substrate of CYP2S1, is in line with the results of Guengerich and collaborators [9], whose detected almost no CYP2S1 activity to oxidize BaP, too. In contrast, HPLC used to analyze metabolism of one of the BaP metabolites, BaP-7,8-dihydrodiol, with either CYP2S1 systems showed their effectiveness to oxidize this xenobiotic (see Supplementary Fig. 1 for CYP2S1 with cumene hydroperoxide); BaP-7,8,9,10-tetrahydrotetrol was identified as the reaction product (Supplementary Fig. 2). As shown in Fig. 3, CYP1A1 or 1B1 reconstituted with POR in liposomes oxidized BaP-7,8-dihydrodiol with up to more than two orders of magnitude higher effectiveness than CYP2S1 reconstituted with POR. On the contrary, CYP2S1 in the presence of cumene hydroperoxide or hydrogen peroxide generated up sevenfold higher levels of

BaP-7,8,9,10-tetrahydrotetrol than CYP2S1 reconstituted with POR. In these systems, the CYP2S1 enzyme exhibited essentially the same (and/or even higher) effectiveness in this reaction than analogous systems of human CYP1A1 or 1B1 (Fig. 3). Essentially no BaP-7,8-dihydrodiol metabolite (BaP-7,8,9,10-tetrahydrotetrol) was detectable when the NADPH-generating system or cumene hydroperoxide/hydrogen peroxide cofactors were omitted from the incubation mixtures (data not shown). The results found indicate that prepared human CYP2S1 is enzymatically active enzyme, being more effective in BaP-7,8-dihydrodiol oxidation in the presence of cumene hydroperoxide or hydrogen peroxide than in the system where CYP2S1 is reconstituted with POR. They also demonstrate that by its potency to oxidize BaP-7,8-dihydrodiol, this CYP can increase the overall metabolism of BaP catalyzed by other CYPs, including CYP1A1 and 1B1, the most important CYPs oxidizing this carcinogen [20, 29].

In the case of ellipticine, only the systems of CYP2S1 containing cumene hydroperoxide and/or hydrogen peroxide were capable of oxidizing this drug (Figs. 4, 5), whereas this CYP reconstituted with POR in liposomes in the presence of NADPH-generating system was without such activity (data not shown). Cumene hydroperoxide was an up to one order of magnitude more effective cofactor for ellipticine oxidation than hydrogen peroxide (Fig. 5a). Of the ellipticine metabolites, 12-hydroxyellipticine and 13-hydroxyellipticine were the major metabolites formed by this CYP2S1 system, while 9-hydroxyellipticine and the ellipticine $N^2$-oxide were the minor ones (Fig. 5a). Negligible amounts of these ellipticine metabolites were generated by CYP2S1 without cofactors (data not shown). The formation of 12-hydroxyellipticine and 13-hydroxyellipticine is the pharmacologically important feature, because these metabolites generate two major deoxyguanosine adducts in DNA [17–19, 30, 31, 32] that are responsible for ellipticine anticancer activity [17–19, 33, 34]. The levels of activation metabolites were increased with increasing concentrations of CYP2S1 with cumene hydroperoxide, while essentially no such effects were found when hydrogen peroxide was used as a cofactor (Fig. 5a). The only low amounts of the ellipticine metabolites were generated by the system of human CYP1A1 in the presence of both peroxides, 12-hydroxyellipticine was even not produced by this CYP at all (Fig. 5b). The system of human CYP1A1 reconstituted with POR in liposomes was not examined in this work, because its efficiency to oxidize this drug was investigated previously in detail; 9-hydroxyellipticine, 7-hydroxyellipticine, and 13-hydroxyellipticine were formed as the major metabolites in this CYP1A1 system, while the ellipticine $N^2$-oxide as a minor product and 12-hydroxyellipticine was not a product of ellipticine oxidation by this enzyme [19, 31, 32]. A pattern of the metabolites formed by this CYP1A1 system is hence quite different from that generated by this enzyme in the presence of either test peroxides (Fig. 5b). The results found demonstrate the effectiveness of CYP2S1 in ellipticine oxidation and confirmed the suggestion of its participation in ellipticine metabolism catalyzed by CYP without POR [17, 23, 24]. Because of the high expression of CYP2S1 in many tumor cells, the results also emphasized its role in metabolism of ellipticine in cancer tissues that was found previously [17, 19, 33, 34].

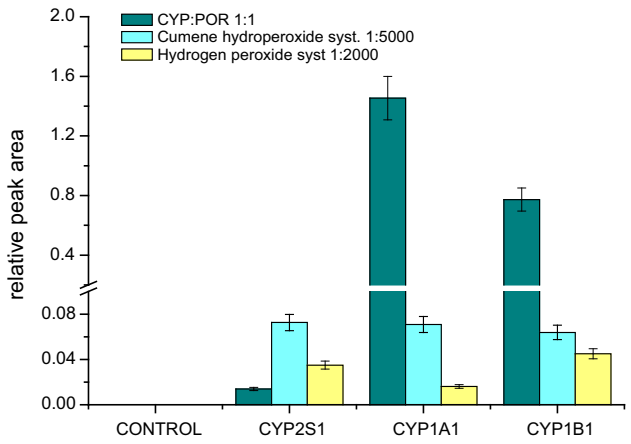


**Fig. 3** Formation of BaP-7,8,9,10-tetrahydrotetrol by human CYP2S1 in different systems. Human CYP1A1 or CYP1B1 known to oxidize BaP- 7,8-dihydrodiol to BaP-7,8,9,10-tetrahydrotetrol were used as positive controls. Data shown are averages and standard deviation from three parallel measurements

## Conclusion

Since functions of many "orphan" CYPs are largely unknown [8–11], their investigation is a challenge for research of many laboratories. Therefore, in this study we examined a function of "orphan" CYP2S1, the enzyme which is able to metabolize several substrates via the NADPH/POR-independent activity [9–11]. For such a study, we prepared enzymatically active human recombinant CYP2S1 and further utilized to evaluate its potency to oxidize one of the anticancer drugs, ellipticine. This antitumor agent was chosen, because it was found that it can be metabolized also by the CYP enzymes that do not need the NADPH/POR system, and we suggested that CYP2S1 might be one of these CYPs [17, 23, 24]. Our data demonstrate that CYP2S1 is indeed capable of oxidizing ellipticine, in the systems containing the peroxide cofactors, therefore, via the NADPH/POR-independent activity. CYP2S1 in the presence of cumene hydroperoxide oxidizes ellipticine predominantly to its activation metabolites, 12-hydroxyellipticine and 13-hydroxyellipticine, the

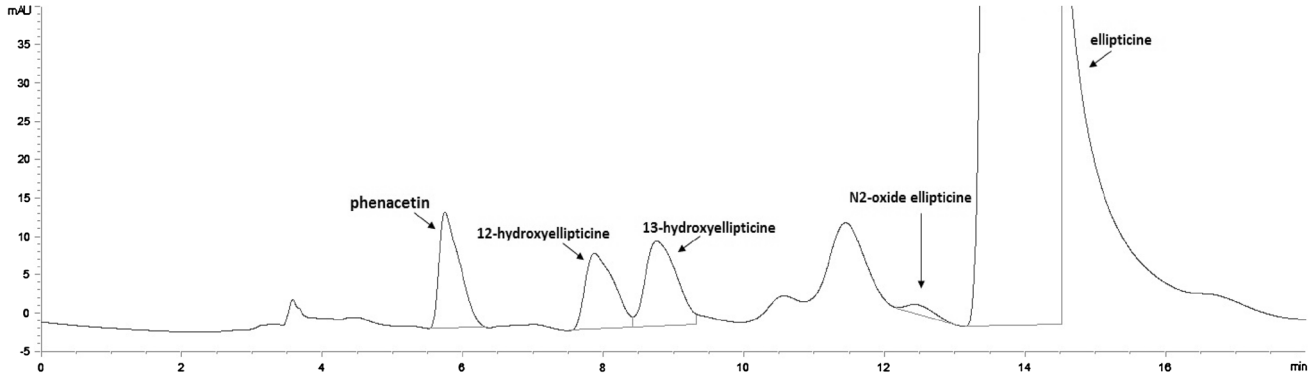


**Fig. 4** HPLC analysis of ellipticine metabolites formed by human recombinant CYP2S1 in the presence of cumene hydroperoxide

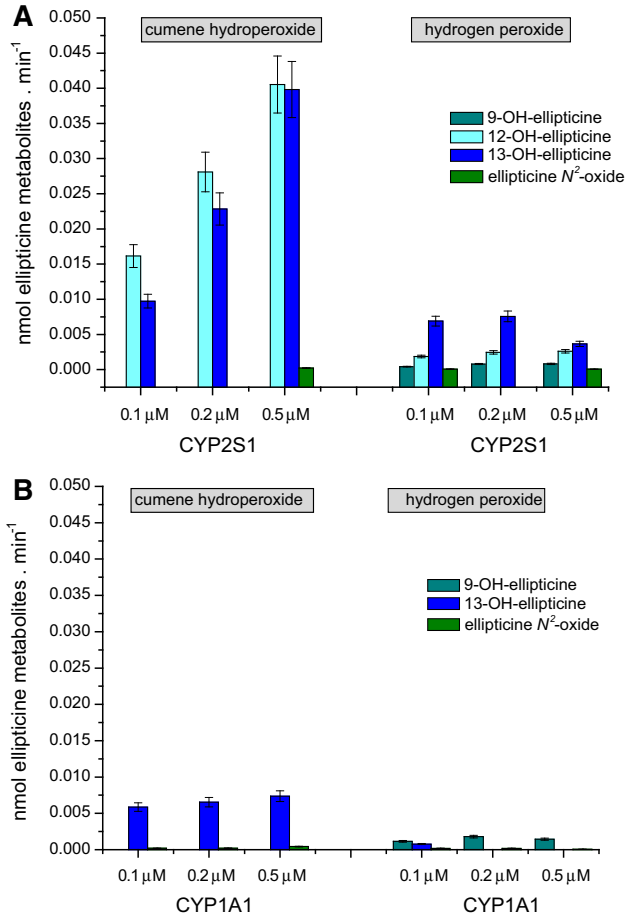


**Fig. 5** Oxidation of ellipticine by human recombinant CYP2S1 (**a**) and CYP1A1 (**b**) expressed in *E. coli* with cumene hydroperoxide or $H_2O_2$. Data shown are averages and standard deviation from three parallel measurements

metabolites responsible for its pharmacological efficiencies that result from formation of covalent ellipticine-derived DNA adducts. These adducts were found to be generated in rat lung and kidney in vivo, indeed even without participation of the NADPH/POR system [17, 18, 23, 24].

Because CYP2S1 can be expressed in several tumor cells sensitive to ellipticine [10, 25, 32–36], the data found in this work suggest that this CYP can contribute to the ellipticine antitumor activity in these cells. This suggestion need, however, to be explored by further studies. Utilization of the tumor cells highly expressing CYP2S1 [10, 25] is planned to be utilized for such studies.

## Experimental

Ellipticine and BaP were from Sigma Chemical Co (St Louis, MO, USA). These and other chemicals used in the experiments were of analytical purity or better. (±)-*Trans*-7,8-dihydroxy-7,8-dihydrobenzo[*a*]pyrene (BaP-7,8-dihydrodiol) was prepared at the Biochemical Institute for Environmental Carcinogenesis, Germany, as described [37].

*Escherichia coli* DH5α cells with the *CYP2S1* gene were a gift of Professor F.P. Guengerich (Vanderbilt University School of Medicine, Nashville, Tennessee, USA). It should be noted that optimization of the conditions suitable for production of plasmid pCW containing the CYP2S1 gene, was carried out in his laboratory and further used for expression of CYP2S1 [9]. It was necessary to modify the C-terminal end of the CYP2S1 cDNA by Histidyl-5-Tag and the N-terminal end before the well-conserved proline-rich region (see [9] for detail).

Human CYP1A1, 1B1 and POR were prepared by heterologous expression in *E. coli* in our laboratory (Department of Biochemistry, Faculty of Sciences, Charles University, Prague, Czech Republic), by J. Milichovský, essentially in the same manner as described previously [38–40].

### Expression of human CYP2S1 in *E. coli*

*Escherichia coli* cultivation was carried out essentially as described previously [9, 41–43]. A single bacterial colony

was picked, and the bacteria were grown overnight in 15 $cm^3$ of a Luria Broth (LB) liquid medium (Sigma Chemical Co, St Louis, MO, USA) containing 100 mg $cm^{-3}$ ampicillin, and 50 mg $cm^{-3}$ kanamycin at 37 °C with shaking at 200 rpm. The overnight culture was inoculated 1:100 into 100 $cm^3$ of a Terrific Broth (TB) medium (Sigma Chemical Co, St Louis, MO, USA) containing 100 mg $cm^{-3}$ ampicilin, 50 mg $cm^{-3}$ kanamycin, and 0.025 % (v/v) of a mixture of trace elements (27 g $FeCl_3 \cdot 6H_2O$, 2.0 g $ZnCl_2 \cdot 4H_2O$, 2.0 g $CaCl_2 \cdot 6H_2O$, 2.0 g $Na_2MoO_4$, 1.0 g $CaCl_2 \cdot 2H_2O$, 1.0 g $CuCl_2$, 0.5 g $H_3BO_3$, and 100 $cm^3$ concentrated HCl per 1 $dm^3$ of distilled water) in a 500 $cm^3$ flask. Sixteen flasks of cultures were incubated for ~4 h at 37 °C with shaking at 220 rpm until they attained an $OD_{600}$ of 0.5–0.7, then were supplemented with 1 mmol $dm^{-3}$ isopropyl $\beta$-D-1-thiogalactopyranoside (IPTG) medium (Sigma Chemical Co, St Louis, MO, USA), 1 mg $cm^{-3}$ arabinose, and 0.5 mmol $dm^{-3}$ a heme precursor, $\delta$-aminolevulinic acid ($\delta$-ALA) (Sigma Chemical Co, St Louis, MO, USA), and cultured for 24 h at 29 °C with shaking at 190 rpm. Induction of GroEL/ES and CYP2S1 synthesis was achieved in the presence of arabinose and IPTG, respectively. The expression level of CYP2S1 was monitored at 12 and 24 h.

*Escherichia coli* membranes were prepared as described previously [44]. All steps were done at 4 °C. The cells were harvested by centrifugation at 5000*g* for 20 min. Pellets were resuspended in 1:20 vol of Tris/sucrose/ethylenediaminetetraacetic acid (EDTA) (TSE) buffer (10 mmol $dm^{-3}$ Tris–acetate, pH 7.4, 500 mmol $dm^{-3}$ sucrose, 0.5 mmol $dm^{-3}$ EDTA). Lysozyme was added to a concentration of 0.2 mg $cm^{-3}$, and the suspensions were diluted twofold with distilled $H_2O$ before incubation on ice for 30 min. The resulting spheroplasts were sedimented at 4000 g at 4 °C for 20 min, and resuspended in 100 mmol $dm^{-3}$ potassium phosphate buffer, pH 7.4, containing 6 mmol $dm^{-3}$ magnesium acetate, 20 % glycerol (v/v), and 10 mmol $dm^{-3}$ $\beta$-mercaptoethanol (ME). The protease inhibitors, phenylmethylsulfonyl fluoride (PMSF), aprotinin, leupeptin, and bestatin (all Sigma Chemical Co, St Louis, MO, USA) were added to a final concentration of 1 mmol $dm^{-3}$, 1 µg $cm^{-3}$, 2, and 1 µmol $dm^{-3}$, respectively. Suspensions of spheroplasts were sonicated ten times for 30 s each, on ice, and centrifuged at 10,000*g* at 4 °C for 20 min. Supernatants were centrifuged at 108,000*g* at 4 °C for 65 min. Sedimented membrane fractions were resuspended in 100 mmol $dm^{-3}$ potassium phosphate buffer, pH 7.4, containing 6 mmol $dm^{-3}$ magnesium acetate, 20 % glycerol (v/v), and 10 mmol $dm^{-3}$ ME. The membrane preparation was stored at −70 °C until use. The reddish pellets represent the CYP containing membrane fraction.

## Purification of recombinant human CYP2S1

Membrane fractions of *E. coli* were diluted up to 2 mg $cm^{-3}$ of protein concentration with 100 mmol $dm^{-3}$ potassium phosphate buffer, pH 7.4, containing 20 % glycerol (v/v), 0.5 mol $dm^{-3}$ NaCl, 10 mmol $dm^{-3}$ ME (solubilization buffer) and solubilized with 1.0 % CHAPS (Sigma Chemical Co, St Louis, MO, USA) (w/v). The detergent was dissolved in solubilization buffer. After stirring for 3 h at 4 °C, the resulting solutions were centrifuged at 108,000*g* at 4 °C for 65 min to eliminate insoluble materials. The supernatants were then applied on a column of Ni–NTA agarose (QIAGEN) (Hilden, Germany) equilibrated with the solubilization buffer [9]. After washing of the column with 10 volumes of 100 mmol $dm^{-3}$ potassium phosphate buffer, pH 7.4, containing 20 % glycerol (v/v), 0.5 mol $dm^{-3}$ NaCl, 0.5 % CHAPS (w/v) and 10 mmol $dm^{-3}$ imidazole, the CYP2S1 enzyme was eluted with 100 mmol $dm^{-3}$ potassium phosphate buffer, pH 7.4, containing 20 % glycerol (v/v), 0.5 mol $dm^{-3}$ NaCl, 0.5 % CHAPS (w/v) and 300 mmol $dm^{-3}$ imidazole. The CHAPS was removed by extensive dialysis against 200-fold volume of 100 mmol $dm^{-3}$ potassium phosphate buffer, pH 7.4 containing 20 % glycerol (v/v), 0.1 mmol $dm^{-3}$ EDTA, and 0.1 mmol $dm^{-3}$ dithiothreitol (DTT) (dialysis buffer). In the last step of dialysis, the dialysis buffer without DTT was used. The final fraction of CYP2S1 was concentrated by ultrafiltration using an YM-30 membrane (Millipore). SDS-PAGE was used to assess the final protein purity.

## Determination of CYP and protein contents

As found by Omura and Sato [45], when CYP is in the reduced state and complexed with CO, it exhibits the classic CO difference spectrum with a maximum at 450 nm. This spectral property is employed for the specific estimation of CYP content and for evaluation whether the purified enzyme exists in a correctly folded protein state. Therefore, the concentration of CYP was estimated by this method, described by Omura and Sato [45] that is based on the absorption of the complex of reduced CYP with CO. The CYP2S1 content was calculated using an extinction coefficient of 91 $[\text{mmol dm}^{-3}]^{-1}$ $cm^{-1}$. Protein concentrations were estimated using a bicinchonic acid assay (BCA, ThermoFisher Scientific, USA) with bovine serum albumin as a standard [46].

## Determination of CYP2S1 protein levels by Western blotting

Samples containing subcellular fractions from bacteria or the purified protein were subjected to electrophoresis on

the 10 % polyacrylamide gel and transferred onto a polyvinylidene fluoride (PVDF) membrane as reported [22, 47]. The membranes were then exposed overnight at 4 °C to the chicken polyclonal antibodies against CYP2S1 prepared as described previously [25] and the antigen–antibody complex was visualized with an alkaline phosphatase-conjugated goat anti-rabbit IgG antibody (1:1428, Sigma-Aldrich, USA) and 5-bromo-4-chloro-3-indolyl-phosphate/nitrobluetetrazolium as chromogenic substrate [48].

## Measurement of CYP2S1 enzyme activities

Enzymatic activity of purified CYP2S1 was analyzed using two systems: (1) CYP2S1 reconstituted with POR in liposomes and (2) CYP2S1 in the presence of cumene hydroperoxide and/or hydrogen peroxide.

Incubation mixtures containing purified CYP reconstituted with human POR contained CYP2S1 (or CYP1A1 or 1B1) and POR. Briefly, CYP was reconstituted as follows (200 pmol CYP with 200 pmol POR, 0.1 mmol $cm^{-3}$ liposomes [dilauroyl phosphatidylcholine, dioleyl phosphatidylcholine, dilauroyl phosphatidylserine (1:1:1) (Sigma Chemical Co, St Louis, MO, USA)], 3 mmol $dm^{-3}$ reduced glutathione, and 50 mmol $dm^{-3}$ HEPES/KOH buffer, pH 7.4) [49]. An aliquot of this mixture was then added to incubation mixtures.

Incubation mixtures used to study metabolism of BaP, BaP-7,8-dihydrodiol, or ellipticine contained 100 mmol $dm^{-3}$ sodium phosphate buffer (pH 7.4), NADPH-generating system (1 mmol $dm^{-3}$ $NADP^+$, 10 mmol $dm^{-3}$ D-glucose-6-phosphate, 1 U per $cm^{-3}$ D-glucose-6-phosphate dehydrogenase, Sigma Chemical Co, St Louis, MO, USA), 0.05 $cm^3$ CYP reconstituted system, 10 μmol $dm^{-3}$ BaP or 133 μmol $dm^{-3}$ BaP-7,8-dihydrodiol or 10 μmol $dm^{-3}$ ellipticine (dissolved in 0.005 $cm^3$ DMSO) in a final volume of 0.5 $cm^3$. The reaction was initiated by adding 0.05 $cm^3$ of the NADPH-generating system. Control incubations were carried out either without CYP enzyme or without the NADPH-generating system or without the substrate. After incubation in open tubes (37 °C, 20 min), 0.005 $cm^3$ of 1 mmol $dm^{-3}$ phenacetin in methanol was added as an internal standard. The reactions catalyzed oxidation of BaP or BaP-7,8-dihydrodiol and ellipticine by human CYP1A1 was linear up to 60 and 30 min, respectively [26, 28, 49]. Metabolites were extracted twice with ethyl acetate (2 × 1 $cm^3$) and evaporated to dryness. The samples were dissolved in 0.025 $cm^3$ methanol and metabolites of the tested substrates formed in these systems separated by HPLC. Metabolites of BaP and BaP-7,8-dihydrodiol were separated by HPLC and identities of their structures were carried out as described [28, 49, 50]. HPLC analysis of ellipticine metabolites and identities of their structures were performed as described previously [26, 31, 32].

Incubation mixtures used to study metabolism of BaP, BaP-7,8-dihydrodiol, or ellipticine in the presence of cumene hydroperoxide or hydrogen peroxide contained 100 mmol $dm^{-3}$ sodium phosphate buffer (pH 7.4), 0.1–0.5 μmol $dm^{-3}$ CYP, 10 μmol $dm^{-3}$ BaP or 133 μmol $dm^{-3}$ BaP-7,8-dihydrodiol or 10 μmol $dm^{-3}$ ellipticine (dissolved in 0.005 $cm^3$ DMSO) in a final volume of 500 $cm^3$. The reaction was initiated by adding cumene hydroperoxide or hydrogen peroxide to their final concentrations of 1 mmol $dm^{-3}$. Control incubations were carried out either without CYP or without peroxides or without substrates. After incubation in open tubes (37 °C, 10 min), 0.005 $cm^3$ of 1 mmol $dm^{-3}$ phenacetin in methanol was added as an internal standard. Metabolites were extracted twice with ethyl acetate (2 × 1 $cm^3$) and evaporated to dryness. The samples were dissolved in 0.025 $cm^3$ methanol and different metabolites formed in these systems were separated by HPLC. Metabolites of BaP, BaP-7,8-dihydrodiol and ellipticine were separated by HPLC and their structure indentified as described above. The peak areas of BaP, BaP-7,8-dihydrodiol, and ellipticine were calculated relative to the peak area of the internal standard (phenacetin), and expressed as relative peak areas.

## Mass spectrometry of purified CYP2S1

The identity and integrity of recombinant protein of human CYP2S1 was verified by MALDI-TOF/TOF (Ultra-FLEX III mass spectrometer, Bruker-Daltonics, Bremen, Germany) mass spectrometer using α-cyano-4-hydroxycinnamic acid as a matrix. The protein band from SDS-PAGE was destained, cysteine residues were modified by iodoacetamide, and protein was digested by trypsin endoprotease (Promega Corp., Madison, USA). The resulting peptide mixture was extracted and the MS and MS/MS spectra of corresponding *m/z* signals for peptide identity verification were acquired and manually interpreted (54 % of protein sequence coverage) [51].

**Acknowledgments** Supported by GACR (Grant 14-18344S) and Charles University (Grant UNCE 204025/2012 and GAUK 1380214). Work at King's College London is also supported by Cancer Research UK (Grant Number C313/A14329).

## References


1. Guengerich FP (2001) Chem Res Toxicol 14:611
2. Guengerich FP (2008) Chem Res Toxicol 21:70
3. Arlt VM, Henderson CJ, Wolf CR, Stiborova M, Phillips DH (2015) Toxicol Res 4:548
4. Riddick DS, Ding X, Wolf CR, Porter TD, Pandey AV, Zhang QY, Gu J, Finn RD, Ronseaux S, McLaughlin LA, Henderson CJ, Zou L, Fluck CE (2013) Drug Metab Disp 41:12
5. Porter TD (2002) J Biochem Mol Toxicol 16:311
6. Rendic S, Di Carlo FJ (2007) Drug Metab Rev 29:413
7. Wienkers LC, Heath LC (2005) Nat Rev Drug Dis 4:825
8. Guengerich FP, Wu ZL, Bartleson CJ (2005) Biochem Biophys Res Commun 338:465
9. Wu ZL, Sohl CD, Shimada T, Guengerich FP (2006) Mol Pharmacol 69:2007
10. Bui PH, Hankinson O (2009) Mol Pharmacol 76:1031
11. Bui PH, Hsu EL, Hankinson O (2009) Mol Pharmacol 76:1044
12. Smith G, Wolf CR, Deeni YY, Dawe RS, Evans AT, Comrie MM, Ferguson J, Ibbotson SH (2003) Lancet 361:1336
13. Rivera SP, Wang F, Saarikoski ST, Taylor RT, Chapman B, Zhang R, Hankinson (2007) J Biol Chem 282:10881
14. Bui P, Imaizumi S, Beedanagari SR, Reddy ST, Hankinson O (2011) Drug Metab Dispos 39:180
15. Xiao Y, Shinkyo R, Guengerich FP (2011) Drug Metab Dispos 39:944
16. International Agency for Research on Cancer (IARC) (2010). Some non-heterocyclic polycyclic aromatic hydrocarbons and some related exposures. In: IARC Monogr Eval Carcinog Risks Hum 92:1
17. Stiborová M, Rupertová M, Frei E (2011) Biochim Biophys Acta 1814:175
18. Stiborová M, Černá V, Moserová M, Mrízová I, Arlt VM, Frei E (2015) Int J Mol Sci 16:284
19. Stiborova M, Frei E (2014) Curr Med Chem 21:575
20. Stiborova M, Moserova M, Cerna V, Indra R, Dracinsky M, Šulc M, Henderson CJ, Wolf CR, Schmeiser HH, Phillips DH, Frei E, Arlt VM (2014) Toxicology 318:1
21. Arlt VM, Stiborova M, Henderson CJ, Thiemann M, Frei E, Aimova D, Singhs R, da Costa GG, Schmitz OJ, Farmer PB, Wolf CR, Philips DH (2008) Carcinogenesis 29:656
22. Arlt VM, Poirier MC, Sykes SE, Kaarthik J, Moserova M, Stiborova M, Wolf R, Henderson CJ, Phillips DH (2012) Toxicol Lett 213:160
23. Stiborová M, Arlt VM, Henderson CJ, Wolf CR, Kotrbová V, Moserová M, Hudecek J, Phillips DH, Frei E (2008) Toxicol Appl Pharmacol 226:318
24. Stiborova M, Moserova M, Mrazova B, Kotrbova V, Frei E (2010) Neuro Endocrinol Lett 31(Suppl 2):26
25. Hodek P, Hrdinova J, Macova I, Soucek P, Mrizova I, Burdova K, Kizek R, Hudecek J, Stiborova M (2015) Neuro Endocrinol Lett 36(Suppl 1):38
26. Kotrbova V, Mrazova B, Moserova M, Martinek V, Hodek P, Hudecek J, Frei E, Stiborova M (2011) Biochem Pharmacol 82:669
27. Stiborova M, Indra R, Moserova M, Cerna V, Rupertova M, Martinek V, Eckschlager T, Kizek R, Frei E (2012) Chem Res Toxicol 25:1075
28. Stiborova M, Moserova M, Cerna V, Indra R, Dracinsky M, Šulc M, Henderson CJ, Wolf CR, Schmeiser HH, Phillips DH, Frei E, Arlt VM (2014) Toxicology 318:1
29. Baird WM, Hooven LA, Mahadevan B (2005) Environ Mol Mutagen 45:106
30. Stiborová M, Sejbal J, Borek-Dohalská L, Aimová D, Poljaková J, Forsterová K, Rupertová M, Wiesner J, Hudecek J, Wiessler M, Frei E (2004) Cancer Res 64:8374
31. Stiborová M, Poljaková J, Martínková E, Ulrichová J, Simánek V, Dvořák Z, Frei E (2012) Toxicology 302:233
32. Poljaková J, Frei E, Gomez JE, Aimová D, Eckschlager T, Hrabeta J, Stiborová M (2007) Cancer Lett 252:270
33. Martinkova E, Dontenwill M, Frei E, Stiborova M (2009) Neuro Endocrinol Lett 30(Suppl 1):60
34. Bořek-Dohalská L, Frei E, Stiborová M (2004) Collect Czech Chem Commun 69:603
35. Poljaková J, Eckschlager T, Hrabeta J, Hrebacková J, Smutný S, Frei E, Martínek V, Kizek R, Stiborová M (2009) Biochem Pharmacol 77:1466
36. Stiborova M, Poljakova J, Mrizova LI, Borek-Dohalska L, Eckschlager T, Adam V, Kizek R, Frei E (2014) Int J Electrochem Sci 9:5675
37. Wohak LE, Krais AM, Kucab JE, Stertmann J, Øvrebø S, Seidel A, Phillips DH, Arlt VM (2014) Arch Toxicol. 90:291. doi:10.1007/s00204-014-1409-1
38. Hanna IH, Teiber JF, Kokones KL, Hollenberg PF (1998) Arch Biochem Biophys 350:324
39. Hanna IH, Reed JR, Guengerich FP, Hollenberg PF (2000) Arch Biochem Biophys 376:206
40. Culka M, Milichovsky J. Jerabek P, Stiborova M, Martinek V (2015) Neuro Endocrinol Lett 36 Suppl 1:29
41. Shimada T, Wunsch RM, Hanna IH, Sutter TR, Guengerich FP, Gillam EMJ (1998) Arch Biochem Biophys 357:111
42. Guengerich FP, Martin MV (2006) Methods Mol Biol 320:31
43. Harnastai IN, Gilep AA, Usanov SA (2006) Protein Expr Purif 46:47
44. Lee SH, Yu HJ, Lee S, Ryu D-Y (2015) Toxicol Lett 239:81
45. Omura T, Sato R (1964) J Biol Chem 239:2370
46. Wiechelman KJ, Braun RD, Fitzpatrick JD (1988) Anal Biochem 175:231
47. Stiborova M, Martinek V, Rydlova H, Hodek P, Frei E (2002) Cancer Res 62:5678
48. Stiborová M, Bieler CA, Wiessler M, Frei E (2001) Biochem Pharmacol 62:1675
49. Indra R, Moserova M, Kroftova N, Sulc M, Martinkova M, Adam V, Eckschlager T, Kizek R, Arlt VM, Stiborova M (2014) Neuro Endocrinol Lett 35(Suppl 2):105
50. Moserová M, Kotrbová V, Aimová D, Sulc M, Frei E, Stiborová M (2009) Interdiscip Toxicol 2:239
51. Ječmen T, Ptáčková R, Černá V, Dračínská H, Hodek P, Stiborová M, Hudeček J, Šulc M (2015) Methods 89:128